


12-2001

Characterization of Biochelators, Membrane Redox Systems, and Quinone Reductases from Wood Degrading Basidiomycetes

Weihong Qi

Follow this and additional works at: <http://digitalcommons.library.umaine.edu/etd>

 Part of the [Plant Biology Commons](#), and the [Wood Science and Pulp, Paper Technology Commons](#)

Recommended Citation

Qi, Weihong, "Characterization of Biochelators, Membrane Redox Systems, and Quinone Reductases from Wood Degrading Basidiomycetes" (2001). *Electronic Theses and Dissertations*. 340.
<http://digitalcommons.library.umaine.edu/etd/340>

This Open-Access Dissertation is brought to you for free and open access by DigitalCommons@UMaine. It has been accepted for inclusion in Electronic Theses and Dissertations by an authorized administrator of DigitalCommons@UMaine.

**CHARACTERIZATION OF BIOCHELATORS, MEMBRANE REDOX
SYSTEMS, AND QUINONE REDUCTASES FROM WOOD
DEGRADING BASIDIOMYCETES**

By

Weihong Qi

B.S. Wuhan University, 1994

M.S. Chinese Academy of Science, 1997

A THESIS

Submitted in Partial Fulfillment of the

Requirements for the Degree of

Doctor of Philosophy

(in Biological Sciences)

The Graduate School

The University of Maine

December, 2001

Advisory Committee:

Jody Jellison, Professor of Plant Pathology, Advisor

Barry Goodell, Professor of Wood Science and Technology

Seanna Annis, Assistant Professor of Mycology

Stylios Tavantzis, Professor of Plant Pathology

Barbara Cole, Professor of Wood Chemistry

**CHARACTERIZATION OF BIOCHELATORS, MEMBRANE REDOX
SYSTEMS, AND QUINONE REDUCTASES FROM WOOD
DEGRADING BASIDIOMYCETES**

By Weihong Qi

Thesis Advisor: Dr. Jody Jellison

An Abstract of the Thesis Presented
in Partial Fulfillment of the Requirements for the
Degree of Doctor of Philosophy
(in Biological Sciences)
December, 2001

Biodegradation of wood by brown rot fungi is dependent upon a non-enzymatic system involving Fenton chemistry. Iron biochelators with molecular weights lower than 1kD are important components in this process. Phenolate biochelators drive a hydroxyl radical generating Fenton reaction by reducing ferric iron. Biochelators may be mineralized or alternately, in some cases oxidized biochelators may be regenerated via a quinone redox cycle. Electron donors for this postulated regeneration have not been identified. Extracellular cellobiose dehydrogenase has also been found to drive the Fenton reaction by generating ferrous iron and hydrogen peroxide. This research compared the production of biochelators and the cellobiose dehydrogenase in white rot, brown rot and non-decay fungi to elucidate the brown rot mechanisms. The transplasma membrane redox system and intracellular quinone reductases were also characterized in the brown rot fungus *Gloeophyllum trabeum*.

All the tested fungi produced iron chelating compounds and cellobiose dehydrogenase. The chemical characteristics and iron-reducing abilities of the biochelators produced varied, with the brown rot fungi producing biochelators showing

significant higher iron reducing ability. The brown rot fungus *Fomitopsis pinicola* produced biochelators with the greatest iron reducing activity.

Gloeophyllum trabeum mycelia showed 1,4-benzoquinone reducing ability. The transplasma membrane redox system was characterized based on its ferricyanide reduction kinetics. The fungus also produced constitutive intracellular NAD(P)H dependent 1,4-benzoquinone reductases. Reduction of 1,4-benzoquinone by intact mycelia and the intracellular enzymes showed different characteristics. An intracellular NADH dependent flavin mononucleotide containing 1,4-benzoquinone reductase was purified from *G. trabeum*. The physical and catalytical properties of the purified enzyme were characterized. The enzyme was highly inducible by 2,6-dimethoxy-1,4-benzoquinone and had a high turn over number for multiple quinones, which indicated it functioned efficiently in quinone metabolism. Quinone reductases can play an important role in pH regulation, protecting hyphae against free radicals, and may in some cases act as one type of electron carrier potentially capable of transporting electrons from the intracellular NADH pool to the extracellular Fenton reaction.

The research described here contributes to the understanding of brown rot degradative mechanisms and to an enhanced understanding of the biochemistry and physiology of the brown rot fungus *G. trabeum*.

ACKNOWLEDGEMENTS

I would like to express my sincere appreciation to my advisor, Professor Jody Jellison, for all of her support, encouragement, and trust. The sharing of her vision and experiences has been a lifetime treasure for me. My special thanks also go to Professor Jellison for her critical reading and correction of the thesis.

I must thank my advisory committee, Professor Goodell, Professor Annis, Professor Tavantzis and Professor Cole for their time, suggestions and encouragement.

I appreciate the help and friendship from my laboratory members, Dr. Andrea Ostrofsky, Dr. Claudia Jasalavich, Dr. Jon Connolly, Kerey Fuller and Jonathan Schilling. I gratefully acknowledge their creating a pleasant working atmosphere. Especially, I thank Dr. Andrea Ostrofsky for her critical reading of the manuscript.

My sincere thanks are due to Dr. Dilip Lakshman in Professor Tavantzis's lab, Dr. Farahad Dastoor in Professor Annis's lab and the visiting scholar Dr. Masaya Nakamura in Professor Goodell's lab for their shared wisdom and techniques.

I would like to thank Ms. Jean Ketch, Ms. Phyllis Brooks, Ms. Donna Pond, Ms. Doreen Turner, Ms. Roseann Cochrane, and Ms. Alma Homola, for their secretarial help.

I received valuable help and support from many other persons at University of Maine and wish to express my thanks to all of them.

I am deeply in debt to my family and friends for their love and patience.

For the research work reported in Chapter 2, I thank Dr. Barry Goodell, Dr. Andrea Ostrofsky and Dr. Jon Connolly for giving helpful background information. The technical assistance of Gang Xu on HPLC analysis is gratefully acknowledged. I also

appreciate the helpful discussion with Yong Shao, and Okuy Lee. This work was made possible by the support from the Maine Agriculture and Forest Experiment Station and USDA grant #96-34-158-13003.

For the research work reported in Chapter 4, I thank Dr. Kenneth Jensen at U.S. Department of Agriculture Forest Products Laboratory, and Dr. Andrzej Paszczynski at University of Idaho for technical advice on shallow basal media liquid cultures. I thank Dr. Claudia Jasalavich, Dr. Farahad Dastoor and Dr. Masaya Nakamura for technical advices on protein purification.

For the research work reported in Chapter 5, I thank Dr. Seanna Annis for suggestions on membrane isolation, and Dr. Dilip Lakshman for technical advice. I also would like to thank Kelley Edwards for his assistance in utilizing the transmission electron microscope. This work was made possible by the support from the Maine Agricultural and Forest Experiment Station, USDA-WUR grant program and University of Maine AGS grant.

TABLE OF CONTENTS

ACKNOWLEDGEMENTS	ii
LIST OF TABLES	x
LIST OF FIGURES	xi

Chapter

1. INTRODUCTION AND LITERATURE REVIEW.....	1
Wood Biodegradation	1
Mechanisms of Wood Biodegradation	4
Mechanisms of White Rot	4
Proposed Mechanisms of Brown Rot	5
Cellobiose Dehydrogenase – Driven Fenton Reaction	5
Oxalic Acid – Driven Fenton Reaction	7
Glycopeptide Ferrous Iron Chelator – Driven Fenton Reaction	8
Phenolate Biochelator – Driven Fenton Reaction	9
Biochelators and Laccase Mediator Systems	14
Dissertation Overview	15
Metabolite Production	16
Plasma Membrane Redox System and Intracellular Quinone – Reducing Enzymes	17
Membrane Isolation	19

Importance of the Projects.....	20
2. MODIFICATION OF THE GROWTH ENVIRONMENT BY WOOD	
INHABITING FUNGI	21
Abstract	21
Introduction	22
Materials and Methods	25
Organisms and Culture Conditions	25
Decay Test	25
Chelator Production by Different Fungi	26
Chelator Production Versus Iron Concentration	29
Modification of the Liquid Media Environment by Fungi	29
Results	31
Decay Test	31
Characterization of Chelator Production by Different Fungi	33
Chelator Production Versus Iron Concentration	42
Modification of the Liquid Media Environment	44
pH Change	44
Change of Extracellular Protein Concentration	45
Biochelator Production	45
Cellobiose Dehydrogenase Activity	47
Quinone Reducing Activity	48
Discussion	50

3. PROPERTIES OF A TRANSPLASMA MEMBRANE REDOX SYSTEM OF THE BROWN ROT FUNGUS <i>GLOEOPHYLLUM TRABEUM</i>	58
Abstract	58
Introduction	59
Materials and Methods	61
Organism and Culture Conditions	61
Collection of Mycelia Mass	62
Determine Mycelial Wet Weight Versus Dry Weight	62
Ferricyanide Reduction	62
Inhibition of Ferricyanide Reduction	62
Effects of Buffers on Ferricyanide Reduction	63
Effect of pH on Ferricyanide Reduction	63
Quinone Reduction by Intact Hyphae or Lysed Hyphae	63
Effect of pH on Quinone Reduction by Intact Hyphae	64
Quinone Reduction by the Culture Filtrate	64
Preparation of Intracellular Enzyme Extract	64
Quinone Reduction by the Intracellular Enzyme Extract	65
Effect of pH on Quinone Reduction by the Intracellular Enzyme Extract	65
Protein Concentration	65
Results	66
Discussion	74

4. PURIFICATION AND CHARACTERIZATION OF AN INTRACELLULAR 1,4-BENZOQUINONE REDUCTASE FROM THE BROWN ROT BASIDIOMYCETE <i>GLOEOPHYLLUM TRABEUM</i>	80
Abstract	80
Introduction	81
Materials and Methods	84
Organism and Culture Conditions	84
Enzyme Extraction.....	85
Enzyme Purification	86
Ammonium Sulfate Precipitation	86
Hydrophobic Interaction	86
Ion Exchange	87
Dye Ligand Affinity	87
Standard Enzyme Assays	87
Protein Measurements	88
Gel Filtration	88
Electrophoresis	89
Flavin Identification	89
Steady – State Kinetics Measurements	90
Stoichiometry of 2,6-DMBQ Reduction	90
Temperature and pH Dependency of the Purified Enzyme	91
Inhibition of the Purified Enzyme	91
Results	92

Induction and Production of Intracellular Quinone Reductases	92
Purification of Quinone Reductase	94
Physical Properties	100
Catalytic Properties	104
pH and Temperature Dependency	108
Inhibition of Quinone Reductase	110
Discussion	113
5. ISOLATION AND CHARACTERIZATION OF PLASMA MEMBRANES FROM THE WOOD DECAY FUNGUS <i>PHANEROCHAETE</i> <i>CHRYSOSPORIUM</i>	122
Abstract	122
Introduction	122
Materials and Methods	125
Organism and Culture Conditions	125
Cell Collection	125
Cell Lysis	126
Plasma Membrane Isolation	126
Protein Determination	127
Enzyme Assays	127
Transmission Electron Microscope Observation	127
Effects of pH on ATPase Activities of Isolated Membrane Fractions.....	128
Results	128

Discussion	132
6. CONCLUSIONS	135
REFERENCES	148
APPENDICES	
Appendix A. Highley's Liquid Media	167
Appendix B. Basal Media	168
Appendix C. Lineweaver – Burk Plots Determining Kinetic Constants.....	170
Appendix D. HPLC Analysis of Biochelator Fractions	174
BIOGRAPHY OF THE AUTHOR	179

LIST OF TABLES

2.1	Fungal growth and biochelator production in the modified Highley's media34	34
2.2	The increase in the absorbance caused by each biochelator fraction after 24 hours in the Ferrozine assay*. The absorbance increase indicates iron reduction is occurring. The increase in the absorbance caused by water control was 0.0138	38
2.3	Biochelator production by <i>Fomitopsis pinicola</i> versus iron concentration in 200ml Highley's liquid media with 1% glucose as the carbon source. Data represents averages of three replicates.....43	43
3.1	Effect of nitrogen deficiency on ferricyanide reduction and growth of <i>G. trabeum</i>66	66
3.2	Effect of inhibitors on ferricyanide reduction rates by <i>G. trabeum</i> . The ratio of inhibitor / mycelia is 100 nmol/mg70	70
3.3	Effect of buffers on ferricyanide reduction and proton excretion by the plasma membrane redox system in <i>G. trabeum</i>70	70
3.4	Reduction of 1,4-benzoquinone by the culture filtrate, hyphae, and intracellular enzyme extract of <i>G. trabeum</i> grown in the shallow basal media71	71
4.1	The effects of inducers, nitrogen levels, and temperatures on intracellular quinone reductase activity in <i>G. trabeum</i>92	92
4.2	Purification of the intracellular quinone reductase from <i>G. trabeum</i> grown in nitrogen limited liquid media95	95
4.3	Determination of the nature of the enzyme-bound flavin by the pH dependency of the fluorescence104	104
4.4	Kinetic constants ^a for the quinone reductase from <i>G. trabeum</i>105	105
4.5	Relative efficiencies of electron acceptors in the quinone reductase reaction106	106
4.6	Enzyme activity levels in the presence of potential quinone reductase inhibitors110	110
5.1	Protein concentration and ATPase activities of membrane fractions from a 24-hour culture of <i>Phanerochaete chrysosporium</i>130	130

LIST OF FIGURES

- 1.1 Generation of extracellular ferrous iron and hydrogen peroxide by *Coniophora puteana* in the proposed cellobiose dehydrogenase -driven Fenton reaction (Schimidhalter and Canevascini, 1993 (a) and (b); Hyde and Wood, 1997; Cameron and Aust, 1999). Cellobiose dehydrogenase also has cellobiose dependent quinone-reducing activity7
- 1.2 The hypothetical role of oxalic acid in oxalic acid - driven Fenton reaction (Schmidt et al., 1981; Shimada et al., 1997)8
- 1.3 Generation of ferrous iron and hydrogen peroxide by *Gloeophyllum trabeum* in the proposed glycopeptide iron chelator - driven Fenton reaction (Enoki et al., 1997)9
- 1.4 Proposed pathways for generation of ferrous iron and hydrogen peroxide extracellularly by *Gloeophyllum trabeum* in the phenolate biochelator - driven Fenton chemistry (Mineralization pathway: Goodell et al., 1997 (a) and (b), 2001; Pracht et al., 2001; Quinone redox cycle and quinone reducing enzymes: Kerem et al., 1999; Paszczynski, et al., 1999; Jensen et al., 2001).
4,5-DMC, 4,5-dimethoxy-1,2-benzenediol.
2,5-DMHQ, 2,5-dimethoxy-1,4-benzenediol.13
- 2.1 Weight loss of spruce blocks caused by the white rot fungus *Phanerochaete chrysosporium* (P), the brown rot fungus *Gloeophyllum trabeum* (G) and the non-decay fungus *Trichoderma viride* (T) in the soil-jar decay test. "C", the control jars. Data represent the averages of triplicate samples. At the end of 16th week, *T. viride* did not caused significant weight loss, while *G. trabeum* and *P. chrysosporium* caused significant weight loss compared with the control treatment (T-test with P<0.05). Major weight loss caused by *G. trabeum* occurred within the first month, while major weight loss caused by *P. chrysosporium* occurred after the first month32

- 2.2 (A) The distribution of phenolate / mixed phenolate derivative compounds in different purification fractions. The biochelators were collected from 1L of fungal culture grown in modified Highley's liquid media with 0.2% glucose and 1% cellulose as the carbon source. The amount of phenolate or mixed phenolate derivative compounds in some fractions from some fungi was too low to be shown clearly in the graph. Data are averages and standard deviations from triplicate samples. "B", the brown rot fungi. B1, *Fomitopsis pinicola*. B2, *Gloeophyllum trabeum*. B3, *Postia placenta*. "W", the white rot fungi. W1, *Trichaptum abietinum*. W2, *Phanerochaete chrysosporium*. W3, *Trametes versicolor*. "N", the non-decay fungi. N1, *Phialocephala fusca*. N2, *Phialophora mutabilis*. N3, *Trichoderma viride*. The amount of phenolate derivative compounds was expressed as the amount of 2,3-dihydroxybenzoic acid. The amount of hydroxamic acid derivative compounds was expressed as the amount of hydroxylamine35
- 2.2 (B) The distribution of hydroxamic acid derivative compounds in different compounds in different purification fractions. The biochelators were collected from 1L of fungal culture grown in modified Highley's liquid media with 0.2% glucose and 1% cellulose as the carbon source. The amount of phenolate or mixed phenolate derivative compounds in some fractions from some fungi was too low to be shown clearly in the graph. Data are averages and standard deviations from triplicate samples. "B", the brown rot fungi. B1, *Fomitopsis pinicola*. B2, *Gloeophyllum trabeum*. B3, *Postia placenta*. "W", the white rot fungi. W1, *Trichaptum abietinum*. W2, *Phanerochaete chrysosporium*. W3, *Trametes versicolor*. "N", the non-decay fungi. N1, *Phialocephala fusca*. N2, *Phialophora mutabilis*. N3, *Trichoderma viride*. The amount of phenolate derivative compounds was expressed as the amount of 2,3-dihydroxybenzoic acid. The amount of hydroxamic acid derivative compounds was expressed as the amount of hydroxylamine36
- 2.3 Ferrozine assays on fungal culture filtrates. Culture filtrates from the brown rot fungi and the non-decay fungi displayed higher iron - reducing ability than those from the white rot fungi. Culture filtrate from the brown rot fungus *Fomitopsis pinicola* showed the highest iron - reducing ability. The ferrozine assay for the culture filtrate of each fungus was carried out in the presence of 30 μM FeIII with 2.5 mM ferrozine reagent in pH 4.5 acetate buffer. The concentration of low molecular weight compounds was 30 μM as determined by the Arnow test and was expressed as the concentration of 2,3-dihydroxybenzoic acid. The total reaction volume was 3 mL. The exception was fungus *Phanerochaete chrysosporium*. Because its production of phenolate derivative compounds could not be detected by the Arnow test, the amount of low molecular weight compounds added into the reaction system was unknown and less than 30 μM 39

- 2.4 Ferrozine assays on the ethyl acetate extracts from fungal culture filtrates. Ethyl acetate fractions mainly containing phenolate derivatives from the brown rot fungi and the non-decay fungi also displayed higher iron - reducing ability than those from the white rot fungi. The ethyl acetate fraction from the non-decay fungus *Phialocephala fusca* had the highest iron - reducing ability. The ethyl acetate fractions from the brown rot fungus *Fomitopsis pinicola* and the non-decay fungi *Trichoderma viride* and *Phialophora mutabilis* displayed similar iron - reducing ability when standardized based upon uniform phenol content, and ranked 2nd. The ferrozine assay for the ethyl acetate extraction of each fungus was carried out in the presence of 30 μ M FeIII with 2.5 mM ferrozine reagent in pH 4.5 acetate buffer. The total reaction volume was 3 mL. For *F. pinicola*, *Gloeophyllum trabeum* and all the non-decay fungi, the concentration of low molecular weight compounds was 30 μ M phenolate derivative compounds. For *Postia placenta* and all the white rot fungi, the amount of low molecular weight compounds added into the reaction system was estimated due to the low initial concentration40
- 2.5 Ferrozine assays on the aqueous residuals of fungal culture filtrates after ethyl acetate extraction. Aqueous residuals from the brown rot fungi and the non-decay fungi also displayed higher iron - reducing ability than those from the white rot fungi. The aqueous residual from the brown rot fungus *Fomitopsis pinicola* showed the highest iron - reducing ability. The ferrozine assay for the aqueous residual of each fungus was carried out in the presence of 30 μ M FeIII with 2.5 mM ferrozine reagent in pH 4.5 acetate buffer. The concentration of low molecular weight compounds was 30 μ M phenolate derivative compounds. The total volume of each reaction system was 3 mL. The exception was *Phanerochaete chrysosporium*. Because its production of phenolate derivative compounds could not be detected by Arnow test, the amount of low molecular weight compound added into the reaction system was unknown41
- 2.6 Changes of modified Highley's liquid media by fungal metabolites of a white rot, a brown rot and a non-decay fungus with time. "P", the white rot fungus *Phanerochaete chrysosporium*. "T", the nondecay fungus *Trichoderma viride*. "G", the brown rot fungus *Gloeophyllum trabeum*. "W", the week. Cellobiose dehydrogenase activity was monitored by using two different electron acceptors, 2,6-Dichloroindophenol (DCPIP) and 2,3-dimethoxy-5-methyl-1,4-benzoquinone. 1 U = 1 μ mol/min. The values shown were the averages and the standard deviations of triplicate samples49

- 3.1 The Reduction of ferricyanide by *G. trabeum* mycelia (A) at different reaction times, (B) at different amounts of mycelial mass, and (C) at different concentrations of ferricyanide. The reduction was linear when the reaction time was within 5 minutes, the ferricyanide concentration was up to 20 mM and when the mycelial mass was up to 120 mg. (A) 89.5 +/- 1.5 mg (dry weight) washed mycelia were used for each reaction. $R^2 = 0.9959$. (B) Indicated amounts of washed mycelia (mg dry weight) were used for each reaction. $R^2 = 0.9267$. (C) 97 +/- 3 mg (dry weight) washed mycelia were used for each reaction. (D) The plot of the wet weight versus the dry weight of *G. trabeum* mycelia. The mycelia were dried by lyophilization. $R^2 = 0.9961$ 68
- 3.2 Effect of pH on ferricyanide reduction by *G. trabeum* mycelia. The reduction rate increased with pH above pH 5. 97 +/- 3 mg (dry weight) washed mycelia were used for each reaction69
- 3.3 Effect of 1,4-benzoquinone concentrations on quinone reduction by *G. trabeum* intracellular enzyme extract (A) and *G. trabeum* mycelia (B). (A) The enzyme activity was based on nmole of NADH oxidized per mg of intracellular protein. In the Lineweave - Burk plot, $R^2 = 0.9984$, $V_{max} = 863 \mu\text{M}/\text{min}$ and $K_m = 156 \mu\text{M}$. (B) The assay was performed with 30 +/- 1 mg (dry weight) washed mycelia. The reduction rates were based on nmole of 1,4 -benzoquinone reduced per mg dry weight of mycelia. In the Lineweaver -Burk plot, $R^2 = 0.9964$, $K_m = 59 \mu\text{M}$, $V_{max} = 17.5 \text{ nmol}/\text{min}/\text{mg}$ 72
- 3.4 Effect of pH on 1,4-benzoquinone reduction by *G. trabeum* mycelia and the intracellular enzyme extract. The reduction was measured with 27 +/- 3 mg (dry weight) mycelia or 0.1 mL of enzyme extract in the 200 mM potassium phosphate buffer at indicated pH, with 100 mM 1,4 - benzoquinone. Reduction rates of washed mycelia were based on nmol of 1,4 - benzoquinone reduced per mg dry weight mycelia. Specific activities of enzyme extracts were based on nmol of NADH oxidized per mg intracellular protein73
- 4.1 Induction of intracellular quinone reductase activity by 2,6-DMBQ in low nitrogen media at 30 °C. The inducer, 2,6-DMBQ was added 3 days after the inoculation. The enzyme specific activity reached the maximum (11.966 U/mg) 3 days after the addition of 2,6-DMBQ, and 6 days after the inoculation94

- 4.2 SDS-PAGE of the protein profiles from *G. trabeum*. The purified enzyme is shown in lane 5. Lanes 1 and 10, molecular weight marker; lane 2, crude intracellular enzyme extract; lane 3, after CL-4B hydrophobic interaction; lane 4, after Q Sepharose Fast Flow ion-exchange; lane 5, after Cibacron Blue 3GA agarose, which is the purified product; lanes 6 and 7, other protein fractions after the hydrophobic interaction column showing low level of quinone - reducing activities; lanes 8 and 9, other ion-exchange eluted fractions. Protein standards (2 μg of each), chromatography fractions (10 μg of each) and the purified quinone reductase (0.5 μg) were loaded. The experiment was performed with a 0.75 mm 15% polyacrylamide gel (16 \times 18 cm) subjected to the constant voltage (200 V) for 2 hours. The gel was stained with Coomassie Blue. The photo was taken by the ChemImager low light digital imaging system.....96
- 4.3 Phenyl Sepharose CL-4B hydrophobic interaction affinity chromatography of the quinone reductase from *G. trabeum*. The first, second and third activity peak corresponds to lane 6, 3, and 7 of figure 4.2, respectively. The sample was eluted with a step reverse ammonium sulfate gradient and a step reverse sodium phosphate gradient. 0-20 mL, 0.5 M ammonium sulfate in 50 mM sodium phosphate buffer (pH 7.0); 21-40 mL, 50 mM sodium phosphate buffer (pH 7.0); 41-60 mL, 4 mM sodium phosphate buffer (pH 7.0); 61-80 mL, water97
- 4.4 Q Sepharose Fast Flow ion-exchange chromatography of the quinone reductase from *G. trabeum*. The sample was eluted with a linear gradient of NaCl. 0-8 mL, equilibrium buffer (20 mM pH 5.2 piperazine buffer); 9-40 mL, the linear gradient (0 to 0.8 M) of sodium chloride in 20 mM piperazine buffer (pH 5.2).....98
- 4.5 Cibacron Blue 3GA agarose dye ligand affinity chromatography of the quinone reductase from *G. trabeum*. 0-8 mL: 10 mM sodium phosphate buffer containing 5 mM MgSO_4 ; 9-25 mL: 10 mM sodium phosphate buffer containing 5 mM MgSO_4 and 0.5 mM NADH. Both the eluted protein and the NADH in elution buffer contributed to the high absorbance at 280 nm99
- 4.6 The molecular weight of the quinone reductase (●) determined by the gel filtration chromatography is 66 KD. The molecular weight standards (○) were bovine serum albumin (66 KD), ovalbumin (45 KD), and carbonic anhydrase (29 KD). The sample (1 mL) which contained 2 mg/mL of each protein standard and 0.5 mg/mL quinone reductase was loaded, and was eluted with gel filtration buffer at 0.37 mL/min flow rate100

- 4.7 (A) Purity confirmation of the quinone reductase by the SDS- PAGE. Lanes 2, 3, and 4, Blue agarose fraction (the purified enzyme) from different purification batches; lane 5, blue agarose fraction recovered from the gel filtration experiment and concentrated by centrifugal filtration; lanes 1 and 6; molecular weight standards, bovine serum albumin (66 KD), ovalbumin (45 KD), carbonic anhydrase (29 KD) and α -lactalbumin (14.2 KD). Protein standards (2 μ g of each) and 0.5 μ g of the purified quinone reductase were loaded. The experiment was performed with a 0.75 mm 15% polyacrylamide gel (16 \times 18 cm) subjected to the constant voltage (200 V) for 2 hours. The gel was stained with Coomassie Blue. The photo was taken with the Chemilmager digital imaging system. (B) Subunit molecular weight of the quinone reductase (\bullet) was 22 KD, determined by SDS-PAGE. The molecular weight standards (\circ) were as listed in (A)101
- 4.8 (A)The quinone reductase (\bullet) displayed a pI value of 4.2 determined by the isoelectric focusing with pI markers (\circ): Amyloglucosidase (3.6), Glucose oxidase (4.2), Trypsin Inhibitor (4.6), β -Lactoglobulin A (5.1), Carbonic anhydrase II (5.4 and 5.9), Carbonic anhydrase (6.6). (B) Purity confirmation of the quinone reductase by the native polyacrylamide gel isoelectric focusing. Protein standards (6 μ g of each) and the purified quinone reductase (1.5 μ g) were loaded. The experiment was performed with a 5% T, 3.3% C polyacrylamide gel (16 \times 18 cm) subjected to the constant voltage (200 V for 1.5 hours, followed by 400 V for 1.5 hours). The proteins were visualized with Coomassie Blue followed by silver stain. The photo was taken with the Chemilmager low light digital imaging system102
- 4.9 Wavelength scan of the native oxidized *G. trabeum* quinone reductase and NADH reduced enzyme. The oxidized enzyme showed maximum absorbance at 375 nm and 450 nm, which is a typical flavin spectrum.....103
- 4.10 The stoichiometry of the quinone reductase catalyzed reduction of 2,6-DMBQ. (A) Reduction of 100 μ M 2,6-DMBQ was monitored in the presence of indicated concentration of NADH. 4 μ g enzyme was used for each assay. (B) The stoichiometry of NADH added versus 2,6-DMBQ reduction. The plot of the moles of 2,6-DMBQ reduced versus the moles of NADH added (0, 50, 100, and 150 μ M) has a slope of 1. The concentration of 2,6-DMBQ reduced was calculated using the Beer-Lambert equation: $Abs = ECl$, in which Abs is the absorbance at 390nm, E is the extinction coefficient (see materials and methods), l is the cuvette pathlength (1cm in this study). The total volume of the reaction system was 1mL. Based on the concentration and the volume, the amount of 2,6-DMBQ reduced could be obtained107

- 4.11 The optimum reaction pH for the quinone reductase from *G. trabeum* is between 5.5 to 7. The effect of pH on activity was measured with sodium citrate-citric acid buffer (pH 3 to 6.3) and sodium phosphate buffer (pH6.5 to 8). Data represents the average and standard deviation of 5 samples108
- 4.12 (A) The optimum reaction temperature for the quinone reductase from *G. trabeum* is between 24 to 40 °C. Data represents the average and standard deviation of 5 samples. (B) The activation energy for the oxidation of NADH was 43.7 kJ/mol calculated by the Arrhenius plot. It was based on the Arrhenius equation: $k=Ae^{-E_a/RT}$, in which A is Arrhenius constant, k is the rate constant ($k=V/[substrate]$), E_a is the activation energy, R is the gas constant (8.317J/Kelvin.mol), T is the temperature in Kelvin degree (°K, °K = °C+273.15). Since [substrate] is constant during the initial rate period, the equation can be written as $V=[substrate] Ae^{-E_a/RT}$ or $\ln V=\ln A[substrate]-E_a/RT$. Consequently the slope of a plot of $\ln V$ versus $1/T$ gives $-E_a/R$ 109
- 4.13 Inhibition of *G. trabeum* quinone reductase by cibacron blue (A) and dicumarol (C). Experiments were carried out in triplicate. (A) Oxidization of NADH (6.25 to 100 µM) was monitored in the presence of 12.5 µM 2,6-DMBQ and Cibacron blue 3GA (0.25, 0.5 and 1 µM). (B) The replot of slope versus Cibacron blue 3GA concentration indicates the K_i value as 0.2 µM. (C) Oxidization of NADH (6.25 to 100 µM) was monitored in the presence of 12.5 µM 2,6-DMBQ and Dicumol (1, 2, and 4 µM). (D) The replot of slope versus Dicumol indicates the K_i value as 0.5 µM111
- 4.14 Enzyme inhibition at 25 µM NADH was observed in the steady state kinetic analysis of *G. trabeum* quinone reductase. 2,6-DMBQ concentrations ranged from 6.25 to 25 µM. Experiments were carried out with triplicate samples112
- 5.1 Phase contrast photograph of hyphae and spores of *P. chrysosporium* after the treatment of snail digestive enzyme (β - glucuronidase type H-1, EC 3.2.1.31, 200 mg were used for 2 g of cells), taken under the Leitz Laborlux S microscope. Swelling spores and hyphae can be observed. Magnification: $\times 800$. The fungal conidia and hyphae (2 g) from MEA plates were inoculated in MEA liquid media (200 mL), grown for 24 hours on Thermolyne type 72000 orbital shaker (200 rpm, room temperature), and were collected by vacuum filtration through Whatman 2 filter paper. Enzyme treatment was performed under 37 °C for 6 hours in 20 mL of 50mM sodium phosphate buffer (pH 6.5, with 5 mM EDTA and 0.59 M sucrose) (Bowman and Slayman, 1981).....129

- 5.2 (A). The effect of pH on ATPase activity of the membrane fraction mem-1 from *Phanerochaete chrysosporium*. The optimum pH 6.7 was similar to the reported optimum pH of plasma membrane ATPase (pH 6.8). (B). The effect of pH on ATPase activity of the membrane fraction mito-2. The optimum pH 8.2 was the same as the reported optimum pH of mitochondrial membrane ATPase131
- 5.3 *Phanerochaete chrysosporium* membrane fraction mem-1 was negatively stained with 1% phosphotungstate acid and observed by transmission electron microscope Philips EM201. Magnification: × 45K. The round/irregular structures lighter in color were membrane fragments132
- C.1. Lineweaver_Burk plot of NADH oxidization by the *G. trabeum* quinone reductase170
- C.2. Lineweaver_Burk plot of 1,4-benzoquinone reduction by the *G. trabeum* quinone reductase170
- C.3. Lineweaver_Burk plot of 2,5-dimethoxy-1,4-benzoquinone reduction by the *G. trabeum* quinone reductase171
- C.4. Lineweaver_Burk plot of 2,6-dimethoxy-1,4-benzoquinone reduction by the *G. trabeum* quinone reductase171
- C.5. Lineweaver_Burk plot of 2,3-dimethoxy-5-methyl-1,4-benzoquinone reduction by the *G. trabeum* quinone reductase172
- C.6. Lineweaver_Burk plot of potassium ferricyanide reduction by the *G. trabeum* quinone reductase172
- C.7. Lineweaver_Burk plot of 2,6-dichloro-indophenol reduction by the *G. trabeum* quinone reductase173
- D.1. HPLC analysis of the culture filtrate from *G. trabeum* at 275.4, 244.5 and 311.9 nm, where the characteristic absorbance peaks of DHBA are expected174
- D.2. HPLC analysis of the ethyl acetate extract from the *G. trabeum* culture filtrate at 275.4, 244.5 and 311.9 nm, where the characteristic absorbance peaks of DHBA are expected175
- D.3. HPLC analysis of the aqueous residual from the *G. trabeum* culture filtrate at 275.4, 244.5 and 311.9 nm, where the characteristic absorbance peaks of DHBA are expected176
- D.4. HPLC analysis of the ethyl acetate extract from the *P. chrysosporium* culture filtrate at 275.4, 244.5 and 311.9 nm, where the characteristic absorbance peaks of DHBA are expected177

- D.5. HPLC analysis of the aqueous residual from the *P. chrysosporium*
Culture filtrate at 275.4, 244.5 and 311.9 nm, where the characteristic absorbance
peaks of DHBA are expected178

Chapter 1

INTRODUCTION AND LITERATURE REVIEW

Wood Biodegradation

Fungi are the major agents responsible for wood biodegradation. Different types of decay are recognized based on the way fungi attack cellulose, hemicellulose, and lignin (Zabel and Morrell, 1992; Eaton, 2000). White rot fungi attack all the cell wall components gradually and leave the wood bleached in color. The fungal hyphae are relatively prolific in the wood cell lumina. The wood cell wall close to the hyphae is eroded first (Eaton, 2000). The wood cell wall that is not in direct contact with fungal hyphae also becomes thinner and more porous (Blanchette, 1994). White rot fungi that will be considered in this work are: *Phanerochaete chrysosporium* Burdsall, *Trametes versicolor* (Linnaeus : Fries) Pilat, *Trichaptum abietinum* (Dickson : Fries) Ryvardeen, *Phlebia brevispora* Nakasone, and *Irpex lacteus* Fries.

Brown rot fungi depolymerize the polysaccharides rapidly. The wood exhibits a darkened color due to the preferential (although not exclusive) utilization of polysaccharides versus lignin. Typically, in laboratory soil block assays, wood blocks may be completely covered with fungal hyphae and fungi are well developed with the wood cell as well. However, it has been reported that, compared with wood degraded by white rot fungi, in the wood degraded by brown rot fungi the fungal hyphae are relatively sparse in the wood cell lumina (Jones and Worrall, 1993 and 1995; Eaton, 2000). Decay is highly diffused (Eaton, 2000). Brown rot fungi that will be considered in this work are: *Gloeophyllum trabeum* (Persoon : Fries) Karsten, *Gloeophyllum striatum* (Swartz : Fries)

Murrill, *Gloeophyllum sepiarium* (Wulfen : Fries) Imazeki, *Postia placenta* (Fries) Larsen et Lombard, *Fomitopsis pinicola* (Swartz : Fries) Karsten, *Coniophora puteana* (Fries) Karsten, *Neolentinus lepideus* (Fries : Fries) Redhead et Ginns, and *Tyromyces palustris* (Berkeley et Curtis) Murrill.

There is also a group of wood-inhabiting non-decay fungi such as mold and stain fungi. They can colonize wood but do not cause significant wood degradation. Wood-inhabiting non-decay fungi that will be considered in this work are: *Trichoderma viride* Persoon : Fries, *Trichoderma reesei* Simmons, *Trichoderma virens* (Miller et al.) von Arx, *Phialocephala fusca* Kendrick, *Phialophora mutabilis* (van Betma) Schol – Schwarz, *Aureobasidium pullulans* (de Bary) Arnaud, and *Sclerophoma pityophila* Funk.

Brown rot fungi form an important group of organisms. They cause the most destructive type of decay in wood structures. The damage costs billions of dollars annually in the United States (Zabel and Morrell, 1992; Paszczynski et al., 1999). They are also essential contributors to biomass recycling and soil fertility in forest ecosystems. Cellulose is the most abundant natural polymer in the world (Sjostrom, 1993). Biodegradation of cellulose is an important step in the global carbon cycle (Kirk, 1987; Kerem et al., 1999). Translocation of metal elements by brown rot fungi can impact forest floor heterogeneity (Jellison et al., 1993; Connolly et al., 1996; Connolly and Jellison, 1995 and 1997).

The cellulolytic systems of brown rot fungi can also play a role in the bioremediation of pollutants. The brown rot fungus *G. trabeum* has been found to degrade polyethylene oxide (PEO) efficiently via one electron oxidation. This organic compound cannot be degraded by white rot basidiomycetes that can depolymerize

ligninocellulose and many other organic chemicals via the free radical based enzymatic combustion system (Kerem et al., 1998). The brown rot fungus *G. striatum* can degrade ciprofloxacin, an antibacterial drug that is not easily biodegraded due to its low water solubility and strong adsorption to the surrounding matrix. Analysis of the metabolites reveals the presence of oxidative decarboxylation or oxidation of the amine moiety, which indicates a hydroxyl radical-based degradation mechanism (Martens et al., 1996; Wetzstein et al., 1999). Both *G. trabeum* and *G. striatum* can degrade 2,4-dichlorophenol and pentachlorophenol (Fahr et al., 1999; Goodell et al., 2001). The characterization of the metabolites also suggests the involvement of one-electron oxidants, such as hydroxyl radicals (Fahr et al., 1999). Brown rot fungi also accumulate and translocate heavy metals from the surrounding environment (Doyle and Jellison, 1996; Fuller et al., 2000).

Some brown rot fungi may have potentially important impacts on the pulp and paper industry. When various species of *Gloeophyllum* are incubated with wood pulp, it has been found that the treated pulps show an incremental increase in brightness, although the degree of polymerization of cellulose also decreases substantially (Job-Cei et al., 1996). The endoglucanases from *G. trabeum* and *G. sepiarium* can efficiently deink xerographic and laser-printed papers (Guebitz et al., 1998). Short-time pinewood chip incubation with *G. trabeum* results in a 40% decrease of energy consumption during thermo-mechanical pulping and in improved fiberboard (Unbehaun et al., 2000). Qian and Goodell (Goodell et al., 2001) have shown that removal of ink in recycling processes can be enhanced by the catechol mediated Fenton reaction.

Better understanding of brown rot mechanisms will help limit the destructive damage caused by these organisms and to broaden the application of brown rot cellulolytic systems in bio-remediation and bio-industry.

Mechanisms of Wood Biodegradation

Mechanisms of White Rot

Both enzymatic and non-enzymatic processes are involved in white rot decay, which is recognized as a free radical based enzymatic combustion (Keyser et al., 1978; Kirk, 1987; Kirk et al., 1986; Schoemaker et al., 1989; Eriksson et al., 1990; Aust, 1995; Cameron and Aust, 1999). White rot fungi produce both polysaccharide and lignin degrading enzymes. Extra-cellular ligninolytic enzymes such as lignin peroxidase, manganese peroxidase, and laccase are key components of the fungal ligninolytic system (Keyser et al., 1978; Erikson et al., 1990; Aust, 1995). Extracellular cellulases, such as endo-1,4- β -glucanase, exo-1,4- β -glucanase, and 1,4- β -glucosidase, are responsible for complete degradation of cellulose and hemicellulose (Schoemaker et al., 1989). The oxidative enzyme cellobiose dehydrogenase participates in both lignin and cellulose degradation. Highly reactive radicals are also produced enzymatically by the ligninolytic enzymes and by cellobiose dehydrogenase (Cameron and Aust, 1999). Free radicals oxidize the lignin, attack the cellulose microfibrils, and cause structural disruption, which facilitates the enzymatic decay process (Kirk, 1987; Aust, 1995; Cameron and Aust, 1999). The combination of enzymatic and non-enzymatic processes leads to gradual decomposition of both lignin and cellulose.

Proposed Mechanisms of Brown Rot

Mechanisms of brown rot decay are less well understood. Research has shown that brown rot fungi do not produce ligninolytic enzymes, such as lignin peroxidase and manganese peroxidase (Milstein et al., 1992; Freitag and Morrell, 1992), although some metabolism and modification of the lignin is observed. Brown rot fungi produce polysaccharide-degrading enzymes, such as endoglucanases, galactosidases and xylanases (Cotoras and Agosin, 1992; Ritschkoff et al., 1994; Green et al., 1995; Guebitz et al., 1998; Mansfield et al., 1998), but the enzymes are too large to penetrate intact wood cell walls (Flournoy et al., 1991). Brown rot decay is characterized by extensive changes in the wood cell wall structure and rapid strength loss. At initial decay stages, brown rot fungi decrease the degree of polymerization (DP) of cellulose rapidly from about 10^4 to 250; before measurable weight losses can be observed (Kirk et al., 1991). It has been suggested that brown rot fungi possess a non-enzymatic oxidative pathway (Highley, 1977 and 1987; Enoki et al., 1989; Ritschkoff, 1996).

Hydroxyl radicals have been proposed as causative agents in brown rot decay, and it has been established that brown rot decay is initiated as a non-enzymatic oxidative degradation process based on the Fenton reaction: $\text{H}_2\text{O}_2 + \text{Fe}^{2+} \rightarrow \text{Fe}^{3+} + \text{OH}^- + \text{HO}\cdot$ (Koenigs, 1974 and 1975; Kirk et al., 1991; Backa et al., 1992; Wood, 1993; Hirano et al., 1997). Multiple theories have been proposed to explain the generation of Fenton reagents (ferrous iron and hydrogen peroxide) by fungi and to elucidate the factors that mediate the Fenton reaction *in vivo*.

Cellobiose Dehydrogenase - Driven Fenton Reaction. A cellobiose dehydrogenase - driven Fenton reaction theory has been proposed by Hyde and Wood (1997). Cellobiose

dehydrogenase (CDH) is an extracellular cellobiose oxidase. It oxidizes cellobiose and other disaccharides by utilizing a large spectrum of electron acceptors, such as ferric iron, quinones and molecular oxygen. The enzyme is a flavohemoprotein produced by many cellulolytic fungi (Ayers et al., 1978; Dekker, 1980; Fahrnich and Irrgang, 1982; Coudray et al., 1982; Canevascini et al., 1991; Bao et al., 1993; Schou et al., 1993 and 1998; Fang et al., 1998; Dumonceaux et al., 1998; Temp and Eggert, 1999; Moukha et al., 1999; Subramaniam et al., 1999; Igarashi et al., 1999; Hallerg et al., 2000; Baminger et al., 2001). CDH has been identified and purified from the brown rot fungus *Coniophora puteana* (Schimidhalter and Canevascini, 1993 (a) and (b)). In the proposed theory (Figure 1.1), *C. puteana* CDH reduces iron to form ferrous iron - oxalate complexes. The complexes then react with hydrogen peroxide to generate hydroxyl radicals (Hyde and Wood, 1997). A difficulty with the theory is that so far, cellobiose dehydrogenase has not been found ubiquitously in brown rot fungi (Schimidhalter and Canevascini, 1993 (a) and (b)). The enzymatic ferric iron reduction rate is also very slow.

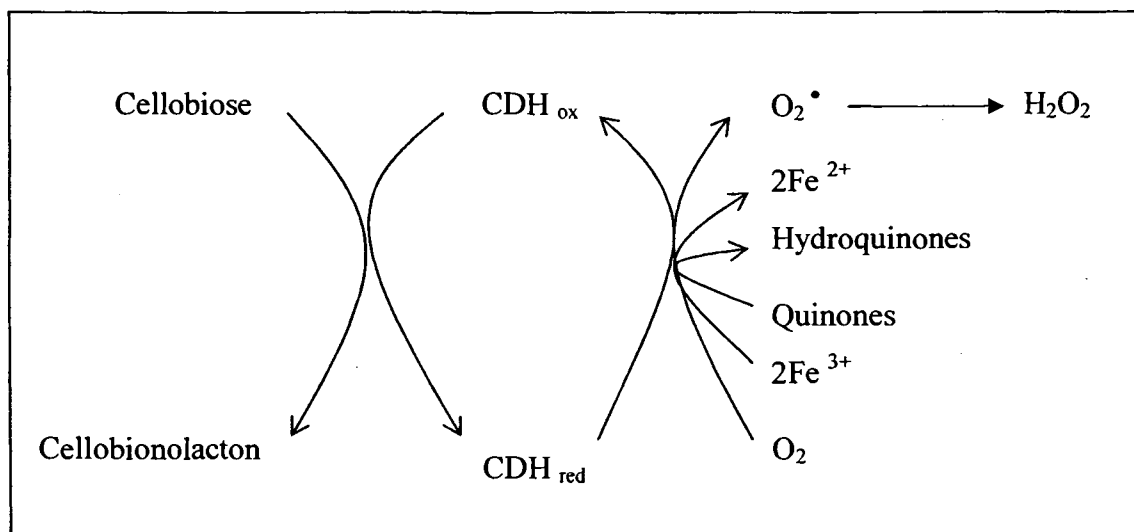


Figure 1.1. Generation of extracellular ferrous iron and hydrogen peroxide by *Coniophora puteana* in the proposed cellobiose dehydrogenase - driven Fenton reaction (Schimidhalter and Canevascini, 1993 (a) and (b); Hyde and Wood, 1997; Cameron and Aust, 1999). Cellobiose dehydrogenase also has cellobiose dependent quinone - reducing activity.

Oxalic Acid - Driven Fenton Reaction. Shimada (1997) has suggested an oxalic acid - driven Fenton reaction. In this model (Figure 1.2), oxalic acid serves as a diffusible metal chelator to reduce ferric iron to ferrous iron (Schmidt et al., 1981; Shimada et al., 1997). But the oxalate - driven ferric iron reduction has been found to be a very slow reaction in the dark. For rapid reduction, light irradiation, which does not exist inside wood cell walls, is necessary (Wood, 1993; Zuo and Hoigne, 1994).

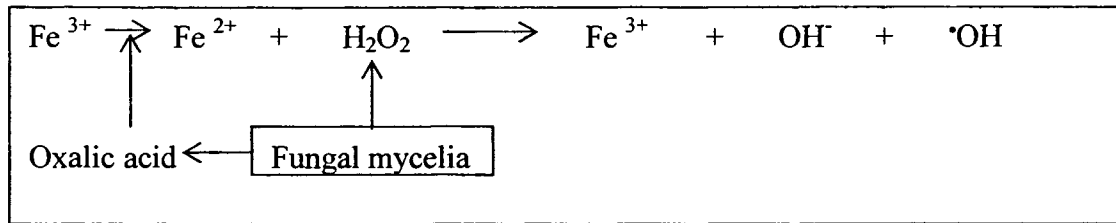


Figure 1.2. The hypothetical role of oxalic acid in oxalic acid - driven Fenton reaction (Schmidt et al., 1981; Shimada et al., 1997).

Glycopeptide Ferrous Iron Chelator - Driven Fenton Reaction. Enoki has proposed that extracellular glycopeptide ferrous iron chelators are produced by brown rot fungi to generate hydroxyl radicals via the Fenton reaction (Enoki et al., 1997). Glycopeptide ferrous iron chelators are extracellular substances with molecular weights between 1 and 12 KD and with single-electron oxidation activity. Such substances have been isolated from the brown rot fungi *G. trabeum* and *T. palustris* (Enoki et al., 1992; Hirano et al., 1995). In this one-electron oxidation system model, the extracellular glycopeptide chelators reduce ferric iron to ferrous iron and chelate the ferrous iron. The glycopeptide chelator - ferrous iron complexes then catalyze the redox reaction between molecular oxygen and unidentified electron donors to produce hydrogen peroxide. Then the glycopeptide chelator - ferrous iron complexes reduce hydrogen peroxide to produce hydroxyl radicals via the Fenton reaction (Figure 1.3). The validity of this proposed mechanism has not been established. When polyethylene glycol (PEG) was used as a model compound for cellulose, *Gloeophyllum trabeum* could not use the glycopeptide

ferrous iron chelators to establish an extracellular Fenton reaction that could cleave the PEG via one electron oxidation (Kerem et al., 1999).

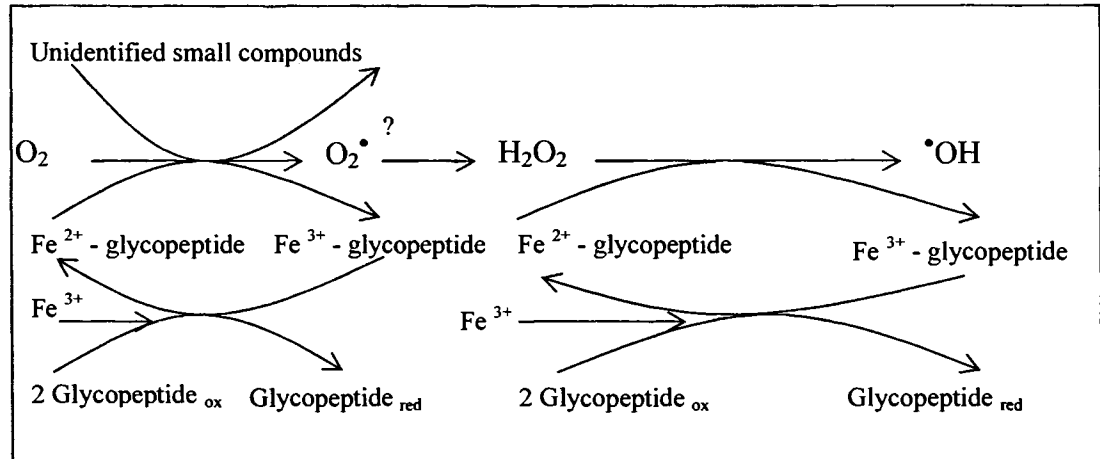


Figure 1.3. Generation of ferrous iron and hydrogen peroxide by *Gloeophyllum trabeum* in the proposed glycopeptide iron chelator - driven Fenton reaction (Enoki et al., 1997).

Phenolate Biochelator - Driven Fenton Reaction. Goodell, Jellison, and colleagues have proposed a phenolate biochelator - driven Fenton reaction (Jellison et al., 1990 (a) and (b), 1991 (a) and (b), 1993, 1996, 1997; Goodell et al., 1996, 1997 (a) and (b), 1999 (a) and (b), 2001; Goodell and Jellison, 1997, 1998 and 1999; Lu et al., 1994; Qian and Goodell, 1999). Both oxalate and phenolate biochelators with molecular weights lower than 1 KD produced by the brown rot fungi are implicated in brown rot decay (Goodell et al., 1996, 1997 (a) and (b), 1999 (a) and (b); Goodell and Jellison, 1997, 1998 and 1999). The oxalate is postulated to reduce pH, to solubilize ferric iron and to function as a pH dependent phase transfer agent. The oxalate could allow biochelators access to iron. Then biochelators reduce iron in an environment with a somewhat higher pH, where it is distant from the fungal mycelia. The phenolate biochelators can reduce ferric iron to

ferrous iron by one-electron oxidizations. The one-electron oxidized biochelators, which are semiquinones, are postulated to catalyze the reduction of ferric iron or molecular oxygen and to be further oxidized to quinones (Goodell et al., 1997 (a) and (b)).

Oxalate production by brown rot fungi and the function of oxalate in pH regulation have been studied (Green et al., 1995; Micales, 1995; Connolly and Jellison, 1995; Connolly et al., 1996). Biochelators are known to be produced by several white rot and brown rot fungi (Fekete et al., 1989). Phenolate biochelators have been isolated from the brown rot fungus *G. trabeum* grown in Highley's liquid media containing cellulose (Highley, 1973; Appendix A). The distribution of *G. trabeum* phenolate biochelators within the wood cell wall has been studied by immunolocalization. Their small size allows biochelators to penetrate microvoids in the wood cell wall that are too small for enzymes to enter (Jellison et al., 1991 (a)). The partially purified phenolate biochelators have been identified as hydroxylated phenylacetic acids, hydroxylated benzoic acids, hydroxylated benzene derivatives and dihydroxyphenyl pentanediol by GC/MS and HPLC/MS (Easwaran, 1994; Goodell et al., 1997 (a) and (b)).

Two other phenolate compounds, 4,5-dimethoxy-1,2-benzenediol (4,5-dimethoxy catechol, 4,5-DMC) and 2,5-dimethoxy-1,4- benzenediol (2,5-dimethoxy hydroquinone, 2,5-DMHQ), have also been isolated and identified from stationary cultures of *G. trabeum* grown in glucose mineral media (Appendix B, Tien and Kirk, 1988). These compounds can serve as iron chelating and reducing biochelators, and can participate in the reduction of oxygen to superoxide anion (Paszczynski et al., 1999). It has been found that 4,5-DMC and 2,5-DMHQ remain in the reduced hydroquinone form through out the fungal growth period. The presence of quinone reducing enzymes in *G. trabeum*, either

extracellular, membrane – bound, or intracellular, have been proposed to explain the production of phenolate compounds by *G. trabeum* (Paszczynski et al., 1999).

Another key metabolite, 2,5-dimethoxy-1,4-benzoquinone (2,5-DMBQ), is produced by *G. trabeum* grown in the glucose mineral media (Kerem et al., 1999). In the presence of this compound and ferric iron, *G. trabeum* mycelia reduced 2,5-DMBQ into 2,5-DMHQ. The direct non-enzymatic reaction between ferric iron and the hydroquinone may lead to both ferric iron reduction and hydrogen peroxide generation. The system can depolymerize the membrane impermeable PEG via one electron oxidization (Kerem et al., 1999).

Research has demonstrated that a single mole of *G. trabeum* phenolate chelator can reduce multiple moles of ferric iron (Goodell et al., 1996, 1997 (a) and (b), 2001). The non-stoichiometric reduction of iron has not been well elucidated. Two different theories, regeneration of biochelators and mineralization of biochelators, have been proposed (Figure 1.4) (Goodell et al., 1997 (a) and (b), 2001; Paszczynski et al., 1999; Kerem et al., 1999; Jensen et al., 2001; Pracht et al., 2001). Regeneration of biochelators via some kind of redox cycle was first suggested by Goodell and colleagues (1996, 1997 (a) and (b)). A quinone redox cycle mediated by quinone - reducing enzymes was suggested later (Paszczynski et al., 1999; Kerem et al., 1999). Recent work by Jensen and colleagues (2001) has shown that 4,5-dimethoxy-1,2-benzoquinone (4,5-DMBQ) can also be reduced to 4,5-DMC by a quinone redox cycle mediated by 2,5-DMHQ. Alternately, mineralization of phenolate biochelators by reducing multiple equivalents of ferric iron has been proposed by Goodell and colleagues (2001). Recent work by Pracht and colleagues (2001) has shown that catechols can be partially or completely mineralized to

CO₂ while reducing ferric iron continuously. Consequently, the catechol fungal biochelators may undergo a similar pathway of mineralization and lead to the non-stoichiometric reduction of iron (Goodell et al., 2001). The relative importance of these two pathways *in vivo* has not been established.

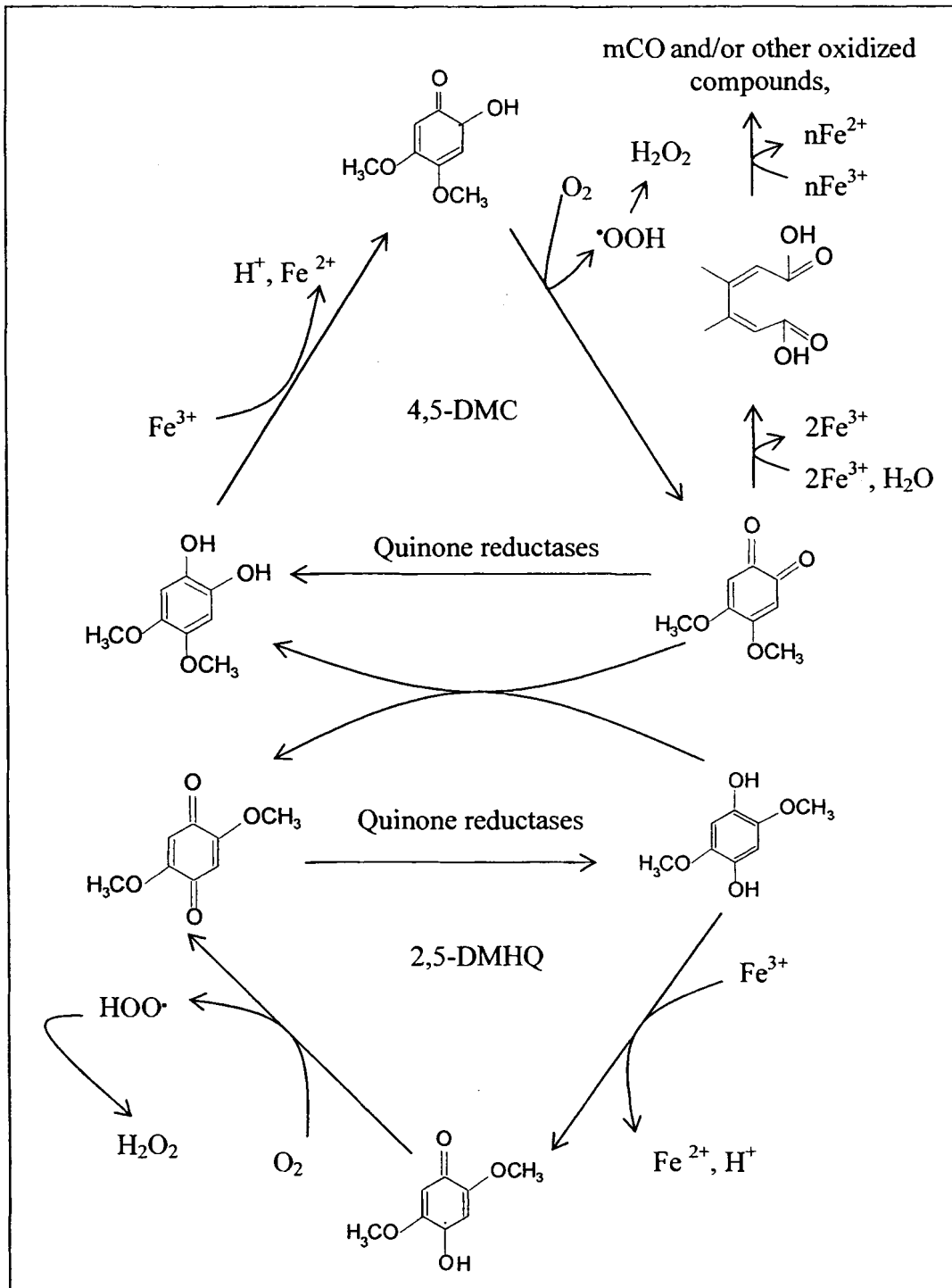


Figure 1.4. Proposed pathways for generation of ferrous iron and hydrogen peroxide extracellularly by *Gloeophyllum trabeum* in the phenolate biochelator - driven Fenton chemistry (Mineralization pathway: Goodell et al., 1997 (a) and (b), 2001; Pracht et al., 2001; Quinone redox cycle and quinone reducing enzymes: Kerem et al., 1999; Paszczyński, et al., 1999; Jensen et al., 2001). 4,5-DMC, 4,5-dimethoxy-1,2-benzenediol. 2,5-DMHQ, 2,5-dimethoxy-1,4-benzenediol.

Biochelators and Laccase Mediator Systems

Biochelators might also be effective as laccase mediators, but as yet this had not been shown (Goodell, personal communication). Laccase is a copper oxidase produced by many white rot fungi. Laccases, lignin peroxidases and manganese-dependent peroxidases are three important enzymes in the white rot ligninolytic systems. Laccase oxidizes aromatic (phenolic) compounds that possess relatively low ionization potentials, producing phenoxy radicals. Non-phenolic compounds are not substrates for laccase. They are oxidized by the cation radicals produced enzymatically (D'Souza et al., 1996). But it has been found that in the presence of some mediators, laccases can also oxidize non-phenolic lignin model compounds. Thus the laccase mediator systems (LMS) extend the spectrum of substrates for laccases (Bourbonnais and Paice, 1990). LMS have received widespread attention for their potential biotechnological applications in bleaching kraft pulp. LMS have also been shown to oxidize various compounds, thus they might be useful in preparative synthesis and bioremediations (Johannes et al., 1996; Bourbonnais et al., 1998; Crestini and Argyropoulos, 1998; Majcherczyk and Johannes, 2000; Johannes and Majcherczyk, 2000; Tsutsumi et al., 2001). More than 100 possible synthesized mediators have already been described (Johannes and Majcherczyk, 2000). It has been known that some of the synthetic mediators are hydroxamic acid type compounds (Goodell, personal communication). Johannes and Majcherczyk (2000) demonstrated that some natural compounds either produced by fungi or present during the biodegradation of lignocellulose could also mediate the laccase, such as phenols, aniline, 4-hydroxybenzoic acid and 4-hydroxybenzyl alcohol. (Johannes and Majcherczyk, 2000). Hydroxylated benzoic acids have been identified as phenolate

biochelators produced by the brown rot fungus *G. trabeum* (Goodell et al., 1997 (a) and (b)). Although production of laccase activity by the brown rot fungi has not been studied extensively, a laccase gene specific sequence has been isolated from *G. trabeum* by PCR utilizing degenerate primers corresponding to the consensus sequences of known laccases (D'Souza, 1996). The PCR product showed high similarity to the laccase genes of the white rot fungi *T. versicolor*, *Coriolus hirsutus*, *C. versicolor*, *Lentinula edodes*, *L. tigrinus*, *Phlebia brevispora*, *P. radiata* and *Ganoderma lucidum*. The presence of laccase activity in *G. trabeum* (Mad-617-R) has also been demonstrated (D'Souza, 1996).

Dissertation Overview

The aims of this dissertation research are:

1. To elucidate brown rot mechanisms by comparing metabolites proposed to play a role in degradation pathways by brown rot fungi with metabolites produced by white rot and wood-inhabiting non-decay fungi. The study examined metabolite production and modification of the growth environment by representatives from different categories of wood-inhabiting fungi.
2. To elucidate possible pathways for quinone reduction in the brown rot fungus *G. trabeum*. A *G. trabeum* plasma membrane redox system with quinone - reducing ability and an intracellular benzoquinone reductase produced by *G. trabeum* were characterized. Fungal plasma membrane isolation was also performed as a preliminary experiment for future studies on fungal plasma membrane redox system and other membrane proteins.

Metabolite Production

Phenolate biochelators have been proposed as an integral part of the cellulolytic systems of brown rot fungi (Goodell et al., 1997 (a) and (b); Jellison et al., 1991 (a) and (b), 1993, 1996, and 1997). Both brown rot and white rot fungi produce low molecular weight, iron-reducing, siderophore-like, metal chelators (Fekete et al., 1989). The production of these biochelators by the wood-inhabiting non-decay fungi has not been completely studied.

CDH has also been suggested to mediate the Fenton reaction in the brown rot fungus *C. puteana* (Schimidhalter and Canevascini, 1993 (a) and (b)). *Phanerochaete chrysosporium* CDH has been proposed to participate in cellulose and lignin degradation by this white rot fungus (Ander, 1994; Ander and Mazullo, 1997; Cameron and Aust, 1999). The enzyme oxidizes cellobiose that is produced in cellulose biodegradation process (Fahnrich and Irrgang, 1982; Schou et al., 1993). It may potentially mediate the Fenton reaction by reducing ferric iron and molecular oxygen, producing destructive hydroxyl radicals that attack ligninocellulose (Cameron and Aust, 1999). The enzyme also participates in lignin biodegradation via its quinone - reducing ability. Quinones are intermediates produced by the ligninolytic enzymes during lignin biodegradation. Quinone reduction is an essential step leading to complete lignin degradation (Schoemaker et al., 1989; Aust, 1995).

Although cellobiose dehydrogenase has been purified from various white rot and soft rot fungi (Ayers et al., 1978; Dekker, 1980; Fahnrich and Irrgang, 1982; Coudray et al., 1982; Canevascini et al., 1991; Bao et al., 1993; Schou et al., 1993 and 1998; Fang et al., 1998; Dumonceaux et al., 1998; Temp and Eggert, 1999; Moukha et al., 1999;

Subramaniam et al., 1999; Igarashi et al., 1999; Hallerg et al., 2000; Baminger et al., 2001), *Coniophora puteana* is the only brown rot fungus from which CDH has been purified and characterized (Schimidhalter and Canevascini, 1993 (a) and (b)). CDH was not produced by *G. trabeum* grown in glucose mineral media (Kerem et al., 1999; Paszcynski et al., 1999).

Some wood-inhabiting non-decay fungi, such as species of *Trichoderma*, can produce significant amounts of cellulase. *Trichoderma reesei* and *T. viride* have been used for the commercial production of cellulase (Samuels, 1996). Incubating pinewood fibers with *T. reesei* also reduces the energy consumption in the production of fiber sheets (Unbehaun et al., 2000). An understanding of why wood-inhabiting non-decay fungi do not cause significant wood degradation while successfully colonizing wood may help to understand the components that are essential for a fungus to attack and break down wood. Experiments were set up with fungal species representatives of white rot, brown rot and wood-inhabiting non-decay fungi. The modifications of the fungal growth environment were monitored. The production of the biochelators was characterized based on biochelator structural types. The production of CDH was characterized by its reduction of two different electron acceptors, 2,6-Dichloroindophenol (DCPIP) and 2,3-dimethoxy-5-methyl-1,4-benzoquinone (coenzyme Q₀).

Plasma Membrane Redox System and Intracellular Quinone - Reducing Enzymes

Quinone reduction is involved in both white rot and brown rot degradation. In white rot decay, quinones are intermediates produced by the ligninolytic enzymes such as peroxidases and laccase during lignin biodegradation. Rapid metabolism of quinone

products shifts the polymerization-depolymerization equilibrium towards degradation (Schoemaker et al., 1989; Ander and Marzullo, 1997). In brown rot decay, quinone - reducing enzymes along with mineralization reactions may mediate the generation and regeneration of phenolate biochelators, which may contribute, along with the mineralization process, to continuous production of Fenton reagents (Goodell et al., 1997 (a) and (b), 2001; Paszczynski, et al., 1999; Kerem et al., 1999). Quinone reducing enzymes may also play vital roles in protecting mycelium against quinone toxicity.

Quinone - reducing enzymes include extracellular cellobiose dependent quinone reducing cellobiose dehydrogenase (CDH) discussed above, intracellular NAD(P)H-dependent quinone reductases, and membrane-bound reductases (Ander and Marzullo, 1997; Paszczynski et al., 1999). Intracellular NAD(P)H dependent quinone oxidoreductases from the white rot fungus *P. chrysosporium* have been characterized (Buswell et al., 1979). Two intracellular NAD(P)H dependent 1,4-benzoquinone reductases from *P. chrysosporium* have been purified (Constam, et al., 1991; Brock et al., 1995; Brock and Gold, 1996). The gene encoding one of the intracellular quinone reductases in *P. chrysosporium* has been cloned and sequenced (Akileswaran et al., 1999). A plasma membrane redox system (PMRS) of *P. chrysosporium* able to reduce quinones has been characterized (Fernando et al., 1990; Stahl and Aust, 1993 and 1995; Stahl et al., 1995). The PMRS and the intracellular quinone reductases of *P. chrysosporium* show different kinetics constant (K_m) and optimal pH (Stahl et al., 1995).

The presence of mycelial quinone - reducing activity in *G. trabeum* has been demonstrated (Paszczynski et al., 1999; Kerem et al., 1999). To elucidate the potential pathways for the quinone reduction in *G. trabeum*, experiments were set up to

characterize the membrane-bound quinone reduction, and to purify and characterize the *G. trabeum* intracellular quinone reductases. The function of these reductases has not been established.

Membrane Isolation

The plasma membrane isolation and characterization is a pre-requisite step for characterization of the outer membrane proteins, such as the siderophore receptors on outer membranes, and the membrane-bound reductase system.

Biochelators produced by wood decay fungi are siderophore-like compounds (Fekete et al., 1989; Jellison et al., 1991). Siderophores are low molecular weight, iron - chelating compounds produced by microorganisms grown under iron deficient conditions. Their function is to acquire iron for cells (Barton and Hemming, 1992). The ubiquitous production of multiple forms of biochelators by wood decay fungi may indicate that in addition to the role biochelators play in mediating the Fenton reaction, biochelators also play a role in general fungal physiology. In the siderophore mediated iron uptake process, bacteria produce specific membrane receptors to uptake the iron-siderophore complex (Barton and Hemming, 1992). However, no siderophore receptors have been found in fungi (Huschka and Winkleman, 1989).

The isolation of plasma membrane from filamentous fungi has been a technical challenge because of the difficulty in obtaining protoplasts from filamentous hyphae. Preliminary studies on the isolation and characterization of plasma membranes from the filamentous wood decay fungus *P. chrysosporium* were performed. The research

provided a basic protocol for future studies on siderophore receptors and the membrane bound reductase system in wood decay fungi.

Importance of the Projects

This work contributes to a better understanding of the role of biochelator – driven Fenton reactions in wood biodegradation by brown rot fungi and leads to a better understanding of the biochemistry and physiology of the brown rot fungus *G. trabeum*. Areas of specific focus include characterization of metabolites produced by various fungi and the isolation and characterization of fungal reductases of potential physiological importance. This research makes a contribution in the general area of the physiology of wood decay organisms and may eventually be helpful in the development of specific, environment – friendly wood preservation strategies based on the physiology of wood decay fungi and wood decay mechanisms.

Chapter 2
**MODIFICATION OF THE GROWTH ENVIRONMENT BY WOOD-
INHABITING FUNGI**

Abstract

Multiple components have been postulated to be involved in the Fenton-based biological degradation of wood by brown rot fungi. Biochelators and cellobiose dehydrogenase have been implicated by different researchers in essential iron reduction steps. Biochelator production by three white rot fungi, three brown rot fungi and three wood-inhabiting non-degradative fungi was examined. All nine species produced chelating compounds. The chemical characteristics and iron-reducing ability of the chelators produced varied. However, the brown rot fungi produced predominately phenolate chelators. Of the species examined, the brown rot fungus *Fomitopsis pinicola* produced chelators with the greatest reducing ability. This fungus has also exhibited ability to accumulate high levels of iron in soil block assays. When liquid cultures of *Phanaerochaete chrysosporium* (white rot fungus), *Gloeophyllum trabeum* (brown rot fungus) and *Trichoderma viride* (non-degradative wood inhabitant) were examined over a four week period, all three replicates of the three fungi showed measurable levels of cellobiose dehydrogenase activity. *Trichoderma* was shown to produce iron-reducing chelators and cellobiose dehydrogenase. It has been previously reported that *Trichoderma* produces large amounts of cellulase and other degradative enzymes. *Trichoderma viride* did not cause weight loss in the 16-week soil block decay test, while both *P. chrysosporium* and *G. trabeum* caused a significant wood degradation. It is interesting

that *Trichoderma* possesses many components of a cellulose degrading system, yet is not associated with the rapid strength losses seen when wood is attacked by brown rot fungi.

Introduction

Biodegradation is one of the factors that limit the utilization of wood. The ability to biodegrade wood lignocellulose is limited to certain fungal species. The brown rot fungi can rapidly and preferentially attack wood cellulose and hemicellulose. They also modify wood lignin significantly. The white rot fungi are able to gradually attack and metabolize both the cellulose and the lignin of wood (Zabel and Morrell, 1992). Wood-inhabiting non-decay fungi do not cause a significant degradation of lignocellulose, although some non-decay fungi, such as *Trichoderma* species, do produce significant amounts of degradative enzymes (Samuels, 1996). What allows brown rot and white rot organisms to initiate and participate in breakdown the cellulose or both cellulose and lignin of the wood, while the wood-inhabiting non-decay microorganisms, which have many of the same degradative enzymes and metabolic pathways, can not, has not been elucidated clearly.

Previous research has shown that low molecular weight, iron-reducing phenolate derivative metal chelators isolated from brown rot fungi are an integral part of the brown rot cellulolytic systems (Jellison et al., 1991 (a) and (b), 1993, 1996, 1997; Goodell et al., 1997 (a) and (b); Paszczynski et al., 1999; Parra et al., 1998). These isolated phenolate derivative chelators not only have a high affinity for ferric iron but also can mediate the reduction of ferric iron to ferrous iron in redox cycling processes at pH values below neutrality. The ferrous iron then reacts with oxidants such as hydrogen peroxide and a

Fenton reaction, $\text{Fe}^{2+} + \text{H}_2\text{O}_2 \rightarrow \text{Fe}^{3+} + \text{HO}\cdot + \text{HO}^-$, will occur to generate destructive hydroxyl radicals, which can depolymerize and oxidize lignocellulose compounds (Goodell et al., 1997 (a) and (b)).

The structures, distribution and iron - reducing ability of phenolate biochelators produced by the brown rot fungus *Gloeophyllum trabeum* have been studied (Jellison et al., 1991 (a); Easwaran, 1994; Goodell, et al., 1997; Paszczynski, 1999). Production of biochelators by other brown rot and white rot fungi has been reported but not well characterized (Fekete et al., 1989). The *G. trabeum* phenolate biochelators are siderophore-like compounds. Siderophores are low molecular weight, iron - chelating compounds produced by microorganisms grown under iron deficient conditions. Their function is to acquire iron for cells. Siderophores are classified as phenol-catecholates, hydroxamates, and carboxylates according to the main chelating groups (Barton and Hemming, 1992). Before the isolation of phenolate biochelators from *G. trabeum*, all of the fungal siderophores found and characterized were hydroxamates (Hofete, 1992).

During the process of iron reduction, the phenolate biochelators themselves are oxidized to quinones and semiquinones. Quinone - reducing enzymes, such as extracellular cellobiose dehydrogenase (CDH), may be important in the recycling and metabolism of these oxidized biochelators and/or other reactive quinones (Paszczynski et al., 1999; Kerem et al., 1999). Alternately, mineralization processes may be dominant (Goodell et al., 2001; Pracht et al., 2001). CDH produced by the brown rot fungus *Coniophora puteana* and the white rot fungus *Phanerochaete chrysosporium* has been proposed to mediate the Fenton reaction by reducing ferric iron and molecular oxygen (Kremer et al., 1992; Hyde and Wood, 1997; Cameron and Aust, 1999).

Cellobiose dehydrogenase, formally known as cellobiose oxidase (Ayers et al., 1978), is a flavohemoprotein produced under cellulolytic conditions. It oxidizes cellobiose, cellodextrins and some other disaccharides using electron acceptors such as ferric iron, cytochromes, quinones, phenoxy radicals and even oxygen. Many cellulolytic fungi have been shown to produce cellobiose dehydrogenase. CDH has been isolated and characterized in the white rot fungi *P. chrysosporium* (Bao et al., 1993; Higham et al., 1994; Raices et al., 1995; Lehner et al., 1996; Li et al., 1996 and 1997; Igarashi et al., 1996, 1998 and 1999; Cohen et al., 1997; Henriksson et al., 1997 and 1998; Habu et al., 1993 and 1997; Vallim et al., 1998; Cameron and Aust, 1999), *Pycnoporus cinnabarinus* (Temp and Eggert, 1999; Moukha et al., 1999), *Schizophyllum commune* (Fang et al., 1998), and *Trametes versicolor* (Dumonceaux et al., 1998). CDH has also been isolated from soft rot fungi *Sporotrichum thermophile* (Coudray et al., 1982; Canevascini et al., 1991; Subramaniam et al., 1999), *Monilia sp.* (Dekker, 1980), *Chaetomium cellulolyticum* (Fahnrich and Irrgang, 1982), *Humicola insolens* (Schou et al., 1993 and 1998; Igarashi et al., 1999), and the plant pathogen *Sclerotium rolfsii* (Baminger et al., 2001). To our knowledge, *Coniophora puteana* is the only brown rot fungus from which CDH has been purified and characterized (Schimidhalter and Canevascini, 1993 (a) and (b)).

In this study, we monitored the production and activities of fungal metabolites previously implicated in the degradation process, such as biochelators and CDH. To determine if different categories of fungi produce structurally and functionally similar chelators, we isolated low molecular weight compounds produced by brown rot fungi *G. trabeum*, *Postia placenta*, *Fomitopsis pinicola*, white rot fungi *P. chrysosporium*, *T.*

versicolor, *Trichaptum abietinum*, and wood-inhabiting non-decay fungi *Trichoderma viride*, *Phialocephala fusca*, *Phialophora mutabilis*. The low molecular weight compounds were characterized based upon siderophore types and iron – reducing ability. Representatives of the white rot, brown rot and wood-inhabiting non-degradative fungi, *G. trabeum*, *P. chrysosporium*, and *T. viride*, respectively, were also examined over a four-week period in liquid media and over a 16-week period in soil block jars. The modification of the liquid media environment by these fungi, such as the change in pH, biochelator production and CDH production, was recorded. The percent weight loss in soil block jar decay assays was also monitored to confirm the absence of significant degradation in blocks colonized by non-decay fungi.

Materials and Methods

Organisms and Culture Conditions

Brown rot fungi *G. trabeum* (ATCC11539), *P. placenta* (Mad 698R), *F. pinicola* (lab isolate, courtesy of J. H. Connolly); white rot fungi *P. chrysosporium* (ATCC 24725), *T. versicolor* (Fp 101664-SP), *T. abietinum* (1247 M5L); and wood-inhabiting non-decay fungi *T. viride* (ATCC 32630), *P. fusca* (ATCC 62326), *P. mutabilis* (ATCC 42792) were maintained on Difco® malt extract agar slants at 4 °C. Four – week old cultures on malt extract agar plates grown at 24 °C were used for inoculations.

Decay Test

A modification of the ASTM soil block assay (ASTM, 1994) was carried out with the brown rot fungus *G. trabeum*, the white rot fungus *P. chrysosporium*, and the non-

decay fungus *T. viride*. The soil was composed of 1:1:1 (dry volume) mixtures of Hyponex® Promix potting soil (Marysville, OH, USA), vermiculite, and sphagnum moss. Deionized distilled water was added to the soil mixture. The moist soil was left over night. The soil was then transferred into 500 mL, wide mouth mason jars to a volume of approximately 250mL. The following day, the soil moisture was re-adjusted by adding deionized distilled water until a little free water could be seen in the bottom of jars. Two birch feeder strips were placed side by side on the surface of the soil in each jar. Jars were capped and autoclaved for 30 minutes at 121 °C. The jars were allowed to incubate 2 days at room temperature and then autoclaved again for 30 minutes at 121 °C. Four blocks of the fungus and growth media were laid on the feeder strips aseptically in each jar to initiate fungal growth. Twelve jars were set up for each fungus. Blocks of sterile medium were laid on the feeder strips aseptically in four jars as controls.

After the jars were incubated for one month at room temperature, oven-dried (100 °C), weighed, autoclaved spruce wood blocks (2.5 × 2.5 × 2.5 cm) were aseptically placed on the fungus covered feeder strips, one wood block per jar.

At weeks two, four, eight and 16, one control jar and three treated jars per fungus were harvested. The blocks were taken out and the fungal mass on the block surface was gently scraped off. Then the blocks were oven-dried (100 °C) and weighed.

Chelator Production by Different Fungi

All glassware was acid washed with 37% HNO₃. The brown rot fungi *G. trabeum*, *P. placenta*, *F. pinicola*, white rot fungi *P. chrysosporium*, *T. versicolor*, *T. abietinum*, and the non-decay fungi *T. viride*, *P. fusca*, *P. mutabilis* were grown in modified liquid

media (Highly, 1973; Appendix A). The iron concentration was modified to 20 μM using ferrous iron sulfate. The carbon source consisted of 0.2% glucose and 1% cellulose.

After 4 weeks, the mycelial mats suspended in the liquid media were collected carefully, freeze dried (VirTis Freezemobiles®), and weighed. Low molecular weight compounds in the liquid media were collected by vacuum filtration through Whatman® No. 2 filters and ultrafiltration in an Amicon® ProFlux™ M12 Tangential filtration system with a molecular weight cut of 1000 D. The filtrate was concentrated by lyophilization (VirTis Freezemobiles®) to about one fifth of the original culture volume. The concentrated culture filtrate was subsequently acidified to pH 3.0 with concentrated HCl, followed by two ethyl acetate extractions. Ethyl acetate extracts were combined and evaporated to dryness at room temperature. The dry materials were resuspended in deionized water to produce the ethyl acetate fraction. The aqueous solution after ethyl acetate extraction was referred to as the aqueous fraction (Jellison et al., 1991 (a)).

The existence of the iron chelators in the original liquid culture and in each fraction was tested by the Chrome azurol S (CAS) assay (Schwyn and Neilands, 1987). CAS assay solution was prepared according to Fekete (Fekete, 1992) and was stored in the dark in a polyethylene bottle. A 0.5 mL of sample or standard was mixed with 0.5 mL of CAS assay solution. The absorbance was read at 630 nm after the color formation stabilized. The chelator standard was 2,3-Dihydroxybenzoic acid.

Phenolate derived compounds were characterized by the Arnow test (Arnow, 1937). The phenolate chelator standard was 2,3-Dihydroxybenzoic acid. The sample or the standard (0.5 mL) was mixed with 0.5 mL of 0.5 N HCl, 0.5 mL of a mixture

containing 10% sodium nitrite and 10% sodium molybdate in water, and 0.5 mL of 1 N NaOH. Absorbance was measured at 515 nm.

Hydroxamic acid derived compounds were characterized by the Csaky test (Csaky, 1948, Ishimaru and Loper, 1992 (a)). The hydroxamic acid standard was hydroxylamine. The sample or the standard (0.2 mL) was mixed with 0.3 mL of 6 N H₂SO₄ in a glass test tube with a polypropylene cap and autoclaved for 30 minutes at 121 °C. Samples were then cooled to room temperature, and 0.6 mL of 35% sodium acetate solution, 0.1 mL of sulfanilic acid solution (in 30% acetic acid), and 0.1 mL of iodine solution (in glacial acetic acid) were added. After 3 minutes, 0.2 mL of 2% NaAsO₂ was added. After the color cleared, 0.2 mL of 0.1% N-1-naphthylethylene diamine solution was added. Absorbance was measured at 520 nm.

The iron reduction abilities of fungal isolates were characterized using the Ferrozine assay (Stookey, 1970). The assay was carried out in 200 mM pH 4.5 acetate buffer in the presence of 30 µM FeIII. Ferrozine reagent (2.5 mM) was added at the beginning of the reaction. The biochelator solution was added to initiate the reaction. The concentration of biochelators was 30 µM as determined by the Arnow test and was expressed as the concentration of 2,3-DHBA. The total reaction volume was 3 mL. The absorbance was monitored at 562 nm.

Fractions from *G. trabeum* were further characterized by HPLC on a Phenomenex Spherex 5 µM C₁₈ 250 × 10 mm column at 30°C using a flow rate of 1.5 mL/min by using the HP series 1050. The mobile phase was 20% methanol containing 1 mM oxalic acid and 1 mM oxalate. The sample (40 µl) was injected using a Hitachi AS-2000

autosampler. Detection was performed using a Hitachi L-4500 Diode array detector at 275, 245 and 312 nm.

Chelator Production Versus Iron Concentration

Highley's liquid media (Highley, 1973; Appendix A) with 4 different iron concentrations were prepared. Glucose (1%) was used in Highley's media as the carbon source in initial experiments. Ferrous iron concentration in Highley's media ranged from 0, 20, 200 to 400 μM and was adjusted by addition of ferrous iron sulfate into iron-free media. Liquid media (200 mL) was distributed into each 500 mL PYREX® flask. Five replicates were set up for each iron concentration. *Fomitopsis pinicola* growing on malt extract agar was used to inoculate flasks. The pH of the liquid media was recorded before and after the growth of the fungus. After 4 weeks, the liquid fraction of the culture was collected by filtration through Whatman® No. 2 filters. The fungal biomass was measured. The iron concentrations of the filtrates were determined by inductively coupled plasma mass spectrometry (ICP). Concentrations of phenolate chelators and hydroxamic acid chelators were determined by the Arnow assay and the Caskey assay, respectively.

Modification of the Liquid Media Environment by Fungi

All glassware was acid washed with 37% HNO_3 . The brown rot fungus *G. trabeum*, the white rot fungus *P. chrysosporium*, and the non-decay fungus *T. viride* were grown in modified Highley's liquid media (Highley, 1973; Appendix A) containing 0.2% glucose and 1% cellulose as the carbon source for 4 weeks at room temperature. At the

end of each week, selected cultures were harvested and the liquid media were collected by vacuum filtration through Whatman® No. 2 filters. Three replicates were set up for each fungus at each time point.

The liquid fraction was characterized with regard to pH, protein concentration (Lowry et al., 1951), phenolate type chelator concentration (Rioux assay, Rioux et al., 1983), hydroxamic acid type chelator concentration (Csaky assay), and cellobiose dehydrogenase (CDH) activity. Electron acceptors 2,6-Dichloroindophenol (DCPIP) and 2,3-dimethoxy-5-methyl-1,4-benzoquinone were used for the detection of CDH activity (Samejima and Eriksson, 1992). The Lowry assay was carried out using bovine serum albumin as the protein standard.

The Rioux assay was carried out with 2.3 mL of deionized, distilled water, 0.2 mL of 20% sulfuric acid, 1.0 mL of sample or standard, 0.1 mL 1% ferric ammonium citrate in 0.009 N sulfuric acid, 0.4 mL of 2 M ammonium fluoride, 0.4 mL of 1% 1,10-phenanthroline monohydrochloride monohydrate, and 0.6 mL of 3 M hexamethylenetetramine. The reaction mixture was incubated at 60 °C for 1 hour. Absorbance was measured at 510 nm.

Cellobiose dehydrogenase catalyzed DCPIP reduction was carried out at 30 °C in 1.9 mL of 50 mM sodium tartrate, pH 4.0 buffer containing 500 µM cellobiose and 75 µM DCPIP. The reaction was initiated by adding 0.1 mL of the liquid fractions. Activity was measured as the decrease of absorbance at 600 nm. The absorption coefficient for DCPIP was $1.6 \text{ mM}^{-1} \text{ cm}^{-1}$ (Samejima and Eriksson, 1992).

Cellobiose dehydrogenase catalyzed quinone reduction was carried out at 30 °C in 1.9 mL of 50 mM sodium tartrate, pH 4.0 buffer containing 500 µM cellobiose and 250

μM 2,3-dimethoxy-5-methyl-1,4-benzoquinone. The reaction was initiated by adding 0.1 mL of the liquid fractions. Activity was measured as the decrease of absorbance at 375 nm. The absorption coefficient for 2,3-dimethoxy-5-methyl-1,4-benzoquinone was $1.2 \text{ mM}^{-1} \text{ cm}^{-1}$ (Samejima and Eriksson, 1992).

Results

Decay Test

Both *P. chrysosporium* and *G. trabeum* caused significant weight loss after 16 weeks of decay in the soil-jar assays. *Gloeophyllum trabeum* caused much more weight loss in spruce wood blocks than *P. chrysosporium* did. The weight loss after 16 weeks was 68.5% (1.977 +/- 0.101g) and 26.7% (0.802 +/- 0.218 g), respectively (Figure 2.1). The non-decay fungus *T. viride* did not cause weight loss. The weight loss of the wood blocks after 16 weeks of incubation with *T. viride* was 1.5% (0.045 +/- 0.002 g), while the weight loss of control wood blocks was 1.3% (0.044 g) (Figure 2.1. A).

Rapid weight loss was caused by *G. trabeum*. The majority of the weight loss occurred within the first month. At the end of week two, the average weight loss per block was 11.9% (0.354 +/- 0.143 g). At the end of week four, weight loss was 46.3% (1.433 +/- 0.371 g), which was more than four times the weight loss in the first two week period. The rate of weight loss slowed down after four weeks. At week eight and week 16, the weight loss was 48.3% (1.669 +/- 0.395 g) and 68.5% (1.977 +/- 0.101 g), respectively (Figure 2.1).

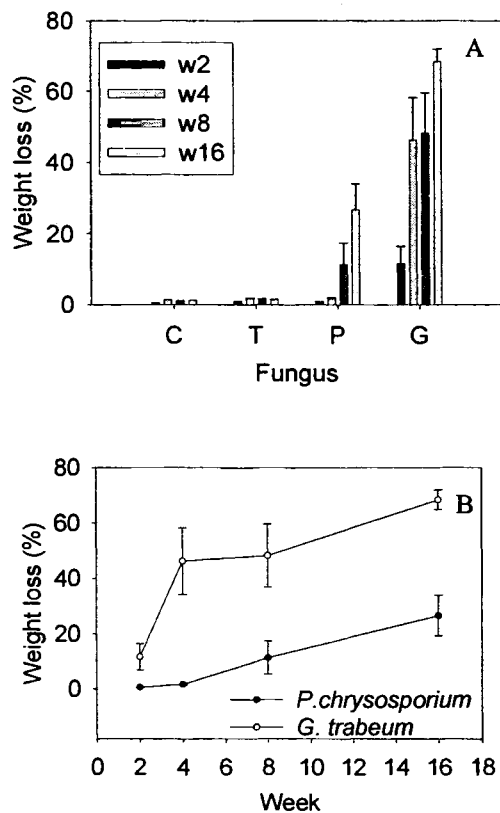


Figure 2.1. Weight loss of spruce blocks caused by the white rot fungus *Phanerochaete chrysosporium* (P), the brown rot fungus *Gloeophyllum trabeum* (G) and the non-decay fungus *Trichoderma viride* (T) in the soil-jar decay test. "C", the control jars. Data represent the averages of triplicate samples. At the end of 16th week, *T. viride* did not cause significant weight loss, while *G. trabeum* and *P. chrysosporium* caused significant weight loss compared with the control treatment (T-test with $P < 0.05$). Major weight loss caused by *G. trabeum* occurred within the first month, while major weight loss caused by *P. chrysosporium* occurred after the first month.

Weight loss caused by *P. chrysosporium* occurred slowly at the beginning. The majority of the weight loss occurred after one month. At the end of week two and four, the weight loss was only 0.7% (0.021 +/- 0.005 g) and 1.7% (0.054 +/- 0.01 g), respectively. After eight weeks, the weight loss was 11.4% (0.341 +/- 0.181 g), which was about 7 times the weight loss observed after four weeks. The rate of weight loss was

sustained in the following weeks. At week 16, the weight loss was 26.7% (0.802 +/- 0.218 g) (Figure 2.1).

After eight weeks, the decay rate was similar for *P. chrysosporium* and *G. trabeum*, which was reflected by the near parallel lines in Figure 2.1.B.

The conditions in our decay test, such as substrates and environmental factors, may not have been ideal for the growth of *P. chrysosporium*, since the growth conditions were originally optimized for the brown rot fungi. The lack of appropriate substrate may contribute to the low initial decay rate and the low weight loss percentage observed. Spruce blocks were used in our decay test. It is known that spruce is not preferred substrate of *P. chrysosporium* and other white rot fungi (Zabel and Morrell, 1992). The wood blocks were placed on the surface of soil instead of being buried in soil. Such growth environment also affects the decay process of *P. chrysosporium* (ASTM, 1994).

Characterization of Chelator Production by Different Fungi

The brown rot fungi and the white rot fungi displayed similar growth in modified Highley's liquid media. There was no significant difference between the unit dry weights of biomass produced. All the fungi tested produced iron biochelators. A positive CAS test indicated the presence of siderophores or other high affinity iron binding compounds (Table 2. 1).

Table 2.1. Fungal growth and biochelator production in modified Highely's media.

Fungi	Rot type	Chrome azurol S test ^a	Unit dry weight of biomass (g/mL)
<i>Fomitopsis pinicola</i>	Brown	+	0.0087
<i>Gloeophyllum trabeum</i>	Brown	+	0.0099
<i>Postia placenta</i>	Brown	+	0.0095
<i>Trichaptum abietinum</i>	White	+	0.0092
<i>Phanerochaete chrysosporium</i>	White	+	0.0115
<i>Trametes versicolor</i>	White	+	0.0115
<i>Trichoderma viride</i>	Non-decay	+	N ^b
<i>Phialocephala fusca</i>	Non-decay	+	N
<i>Phialophora mutabilis</i>	Non-decay	+	N

a. "+", positive

b. "N", not measured due to technical difficulties. The non-decay fungi did not form mycelia mats that could be separated from the cellulose powder added into the liquid media. Data are averages of triplicate samples.

The three brown rot fungi and the three non-decay fungi produced phenolate-derived compounds that were distributed both in the organic phase and the aqueous phase. *Phanerochaete chrysosporium* did not produce detectable levels of phenolate type iron chelating compounds as detected by the Arnou assay. The white rot fungi *T. versicolor* and *T. abietinum* produced phenolate type compounds that were only found in the aqueous phase (Figure 2.2). All of the fungi produced hydroxamic acid derived compounds, which mainly occurred in the aqueous phase, except for the hydroxamic biochelators produced by *G. trabeum* (Figure 2.2).

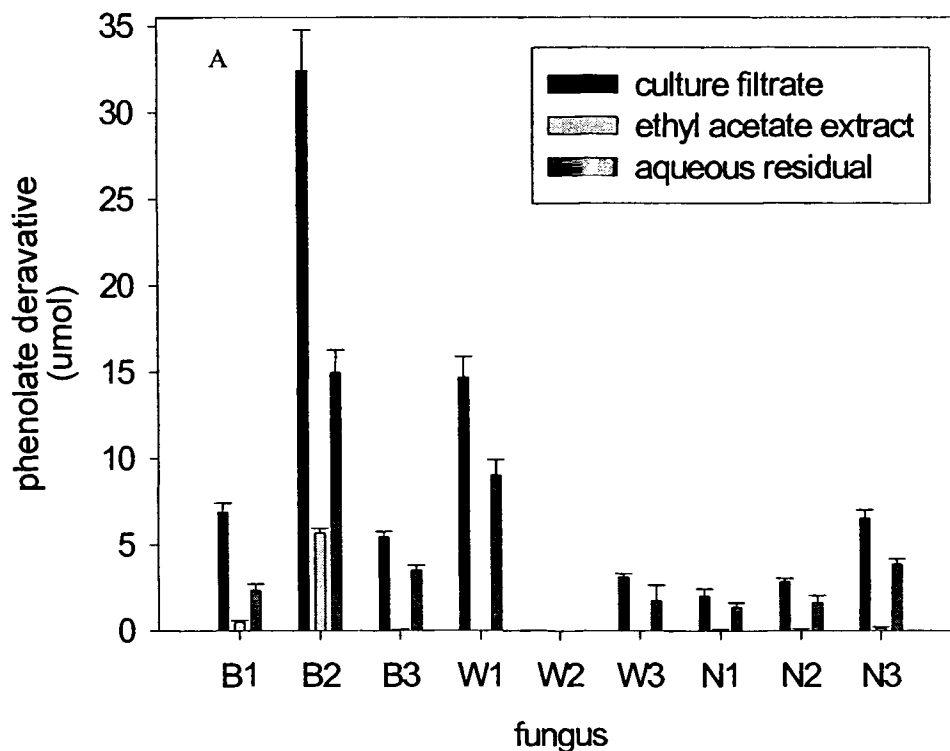


Figure 2.2. (A) The distribution of phenolate / mixed phenolate derivative compounds in different purification fractions. The biochelators were collected from 1L of fungal culture grown in modified Highley's liquid media with 0.2% glucose and 1% cellulose as the carbon source. The amount of phenolate or mixed phenolate derivative compounds in some fractions from some fungi was too low to be shown clearly in the graph. Data are averages and standard deviations from triplicate samples. "B", the brown rot fungi. B1, *Fomitopsis pinicola*. B2, *Gloeophyllum trabeum*. B3, *Postia placenta*. "W", the white rot fungi. W1, *Trichaptum abietinum*. W2, *Phanerochaete chrysosporium*. W3, *Trametes versicolor*. "N", the non-decay fungi. N1, *Phialocephala fusca*. N2, *Phialophora mutabilis*. N3, *Trichoderma viride*. The amount of phenolate derivative compounds was expressed as the amount of 2,3-dihydroxybenzoic acid. The amount of hydroxamic acid derivative compounds was expressed as the amount of hydroxylamine.

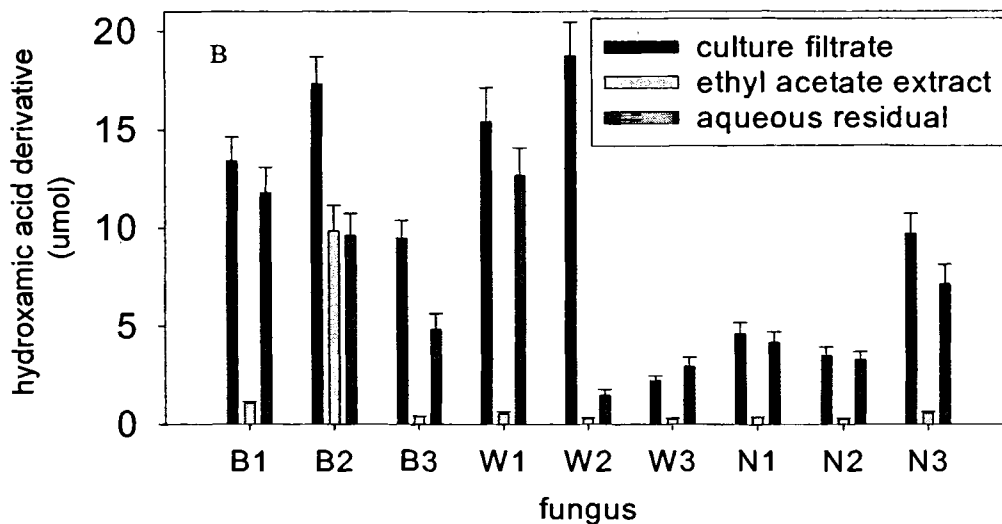


Figure 2.2. (B) The distribution of hydroxamic acid derivative compounds in different purification fractions. The biochelators were collected from 1L of fungal culture grown in modified Highley's liquid media with 0.2% glucose and 1% cellulose as the carbon source. The amount of phenolate or mixed phenolate derivative compounds in some fractions from some fungi was too low to be shown clearly in the graph. Data are averages and standard deviations from triplicate samples. "B", the brown rot fungi. B1, *Fomitopsis pinicola*. B2, *Gloeophyllum trabeum*. B3, *Postia placenta*. "W", the white rot fungi. W1, *Trichaptum abietinum*. W2, *Phanerochaete chrysosporium*. W3, *Trametes versicolor*. "N", the non-decay fungi. N1, *Phialocephala fusca*. N2, *Phialophora mutabilis*. N3, *Trichoderma viride*. The amount of phenolate derivative compounds was expressed as the amount of 2,3-dihydroxybenzoic acid. The amount of hydroxamic acid derivative compounds was expressed as the amount of hydroxylamine.

In the Ferrozine test, the iron reduction ability of each fraction is proportional to the increase in absorbance at wavelength 562nm caused by the fraction. Culture filtrates from the brown rot fungi and the non-decay fungi caused a greater absorbance increase in the Ferrozine test than did the white rot fungi, indicating greater iron - reducing capacities. Phenolate compounds produced by *T. abietinum* in culture filtrate caused an increase in absorbance of only 0.217 after 24 hours (Table 2.2). For *G. trabeum*, *P. placenta*, and *F. pinicola*, the same amount of phenolate compounds in the culture filtrates caused 0.335, 0.929 and 1.639 absorbance increases respectively (Table 2.2, Figure 2.3). All the fractions from *F. pinicola* caused extremely high absorbance increases. The aqueous fraction from *F. pinicola* caused an absorbance increase as high as 2.132, even though it contained a very small amount of phenolate compounds (Table 2.2, Figure 2.3, 2.4, 2.5). When the ethyl acetate extraction fractions (containing mainly phenolate derivatives) were examined, those from the non-decay fungi caused higher absorbance increases than did those from the other fungi (Table 2.2, Figure 2.4).

Table 2.2. The increase in the absorbance caused by each biochelator fraction after 24 hours in the Ferrozine assay*. The absorbance increase indicates iron reduction is occurring. The increase in the absorbance caused by water control was 0.01.

Fungus	Absorbance increase in the Ferrozine assay		
	Culture filtrates	Ethyl acetate extract	Aqueous fraction
<i>F. pinicola</i>	1.639	0.428	2.132
<i>G. trabeum</i>	0.335	0.275	0.344
<i>P. placenta</i>	0.929	0.186	0.56
<i>T. abietinum</i>	0.217	0.152	0.3
<i>P. chrysosporium</i>	0.252	0.212	0.355
<i>T. versicolor</i>	0.178	0.234	0.376
<i>T. viride</i>	1.489	0.575	1.205
<i>P. fusca</i>	1.457	0.72	1.055
<i>P. mutabilis</i>	0.41	0.471	0.267

* Bold numbers indicate the absorbance increase caused by 0.09 μ mol phenolate type compounds determined by the Arnou assay. Non-bold numbers indicate the absorbance increase caused by a lesser and unknown amount of the phenolate type compounds.

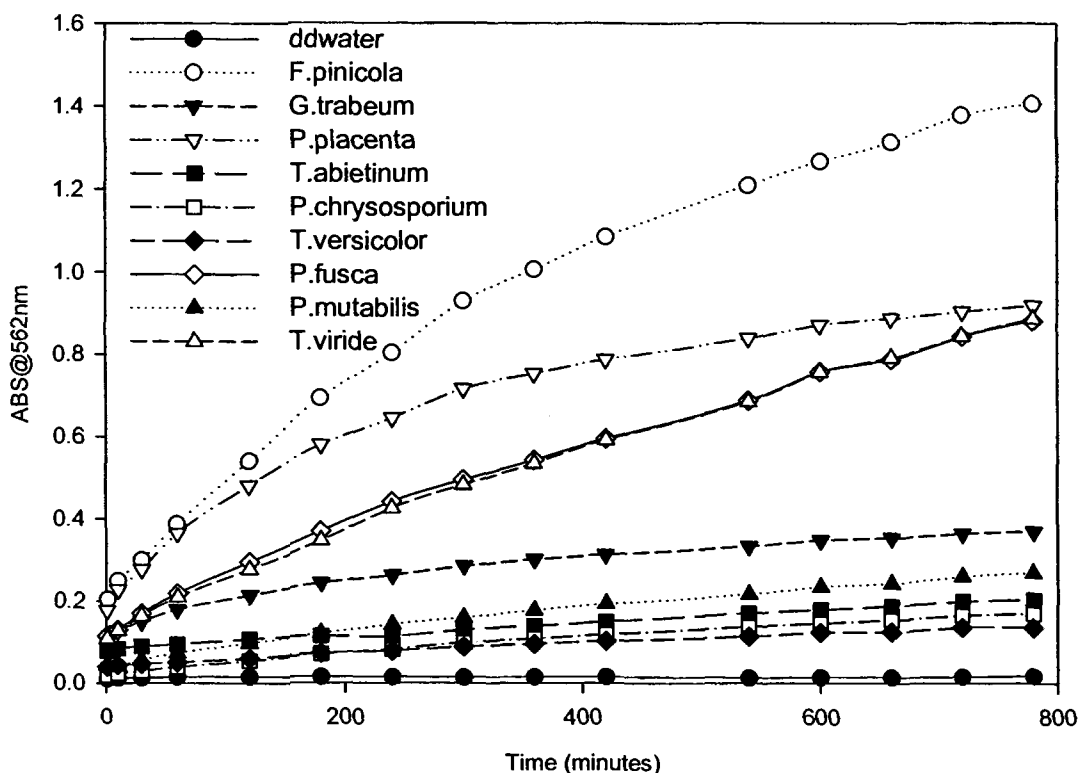


Figure 2.3. Ferrozine assays on fungal culture filtrates. Culture filtrates from the brown rot fungi and the non-decay fungi displayed higher iron - reducing ability than those from the white rot fungi. Culture filtrate from the brown rot fungus *Fomitopsis pinicola* showed the highest iron - reducing ability. The ferrozine assay for the culture filtrate of each fungus was carried out in the presence of 30 μM FeIII with 2.5 mM ferrozine reagent in pH 4.5 acetate buffer. The concentration of low molecular weight compounds was 30 μM as determined by the Arnow test and was expressed as the concentration of 2,3-dihydroxybenzoic acid. The total reaction volume was 3 mL. The exception was fungus *Phanerochaete chrysosporium*. Because its production of phenolate derivative compounds could not be detected by the Arnow test, the amount of low molecular weight compounds added into the reaction system was unknown and less than 30 μM .

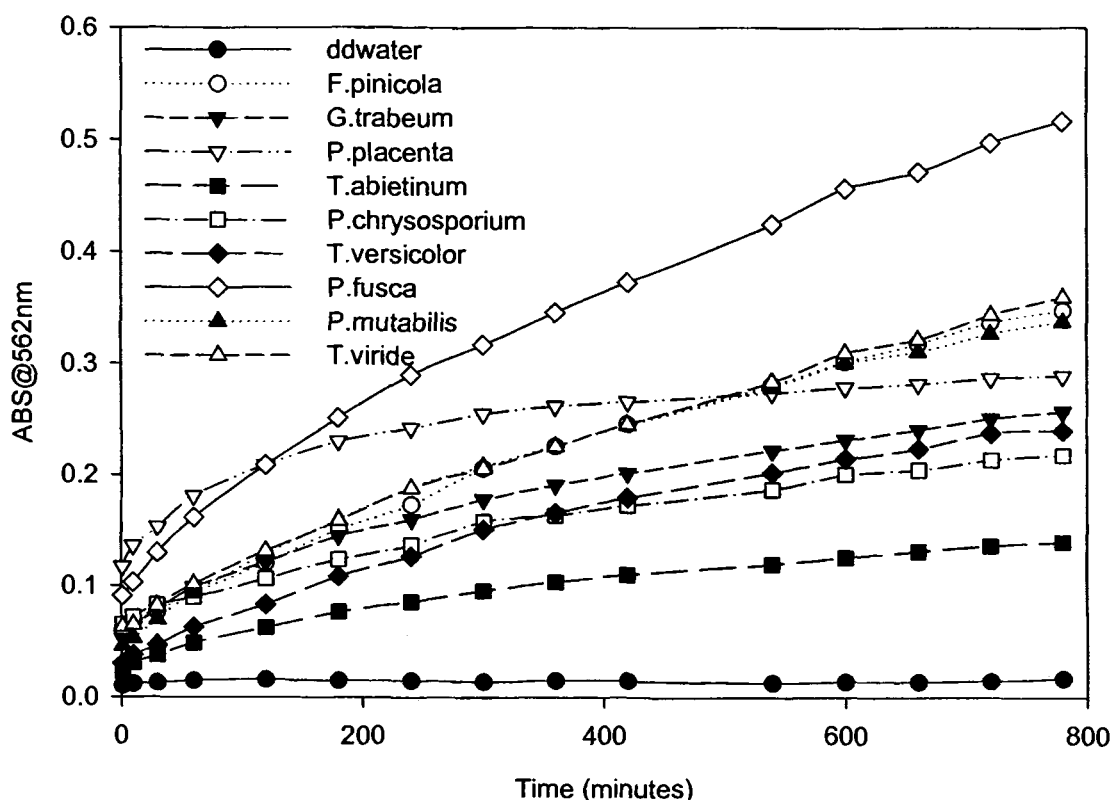


Figure 2.4. Ferrozine assays on the ethyl acetate extracts from fungal culture filtrates. Ethyl acetate fractions mainly containing phenolate derivatives from the brown rot fungi and the non-decay fungi also displayed higher iron-reducing ability than those from the white rot fungi. The ethyl acetate fraction from the non-decay fungus *Phialocephala fusca* had the highest iron-reducing ability. The ethyl acetate fractions from the brown rot fungus *Fomitopsis pinicola* and the non-decay fungi *Trichoderma viride* and *Phialophora mutabilis* displayed similar iron-reducing ability when standardized based upon uniform phenol content, and ranked 2nd. The ferrozine assay for the ethyl acetate extraction of each fungus was carried out in the presence of 30 μ M FeIII with 2.5 mM ferrozine reagent in pH 4.5 acetate buffer. The total reaction volume was 3 mL. For *F. pinicola*, *Gloeophyllum trabeum* and all the non-decay fungi, the concentration of low molecular weight compounds was 30 μ M phenolate derivative compounds. For *Postia placenta* and all the white rot fungi, the amount of low molecular weight compounds added into the reaction system was estimated due to the low initial concentration.

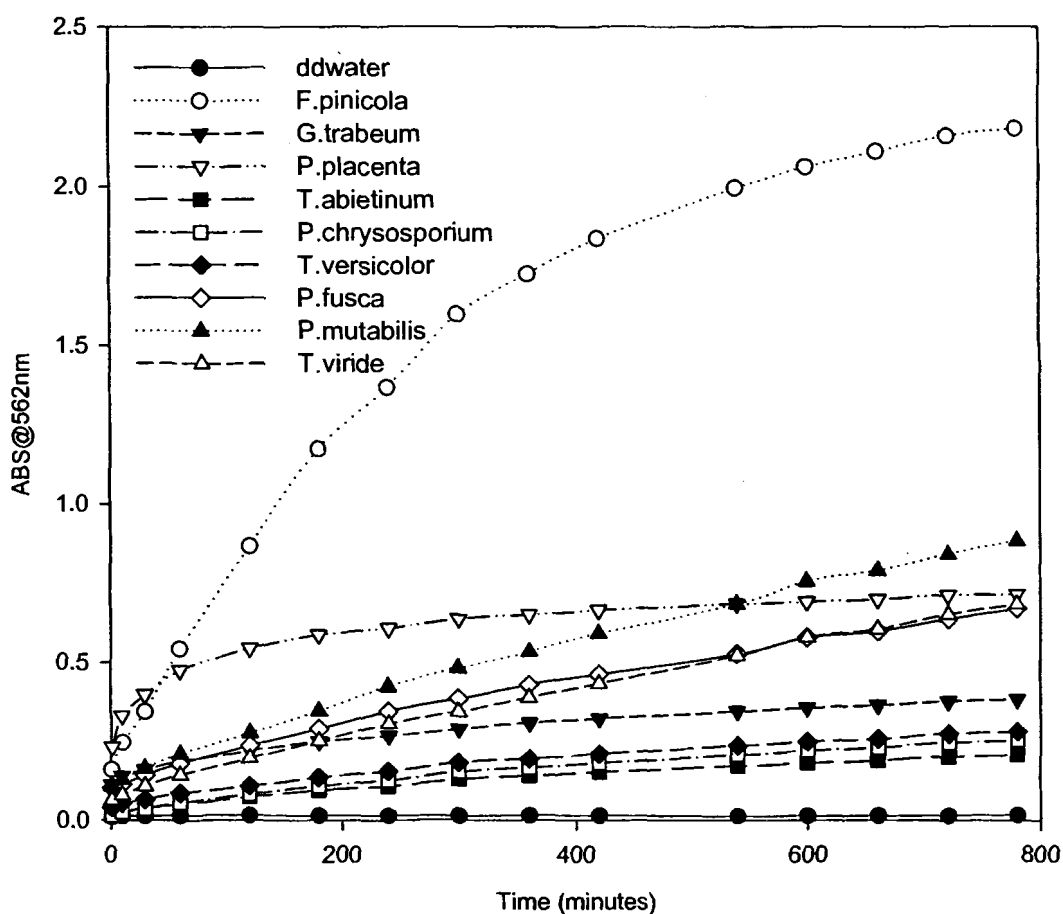


Figure 2.5. Ferrozine assays on the aqueous residuals of fungal culture filtrates after ethyl acetate extraction. Aqueous residuals from the brown rot fungi and the non-decay fungi also displayed higher iron - reducing ability than those from the white rot fungi. The aqueous residual from the brown rot fungus *Fomitopsis pinicola* showed the highest iron - reducing ability. The ferrozine assay for the aqueous residual of each fungus was carried out in the presence of 30 μM FeIII with 2.5 mM ferrozine reagent in pH 4.5 acetate buffer. The concentration of low molecular weight compounds was 30 μM phenolate derivative compounds. The total volume of each reaction system was 3 mL. The exception was *Phanerochaete chrysosporium*. Because its production of phenolate derivative compounds could not be detected by Arnow test, the amount of low molecular weight compound added into the reaction system was unknown.

The culture filtrate, ethyl acetate extraction and aqueous residue from *G. trabeum* and *P. chrysosporium* were analyzed by HPLC (Appendix D). In the ethyl acetate extraction from *G. trabeum*, major elution peaks appeared at 17.5 min at detection wavelength 275 nm, 244 nm and 312 nm. The peaks correspond to iron reducing DHBA-like compounds (Xu, personal communication). Lesser amounts of DHBA-like compounds were also found in the aqueous fraction from *G. trabeum*. Such peaks were not observed with *P. chrysosporium* fractions, which indicates biochelators produced by the two fungi are different structurally. Another major type of compounds left in the aqueous fraction from *G. trabeum* was eluted at 22 minutes at 244 nm. It was not determined if this type of compounds also have iron reducing ability. Other extraction methods should be utilized to further separate the compounds produced by *G. trabeum* in order to identify additional compounds with high iron reducing ability.

Chelator Production Versus Iron Concentration

Although ferrous iron was added into the modified Highley's liquid media at the final concentrations of 0, 20, 200, and 400 μM , most of the iron precipitated in the media. The soluble iron in the media before inoculation was 0, 2, 4, and 7 μM , respectively. In iron deficient Highley's media, 20 μM of ferrous iron is generally added (Jellison et al., 1991). Thus all the media were initially iron deficient media in terms of soluble iron (Table 2.3).

Table 2.3. Biochelator production by *Fomitopsis pinicola* versus iron concentration in 200 mL Highley's liquid media with 1% glucose as the carbon source. Data represents averages of three replicates.

Fe ²⁺ added (μ M)	Before fungal growth		After the fungal growth						
	Soluble Fe ²⁺ (μ M)	pH	Soluble Fe ²⁺ (μ M)	pH	Biomass (g)	Chelator production			
						Phenolate		Hydroxamic	
						μ M	μ mol/g	μ M	μ mol/g
0	0	3.87	5	3.30	0.06	8.10	27.00	0.05	0.20
20	2	3.92	16	2.44	0.26	16.50	12.70	0.12	0.10
200	4	3.7	209	2.68	0.26	18.30	14.10	12.50	9.60
400	7	3.51	376	2.81	0.24	16.00	13.60	12.00	10.20

The addition of ferrous iron decreased the pH of the liquid media. The pH values of the media of 0, 20, 200 and 400 μ M added iron before inoculation were 3.87, 3.92, 3.7, and 3.51, respectively (Table 2.3).

The growth of *F. pinicola* decreased the pH of the liquid media. The pH values of the media after one month of fungal growth were 3.30, 2.44, 2.68, and 2.81, respectively. The fungus grew poorly in the media without added iron. It showed similar levels of growth in the media containing 20, 200 and 400 μ M additional iron (Table 2.3).

The decreasing pH and the production of chelators and other fungal metabolites dissolved the precipitated iron. After the fungal growth, the iron concentrations were 5, 16, 209, and 376 μ M, respectively. The iron concentrations of 5 μ M and 209 μ M were higher than the original known iron concentrations of 0 μ M and 200 μ M. The small amount of extra iron may have come from iron contamination of chemicals used in media preparation (Table 2.3).

Under iron deficient conditions (0-20 μ M ferrous iron), more phenolate biochelators per gram of fungal biomass were produced than hydroxamic biochelators. Within this iron concentration range, the less iron available, the higher the amount of

phenolate derivative biochelators produced by unit amount of cells (Table 2.3). However, the fungal biomass was very limited in the media without iron added. About double the $\mu\text{M/g}$ of phenolate chelators were produced in the media with $0\mu\text{M}$ of ferrous iron compared to the other media with higher iron level. This suggests only a limited iron repressibility exists in *F. pinicola* compared to the higher levels of iron repressibility existed in previous work (Chen, 1994; Barton and Hemming, 1992).

Further increasing the amount of ferrous iron in the media to $200\mu\text{M}$ did not significantly affect the production of phenolate type biochelators, while the production of hydroxamic acid derivatives increased significantly (Table 2.3). This may indicate that different regulation mechanisms exist for the production of these two types of biochelators. When the amount of iron was increased to $400\mu\text{M}$, the production of either type of biochelators did not change (Table 2.3).

Fomitopsis pinicola grown in the modified Highley's liquid media ($20\mu\text{M}$ ferrous iron) with 1% cellulose and 0.2% glucose as the carbon source produced more hydroxamic acid derivatives (Figure 2.2). But most of the biochelators produced by *F. pinicola* grown in Highley's media ($20\mu\text{M}$ ferrous iron) with glucose as the sole carbon source were phenolate types (Table 2.3).

Modification of the Liquid Media Environment

Three representative fungi, *P. chrysosporium*, *G. trabeum* and *T. viride*, were selected for further examination (Figure 2.6).

pH Change. The growth of all three fungi caused the media pH to decrease with time from an original value of pH 4.5. The white rot fungus *P. chrysosporium* and the brown rot fungus *G. trabeum* decreased the pH gradually within the 4 weeks, while the non-

decay fungus *T. viride* decreased the pH sharply within the first week. In the following weeks, the pH decreased slightly or remained unchanged. At the end of 4 weeks of growth, *T. viride* caused the greatest pH decrease. *Phanerochaete chrysosporium* decreased pH more sharply than *G. trabeum* did within the first week, but by week four the decrease in pH by *P. chrysosporium* and *G. trabeum* was almost the same, 1.18 and 1.15 pH units respectively (Figure 2.6). In studies extending over longer periods, *G. trabeum* is usually observed to lower the pH to a greater extent than does *P. chrysosporium* (Jellison, unpublished).

Change of Extracellular Protein Concentrations. For *P. chrysosporium*, the extracellular protein concentration was greatest at week one, then decreased with time. For *T. viride*, the protein concentration was greatest after two weeks, then decreased with time. For *G. trabeum*, the protein concentration also was greatest at week one, then decreased with time until week four. At its highest concentration, *P. chrysosporium* produced the highest amount of extracellular protein (0.038 $\mu\text{g}/\mu\text{l}$). *Gloeophyllum trabeum* ranked second (0.034 $\mu\text{g}/\mu\text{l}$) and *T. viride* was the third (0.023 $\mu\text{g}/\mu\text{l}$). Data were not shown in Figure 2.6. The higher protein concentration at early weeks might be experiment errors caused by the nitrogen source in the liquid media. Alternative methods for protein concentration determination should be used to repeat this experiment.

Biochelator Production. Determined by the Rioux assay, *Gloeophyllum trabeum*, *P. chrysosporium* and *T. viride* all produced phenolate type chelators in this experiment. After grown in the modified Highley's liquid media for 4 weeks, *G. trabeum* produced the highest amount of phenolate chelator (26.99 μM) and *P. chrysosporium* produced the

least amount (14.67 μM). *Trichoderma viride* produced an intermediate level of phenolate type chelators (18.09 μM) (Figure 2.6).

When the phenolate biochelator production in modified Highley's liquid media was detected by the Arnou assay (Figure 2.2), *G. trabeum* produced about 32 μM phenolate compounds. *Trichoderma viride* produced about 6 μM phenolate compounds. The amount of phenolate biochelators produced by *P. chrysosporium* was not detectable. It's known that the Rioux assay is more sensitive than the Arnou assay since it has a broader spectrum of substrates. The Rioux assay detects both *p*-diol (hydroquinones) and *o*-diols (catechols), while the Arnou assay is specific for *cis*-diols (catechols) (Barton and Hemming, 1992). The amounts of phenolate biochelators produced by both *P. chrysosporium* and *T. viride* increased when the production was detected by the Rioux assay (Figure 2.2 and Figure 2.6), which can be easily explained by the property of the Rioux assay mentioned above. This implies *P. chrysosporium* and *T. viride* produce more hydroquinones than catechols. The differences between these two sets of experiments, such as culture temperatures, media compositions, ages of inoculums, and so on, can also contribute to the increasing production. The amounts of phenolate biochelators produced by *G. trabeum* decreased when the production was detected by the Rioux assay (Figure 2.2 and Figure 2.6), which may be due to the differences between these two sets of experiments mentioned above. It has been reported that *G. trabeum* produced much more catechol compounds than hydroquinone compounds (Jensen et al., 2001). Consequently it is expected that the Rioux assay and the Arnou assay should give similar results when used to detect the amounts of phenolate biochelators produced by *G. trabeum*.

Gloeophyllum trabeum, *P. chrysosporium* and *T. viride* all produced hydroxamic acid type chelators (Figure 2.6), which is consistent with the results obtained from the previous experiment shown in Figure 2.2. However, the amounts of hydroxamic biochelators produced by the same fungus varied in these two experiments (Figure 2.2 and Figure 2.6). At week four, the amounts of hydroxamates produced by *P. chrysosporium* were about 5 μM (Figure 2.6) and 18 μM (Figure 2.2), respectively. The amounts of hydroxamates produced by *T. viride* were about 35 μM (Figure 2.6) and 10 μM (Figure 2.2), respectively. The amounts of hydroxamates produced by *G. trabeum* were about 8 μM (Figure 2.6) and 17 μM (Figure 2.2), respectively. The reasons why the hydroxamate production was so different between these two experiments are not known.

Shown in the time study, the phenolate biochelator production and the hydroxamic biochelator production by the tested fungi changed irregularly between weeks. The reasons are not known. But overall, the concentration of phenolate type chelators was greatest at week four for all three fungi tested. The higher level of production of phenolates by *G. trabeum* was particularly pronounced during the early weeks (Figure 2.6). For all fungi tested the hydroxamate production was greatest at week three (Figure 2.6).

Cellobiose Dehydrogenase Activity. By monitoring DCPIP reduction, all three tested fungi showed detectable CDH activity (Figure 2.6). *Phanerochaete chrysosporium* and *G. trabeum* displayed a similar trend; from week one to week three, the activity decreased with time, then it increased at week four. *Phanerochaete chrysosporium* displayed its greatest CDH activity at week four and *G. trabeum* at week one. For *T. viride*, the CDH activity increased from week one to week two, maximizing at week two then decreased.

Quinone - Reducing Activity. The extracellular cellobiose dependent quinone reducing ability of the three fungi was studied by monitoring 2,3-dimethoxy-5-methyl-1,4-benzoquinone reduction,. At week one, none of the three fungi tested showed extracellular quinone - reducing activity. However, activity increased with time, maximizing at week three, then decreased. The liquid media of *T. viride* showed the highest amount of quinone reduction of the fungi tested (Figure 2.6). Average levels of quinone reduction ranged from below 2 U for *P. chrysosporium* at 2 weeks to over 12 U for *T. viride* at 2 and 3 weeks and 6 U for *G. trabeum* at 3 weeks.

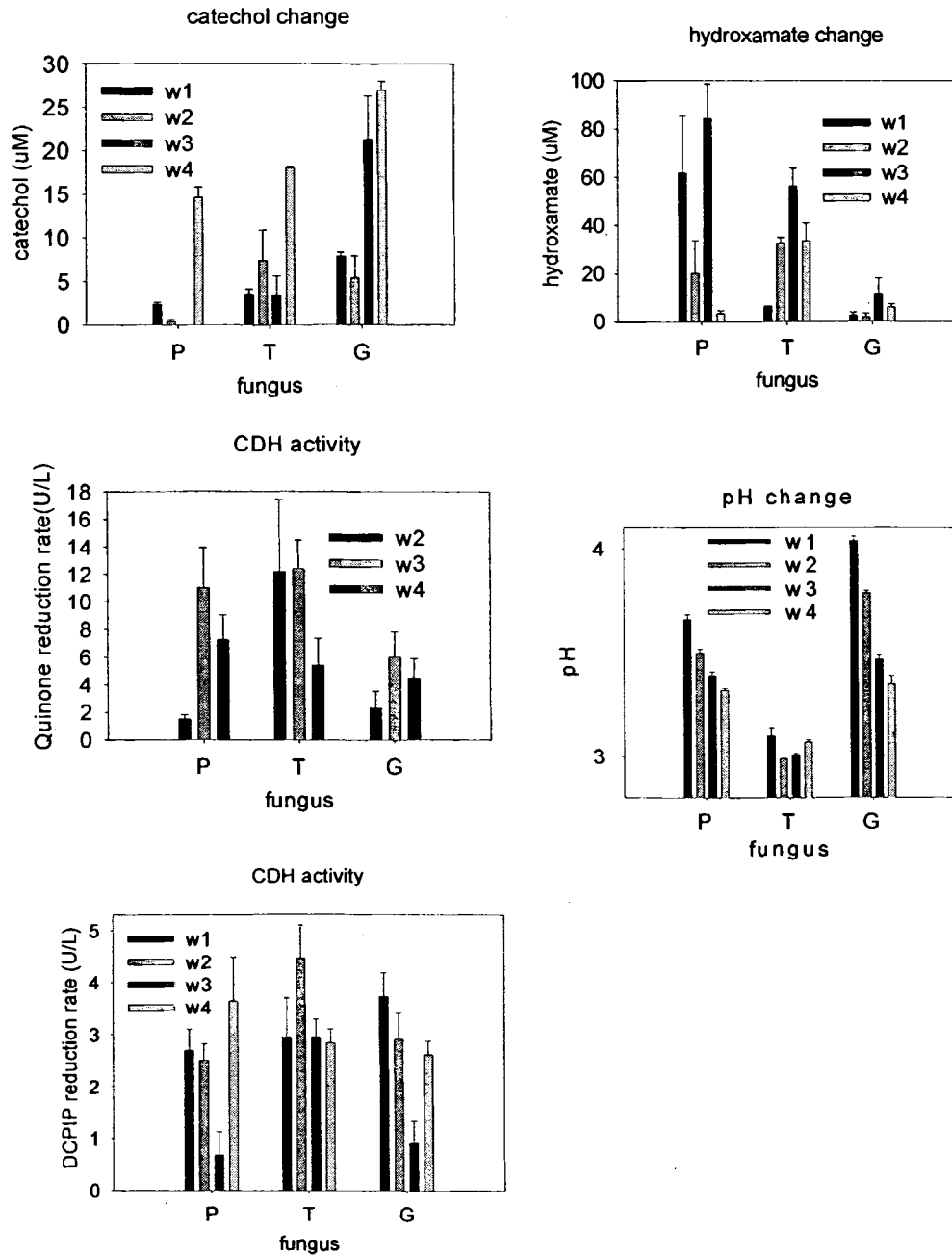


Figure 2.6. Changes of modified Highley's liquid media by fungal metabolites of a white rot, a brown rot and a non-decay fungus with time. "P", the white rot fungus *Phanerochaete chrysosporium*. "T", the non-decay fungus *Trichoderma viride*. "G", the brown rot fungus *Gleophyllum trabeum*. "W", the week. Cellobiose dehydrogenase activity was monitored by using two different electron acceptors, 2,6-Dichloroindophenol (DCPIP) and 2,3-dimethoxy-5-methyl-1,4-benzoquinone. 1 U = 1 $\mu\text{mol}/\text{min}$. The values shown were the averages and the standard deviations of triplicate samples.

Discussion

The soil block decay test confirms previous observations concerning different types of wood degradation. The wood-inhabiting non-decay fungus *T. viride* colonized but did not significantly decrease the weight of spruce blocks. The brown rot fungus *G. trabeum* caused rapid weight loss. The white rot fungus *P. chrysosporium* degraded wood and caused weight loss gradually (Worrall et al., 1997). Apparent weight loss was monitored in our decay test (Figure 2.1). Measurements of apparent weight loss may underestimate actual weight loss by up to as much as 42%. Work by Jones and Worrall (1993 and 1995) has showed that when the fungal biomass in decayed wood is measured by using glucosamine as an indicator, after 12 weeks of decay, birch blocks contain 31.3% *T. versicolor* fungal mass, and 9.0% *G. trabeum* fungal mass. Thus *G. trabeum* and *P. chrysosporium* actually cause more significant weight losses than what was observed in our decay test. Although it has not been studied, the *T. viride* inhabiting wood blocks might also contain certain amount of *T. viride* fungal mass.

After grown in the modified Highley's liquid media for 4 weeks, *Phanerochaete chrysosporium* produced more hydroxamic acid type chelator than phenolate type chelators. The reverse was seen for *G. trabeum*. *Trichoderma* also produced more hydroxamates than phenolates (Figure 2.2 and Figure 2.6). *Phanerochaete chrysosporium* produced the highest amount of hydroxamic acid type chelators, while *G. trabeum* produced the highest amount of phenolate types (Figure 2.2 and Figure 2.6). *Gloeophyllum trabeum* was characterized by an ability to produce much higher levels of phenolate chelators during the early weeks of growth than did either of the other fungi tested (Figure 2.6).

The phenolate compounds produced by different categories of fungi showed a differential partitioning in ethyl acetate extraction. Some phenolate type compounds produced by brown rot fungi could be extracted by ethyl acetate but none of those produced by the white rot fungi could (Figure 2.2). This may suggest some phenolate type compounds from the brown and white rot fungi are different in polarity, structure, and possibly function.

For most of the fungi, ethyl acetate extraction could efficiently exclude the hydroxamate type compounds, and most of these compounds were left in the aqueous fraction after extraction (Figure 2.2). This confirms the selectivity of the ethyl acetate extraction. The only exception was *G. trabeum* (Figure 2.2 B).

However, it can be observed that ethyl acetate fraction and the aqueous residue contained both phenolates and hydroxamates. This is because phenolates with higher polarity will be more difficult to extract completely in the ethyl acetate phase and hydroxamates with lower polarity will tend to be extracted in the ethyl acetate phase. Consequently it is an artificial way to label the ethyl acetate extraction as phenolates and the aqueous fraction as hydroxamates.

The culture filtrates from the brown rot fungi showed higher iron reduction ability than the culture filtrates from the white rot fungi (Table 2.2 and Figure 2.3). This suggests again that there are differences in function and structure between iron-chelators produced by the white rot and the brown rot fungi. It is interesting to note that the mixed compounds produced by the non-decay fungi (Table 2.2 and Figure 2.3), especially the compounds extracted by ethyl acetate (Table 2.2 and Figure 2.4), also show very high iron - reducing ability. This suggests that these non-decay fungi also produce biochelators

that can potentially play an important role in a chelator - driven Fenton reaction when other factors permit this to occur.

The relevance of these observations on biochelator production to decay mechanisms is not entirely clear. The ubiquitous production of biochelators by all fungi tested suggests that biochelators may play various roles in the physiology of fungi. For example, biochelators may act as laccase mediators, or participate in iron uptake.

We expected that biochelators extracted by ethyl acetate would have the highest iron reducing ability. This was only true for the non-decay fungus *P. mutiabilis* (Table 2.2). For all the other eight fungi tested, the ethyl acetate fraction showed a lower iron-reducing ability than did the aqueous fraction (Table 2.2), probably indicating incomplete extraction. When the three fractions from *G. trabeum* were analyzed with HPLC (Appendix D), it was found that in the ethyl acetate extraction, most compounds were iron reducing DHBA-like compounds. Lesser amounts of DHBA-like compounds were also found in the aqueous fraction. Thus the ethyl acetate extraction was selective but not complete for DHBA-like phenolate compounds. Increasing the times of ethyl acetate extraction or utilizing other extraction methods would help to isolate more phenolate compounds with iron reducing ability from the aqueous fraction.

Low levels of CDH activity were detected in *P. chrysosporium*, *G. trabeum* and *T. viride* by the reduction of DCPIP and 2,3-dimethoxy-5-methyl-1,4-benzoquinone (Figure 2.6). Presence of CDH activity in *P. chrysosporium* culture is consistent with previous research (Bao et al., 1993; Higham et al., 1994; Raices et al., 1995; Lehner et al., 1996; Li et al., 1996 and 1997; Igarashi et al., 1996, 1998 and 1999; Cohen et al., 1997; Henriksson et al., 1997 and 1998; Habu et al., 1993 and 1997; Vallim et al., 1998;

Cameron and Aust, 1999). This is the first report regarding the presence of CDH in *G. trabeum* and *T. viride* cultures. It has been reported that CDH was not produced by *G. trabeum* grown in glucose mineral media (Kerem et al., 1999). Our results, however, show CDH production in the presence of cellulose (Figure 2.6). The results confirm that CDH is a cellulose induced enzyme produced under cellulolytic conditions, and suggest that previous difficulties detecting CDH production (Kerem et al., 1999) may have been due to inappropriate culture conditions.

The low level and irregular CDH production over time might be because most CDH was absorbed on the surface of the cellulose. Shake cultures have been shown to increase the production and release of the CDH into liquid media (Igarashi et al., 1996). It has also been reported that supplementing the liquid media with bovine calf serum increases the CDH production in *P. chrysosporium* (Habu et al., 1997).

Genes encoding CDH in *P. chrysosporium*, *P. cinnabarinus*, *T. versicolor*, and *S. thermophile* have been cloned and characterized. The enzymes from different fungi showed high protein sequence identity (Raices et al., 1995; Li et al., 1996 and 1997; Vallim et al., 1998; Moukha et al., 1999; Dumonceaux et al., 1998; Subramaniam et al., 1999). Thus, it should also be possible to characterize the CDH in the brown rot fungi and the non-decay fungi directly at gene level.

CDH has been proposed to drive the Fenton reaction in white rot fungi (Cameron and Aust, 1999) and in the brown rot fungus *C. puteana* (Hyde and Wood, 1997) by reducing ferric iron and molecular oxygen. The quinone - reducing ability of CDH may contribute to the biochelator - driven Fenton reaction. It may also play a role in regenerating oxidized biochelators (Paszczynski et al., 1999; Kerem et al., 1999).

Biochelators are oxidized to quinones by reducing ferric iron (Goodell et al., 1997 (a) and (b); Paszczynski et al., 1999; Kerem et al., 1999). CDH may reduce the oxidized biochelators to corresponding hydroquinones/catechols by using cellobiose as the electron donor. Such a CDH mediated quinone redox cycle could be one possible pathway for the continuous iron reduction necessary to perpetuate the Fenton reaction. However, the electron donor of CDH, cellobiose, is a product of cellulases during enzymatic cellulose biodegradation, and the size of CDH is also too big for the enzyme to diffuse in the solid wood cell wall. As a result, regeneration of biochelators by the CDH mediated quinone redox cycle would be unlikely to occur at the early stage of brown rot decay. Alternate possibilities including biochelator mineralization may be more feasible (Goodell et al., 2001; Goodell, 2002; Pracht et al., 2001).

CDH may also participate in the production of hydroxamic acid type biochelators. It has been reported that CDH oxidizes cellobiose resulting from cellulose degradation to cellobionolactone, determined as a hydroxamic acid derivative (Westermarck and Eriksson, 1975; Higham et al., 1994). It was shown that the carbon source affected the production of biochelators by *F. pinicola*. When cellulose and glucose were used as the combined carbon source, the fungus produced about equal amounts of phenolate derivatives and hydroxamic acid derivatives in iron deficient media (20 μ M ferrous iron) (Figure 2.2). However, phenolate types were produced mostly when glucose was the only carbon source in iron deficient media (20 μ M ferrous iron) (Table 2.3). As noted in our work, CDH is a cellulose induced enzyme. Thus the presence of CDH under cellulolytic conditions might contribute to the increased production of hydroxamic acid derivatives by cultures grown on cellulose as a carbon source.

In our study, the wood-inhabiting non-decay fungi tested produced moderate levels of both phenolate type and hydroxamic acid type chelators (Figure 2.2 and Figure 2.6). The biochelators produced also showed iron - reducing ability, which was higher than the iron-reducing activity of the chelators produced by the white rot fungi and some of the brown rot fungi tested (Table 2.2, Figure 2.3, Figure 2.4 and Figure 2.5). *Trichoderma viride* caused a rapid pH decrease during the time period monitored and showed detectable CDH activity (Figure 2.6).

Although not measured in this study, *Trichoderma* is known to produce large amounts of cellulase and other degradative enzymes. *Trichoderma reesei* and *T. viride* have been used for the commercial production of cellulase (Samuels, 1996). It has also been reported that when the ability of different fungi to penetrate micropores of various pore size in polycarbonate membranes was tested, the non-decay fungi *Aureobasidium pullulans* and *Sclerophoma pityophila* were able to penetrate micropores of very small dimensions (0.2 μm) rapidly and caused erosion. Neither *G. trabeum* nor *P. chrysosporium* could penetrate the membranes (Bardage and Geoffrey, 1998). However, as shown in the soil block decay test, *Trichoderma viride* did not degrade spruce blocks. The ability of a non-decay fungus such as *Trichoderma* to produce many of the components postulated to be involved in wood biodegradation is still not explained and clearly has implications for understanding wood degradation and preservation.

It should be noted that in the pH change time study, *Trichoderma* decreased the pH sharply in the modified Highley's media at the first week and made the pH much lower than the pH detected in cultures of *G. trabeum* and *P. chrysosporium* at the same growth time. pH reduction may be one of the mechanisms used by *Trichoderma* during

competitive growth to modify the environment for fast establishment of itself. In the dual agar cultures of *Trichoderma virens* with the white rot fungi: *T. versicolor*, *Phlebia brevispora*, *Irpex lacteus*, and the brown rot fungi, *P. placenta*, *Neolentinus lepideus*, and *G. trabeum*, *Trichoderma* rapidly overgrew and killed the decay fungi (Highley, 1997; Highley et al., 1997). Although the filter-sterilized filtrates from *T. virens* showed a similar fungistatic effect against the decay fungi in agar media, weight loss in wood blocks treated with such filtrates was only slightly reduced when exposed to decay fungi in soil-block tests. Thus, living *T. virens* was needed to inhibit wood decay. *Trichoderma* species have also been used in biological control of several plant diseases (Highley, 1997; Highley et al., 1997).

In summary, all fungal species tested could produce iron chelators, but the patterns of production and iron - reducing abilities varied, which indicates biochelators produced by different categories of fungi may be different in structure and function. The ubiquitous production of biochelators by the fungi tested suggests biochelators may play a role in general fungal physiology, such as iron uptake. Biochelators from the brown rot fungi showed higher iron reduction ability than did those from the white rot fungi. The brown rot fungus *Fomitopsis pinicola* produced biochelators with the highest iron - reducing ability. These results support the theory that biochelator mediated Fenton reactions play a role in brown rot biodegradation of wood.

In the presence of cellulose, all the fungi tested produced low levels of CDH activity in the media. The results are consistent with the observations that the enzyme is induced by cellulose but little of the activity is released into the media because the enzyme is bound to cellulose strongly via a cellulose - binding site. CDH might help

mediate an extracellular quinone redox cycle by which oxidized biochelators can be reduced, but the absence of the electron donor (cellobiose) at the early non-enzymatic decay stage and the size of the enzyme suggest that a CDH mediated quinone redox cycle would not occur at the initial decay stage.

Chapter 3

PROPERTIES OF A TRANSPLASMA MEMBRANE REDOX SYSTEM OF THE BROWN ROT FUNGUS *GLOEOPHYLLUM TRABEUM*

Abstract

Ubiquitous transplasma membrane systems contribute to quinone reduction, which is an important reaction in fungal physiology. A transplasma membrane redox system of the brown rot fungus *Gloeophyllum trabeum* was characterized based upon its ferricyanide reduction kinetics. Nitrogen deficiency did not statistically affect the ferricyanide reduction rates, but carbon limitation decreased the reduction activity. Ferricyanide reduction rates depended on initial ferricyanide concentration and initial mycelial mass. Reduction rates were within linear range when the ferricyanide concentration was up to 20 mM and when mycelial mass was up to 120 mg (dry weight) in 200 mM potassium phosphate buffer (pH 8.0). Specific activity of approximately 12 nmol/min/mg of mycelia (dry weight) was obtained in potassium phosphate buffer (pH 8.0, 200 mM) with 10 mM ferricyanide and 97 +/- 3 mg dry weight of mycelia. The rates increased with pH above the fungal physiological pH (pH 5). Ferricyanide reduction was inhibited by carbonyl cyanide m-chloromethoxyphenyl hydrazone, 2,4-dinitrophenol (DNP-OH) and sodium azide at 100 nmol/mg mycelia (dry weight) but not by potassium cyanide. The ferricyanide reduction rate was statistically lower in HEPES buffer (pH 8.0) than in potassium phosphate buffer (pH 8.0). The plasma membrane redox system of *G. trabeum* showed 1,4-quinone - reducing ability. The reaction had an optimum pH of 7.0, a K_m of 59 μ M, and a V_{max} of 17.5 nmol/min/mg mycelia (dry weight). *Gloeophyllum*

trabeum also produced intracellular NAD(P)H dependent 1,4-benzoquinone reductases. Reduction of 1,4-benzoquinone by the crude intracellular enzyme extract had a pH optimum of 6.5, a K_m of 156 μM , and a V_{max} of 863 nmol/min/mg protein.

Introduction

A membrane-bound redox system with quinone-reducing ability (Fernando et al., 1990; Stahl and Aust, 1993 and 1995; Stahl et al., 1995) has been characterized in the white rot fungus *Phanerochaete chrysosporium*. The transplasma membrane redox system (PMRS) is the plasma membrane-bound electron transport chain or the plasma membrane-bound oxidoreduction system that is ubiquitous in all organisms. The enzyme activities associated with PMRS include ferrireductase, NADH:ubiquinone oxidoreductase, NADH:acceptor oxidoreductase and many others. The primary electron donors are cytoplasmic NADH and NADPH. The electron acceptors include molecular oxygen, ferric ions, ascorbate free radicals, and quinones. Quinones and non-heme iron have also been found as the cofactors of some systems (Medina et al., 1997). For example, animal PMRSs contain ubiquinone as an electron shuttle (Sun et al., 1992). The quinone vitamin K is in plant plasma membranes (Barr et al., 1990). Several NAD(P)H-quinone oxidoreductases have been purified from the plasma membrane of higher plants (Berczi and Moller, 2000). Sodium transport NADH-quinone reductases have been purified from many bacteria (Unemoto and Hayashi, 1993).

PMRSs contribute to many important cell functions, such as modulation of membrane potential, proton extrusion and control of internal pH, and iron uptake and cell defense (Medina et al., 1997). For example, a cytochrome system that directly drives iron

uptake at the plasma membrane of plant cells (Lundegardh, 1945), an inducible Turbo system for iron reduction and uptake in plant root cells (Bienfait, 1985), and a membrane – bound ferrireductase system in yeast *Saccharomyces cerevisiae* (Lesuisse et al., 1996) have been studied. The PMRS in *S. cerevisiae* has also been proposed to drive potassium - proton and potassium - sodium exchange (Conway and Kernan, 1955). The PMRS in the mold *Dendryphiella salina* has been suggested to be involved in the oxidation and reduction of polyols (Medina et al., 1997). The NAD(P)H-quinone oxidoreductases in plant PMRSs may act as antioxidants in cell defense (Medina et al, 1997). The NADH quinone reductases in bacterial PMRSs play an important role in bacterial energetics (Unemoto and Hayashi, 1993). The PMRS of the white rot fungus *P. chrysosporium* has been found to be able to reduce free radicals and several quinones (Stahl et al., 1995). It has been proposed that the *P. chrysosporium* PMRS plays an important role in extracellular pH regulation, bioremediation of highly oxidized contaminants, and cell protection against the extracellular free radical generating ligninolytic systems (Stahl et al., 1995). Traditionally PMRSs have been studied by using membrane impermeable electron acceptors such as ferricyanide on intact cells and characterized regarding the kinetics of ferricyanide reduction (Conway and Kernan, 1955; Crane et al., 1982; Medina et al., 1997).

The role of membrane bound redox systems in brown rot fungi has not been extensively studied. Intact hyphae of *G. trabeum* have been found to reduce 2,5-dimethoxy-1,4-benzoquinone (2,5-DMBQ) in sodium phosphate buffer (50 mM, pH 4.1) (Kerem et al., 1999). It has also been reported that intact *G. trabeum* hyphae can reduce 2,3-dimethoxy- 5-methyl-1,4-benzoquinone added into a basal media, although

extracellular quinone - reducing activity has not been detected on basal media alone (Kerem et al., 1999). Purification and further characterization of this activity has not previously been attempted.

In this study, the reduction of 1,4-quinone by intact *G. trabeum* hyphae and by the crude intracellular enzyme extract from *G. trabeum* (Brock et al., 1995) was studied and compared. The transplasma membrane redox system of *G. trabeum* was characterized based on the kinetics of ferricyanide reduction. The purpose of this work was to better understand the characteristics of *G. trabeum* PMRS and what role it might play in biodegradative processes and basic fungal physiology.

Materials and Methods

Organism and Culture Conditions

Stock cultures of *Gloeophyllum trabeum* ATCC 11539 were maintained on Difco® malt extract agar slants at 4 °C. Cultures were grown on BBL® potato dextrose agar (PDA) plates (20 mL/plate) at 30 °C for a week. The PDA with the fungus was homogenized with sterile distilled water at the ratio of 1:4 (weight ratio) in a sterile Osterizer® blender aseptically, three times in 15-second bursts with 1 minute between each burst. The resulting mixture was used to inoculate aseptically the stationary 4-liter PYREX® flasks that contained 90 mL of basal growth media (Tien and Kirk, 1988). Ten mL homogenate was inoculated into each flask (Kerem et al., 1999). The nitrogen levels of the basal media were 1.1 mM (low - nitrogen) and 11 mM (high - nitrogen), respectively. Cultures were grown at 30 °C for one week.

Collection of Mycelia Mass

The mycelia were collected by vacuum filtration through Whatman® No. 2 filters and washed with an equal volume of 4 °C deionized distilled water.

Determine Mycelial Wet Weight Versus Dry Weight

Different amounts of fresh mycelia were dried by lyophilization using a VirTis® Lyophilizer. The dry weights were measured and plotted versus the wet weights.

Ferricyanide Reduction

In a typical reaction (Stahl and Aust 1995, Avron and Shavit 1963), washed mycelia (97 +/- 3 mg, dry weight) were incubated with ferricyanide (10 mM) in 200 mM potassium phosphate buffer (pH 8.0) for 5 minutes. The total volume was 5 mL. The assays were carried out in 20 mL PYREX® beakers and run through Whatman® glass microfibre filters at the end of the reaction time. The ferrocyanide concentration was determined spectrophotometrically (Avron and Shavit, 1963) at 535 nm. The molar absorbance coefficient of ferrocyanide was $10,800 \text{ M}^{-1}\text{cm}^{-1}$. The dry weight of the mycelia was determined via the standard curve prepared.

Inhibition of Ferricyanide Reduction

Washed mycelia (100 +/- 10 mg dry weight) were suspended in 65 mL potassium phosphate buffer (200 mM, pH 8.0) containing 200 μM of the inhibitor being tested. Potassium cyanide (KCN, 10 mM) and sodium azide (NaN_3 , 10 mM) were prepared in water. Carbonyl cyanide m-chlorophenyl hydrazone (CCCP, 10 mM) and 2,4-

dinitrophenol (DNP-OH, 10 mM) were prepared in acetone. Water or acetone alone added to the buffer represented the controls. The mycelia – buffer mixtures were pre-incubated for 15 minutes with each inhibitor or control (Stahl and Aust, 1995). Potassium ferricyanide was subsequently added and the mixtures were further incubated for 5 minutes. Ferricyanide reduction was detected as described previously.

Effects of Buffers on Ferricyanide Reduction

The assays were carried out with 35 +/- 2 mg of mycelia (dry weight) in 5 mL of 200 mM, pH 8.0 potassium phosphate buffer, sodium phosphate buffer, or HEPES (N-[2-Hydroxyethyl]piperazine-N'-[2-ethanesulfonic acid) buffer as described previously.

Effect of pH on Ferricyanide Reduction

The assays were carried out with 97 +/- 3 mg of mycelia (dry weight) in 5 mL of 200 mM phosphate buffer (pH 6 to 8) or 200 mM sodium citrate buffer (pH 3 to 5) as described previously.

Quinone Reduction by Intact Hyphae or Lysed Hyphae

Lysed mycelia were obtained by breaking mycelia in an Osterizer® blender with 50 mM sodium phosphate buffer (pH 7.0), followed by centrifuging at $17,418 \times g$ for 20 minutes (Beckman J2-21 centrifuge with a JA-20 rotor). The pellet was collected. Fresh mycelia or lysed mycelia (27 to 30 mg, dry weight) was added into 5.0 mL pH 8.0 (unless otherwise noted) 200 mM potassium phosphate buffer with 80 μ M 1,4 benzoquinone (Stahl et al., 1995). The assays were carried out in 20 mL PYREX® beakers and run

through Whatman® glass microfibre filters at the end of the reaction time. The product 1,4-hydroquinone was detected at 288 nm with extinction coefficient as $2670 \text{ M}^{-1}\text{cm}^{-1}$. The absorbance was corrected for the contribution by the reactant 1,4-benzoquinone at 288 nm with extinction coefficient as $450 \text{ M}^{-1}\text{cm}^{-1}$. The reactant 1,4-benzoquinone was detected at 245 nm with extinction coefficient as $15600 \text{ M}^{-1}\text{cm}^{-1}$. Each reaction was carried out with three replicates.

Effect of pH on Quinone Reduction by Intact Hyphae

The assays were carried out with 27 +/- 3 mg of mycelia (dry weight) in 200 mM phosphate buffer (pH 6.5 to 8.7) or 200 mM sodium citrate buffer (pH 4.5 to 6) as described previously.

Quinone Reduction by the Culture Filtrate

Cellobiose dehydrogenase catalyzed quinone reduction was carried out at 30 °C in 1.9 mL of 50 mM sodium tartrate, pH 4.0 buffer containing 500 µM cellobiose and 250 µM 2,3-dimethoxy-5-methyl-1,4-benzoquinone. The reaction was initiated by adding 0.1 mL of the liquid fraction. Activity was measured as the decrease of absorbance at 375 nm. The extinction coefficient of 2,3-dimethoxy-5-methyl-1,4-benzoquinone was $1.2 \text{ mM}^{-1} \text{ cm}^{-1}$ (Samejima and Eriksson, 1992).

Preparation of Intracellular Enzyme Extract

The protocol was modified from the procedure described by Brock and colleagues (1995). Frozen mycelia were broken in an Osterizer® blender with extract buffer (50 mM

sodium phosphate pH 7.0, 1 mM EDTA, 0.004% phenylmethylsulfonyl fluoride), transferred to a VWRbrand® tissue grinder, and homogenized three times. The homogenate was centrifuged at $17,418 \times g$ for 20 minutes (Beckman J2-21 centrifuge with a JA-20 rotor) and the supernatant was collected.

Quinone Reduction by the Intracellular Enzyme Extract

Intracellular quinone - reducing activity was determined by following the oxidation of NADH at 340 nm (Brock et al., 1995). Standard reaction mixtures in 1 mL consisted of 50 mM sodium citrate buffer (pH 6.0), 100 μ M 1,4-benzoquinone, and 0.01 mL of enzyme extraction. Reactions were initiated by the addition of 200 μ M NADH. Reaction time was 10 minutes. Enzyme assays were carried out at room temperature with a Beckman DU®-64 spectrophotometer.

Effect of pH on Quinone Reduction by the Intracellular Enzyme Extract

The assays were carried out with 0.01 mL of the intracellular enzyme extract in 50 mM phosphate buffer (pH 6.5 to 8.7) or 50 mM sodium citrate buffer (pH 4.5 to 6) as described previously.

Protein Concentration

Protein concentrations were measured by the Lowry assay (Lowry et al., 1951), with bovine serum albumin as the protein standard.

Results

Nitrogen deficiency limited the growth of *G. trabeum* in the shallow basal media (Table 3.1). After one week of growth, the mycelial mass in nitrogen sufficient media (11 mM of ammonium) was 0.9 mg/mL, while that in nitrogen deficient media (1.1 mM of ammonium) was only 0.3 mg/mL.

The ferricyanide reduction rate of the *G. trabeum* PMRS was statistically the same for the mycelia grown in nitrogen deficient media and the mycelia grown in nitrogen sufficient media. However, the older mycelia from both media lost about half of their reduction capability (Table 3.1). The decrease of reduction capability may be because the older cultures contain a greater amount of inactive hyphae.

The mycelial mass from nitrogen deficient media was used in this study in order to simulate the nitrogen deficient wood environment.

Table 3.1. Effect of nitrogen deficiency on ferricyanide reduction and growth of *G. trabeum* ^a.

Culture age (week)	Fungal growth and ferricyanide reduction			
	1.1mM of ammonium		11mM of ammonium	
	Ferricyanide reduction rate (nmol/mg/min)	Mycelia mass (mg/mL, Wet weight)	Ferricyanide reduction rate ^b (nmol/mg/min)	Mycelia mass ^c (mg/mL, Wet weight)
1	12 +/- 1.9	0.3 +/- 0.05	10.9 +/- 2.1	0.9 +/- 0.03
2	5.5 +/- 2.46	0.3 +/- 0.03	4.5 +/- 0.95	1.2 +/- 0.04

^a Ferricyanide reduction rates were determined by using 76 +/- 15 mg (dry weight) washed mycelia. All data represent averages and standard deviations of triplicate samples.

^b The ferricyanide reduction rate of mycelia from the nutrient sufficient condition was statistically the same as that from the nutrient deficient condition at $P < 0.05$.

^c The mycelia mass from the nutrient sufficient condition (11 mM nitrogen) was statistically higher than that from nutrient deficient condition (1.1 mM) at $P < 0.05$.

To find out the linear range of the reaction, we studied the effects of reaction time, concentration of ferricyanide, and amount of mycelia on ferricyanide reduction (Figure 3.1). The reaction was within a linear range when the reaction time was less than or equal to 5 minutes, when the ferricyanide concentration was up to 20 mM, and when the mycelial amount was up to 120 mg (dry weight). The linear regression correlation coefficients were 0.9959, 0.9906, 0.9267, respectively. Specific activity of 12 nmol/min/mg (mycelial dry weight) was obtained with 10 mM ferricyanide and 97 +/- 3 mg dry weight of mycelia in pH 8.0 potassium phosphate buffer after 5 minutes. The mycelial wet weight or dry weight was estimated based on the standard curve (Figure 3.1).

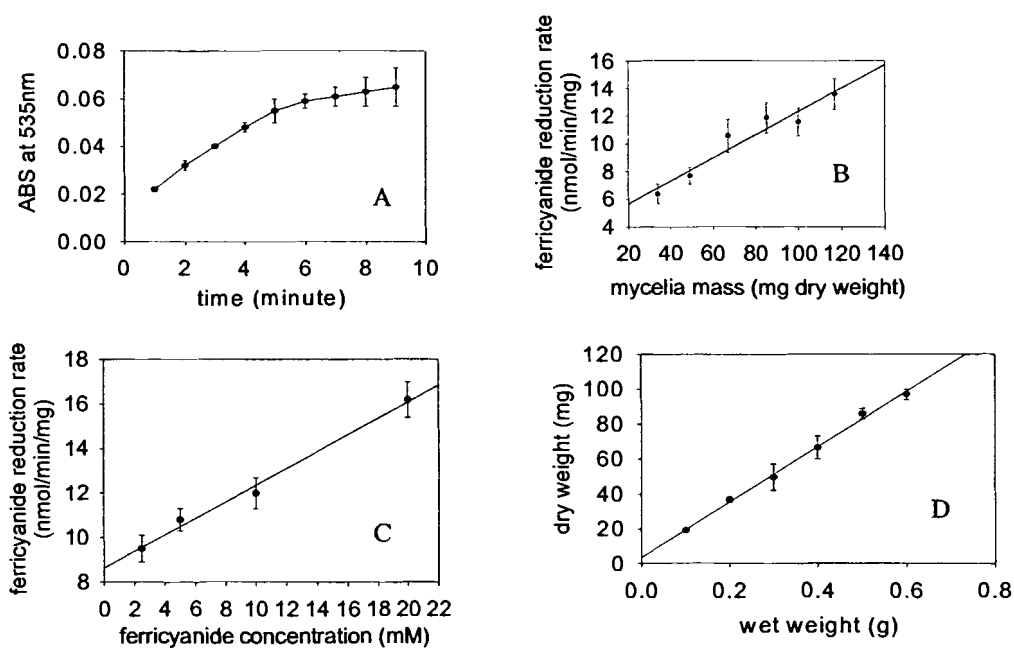


Figure 3.1. Reduction of ferricyanide by *G. trabeum* mycelia (A) at different reaction times, (B) at different amounts of mycelial mass, and (C) at different concentrations of ferricyanide. The reduction was linear when the reaction time was within 5 minutes, the ferricyanide concentration was up to 20 mM and when the mycelial mass was up to 120 mg. (A) 89.5 \pm 1.5 mg (dry weight) washed mycelia were used for each reaction. $R^2 = 0.9959$. (B) Indicated amounts of washed mycelia (mg dry weight) were used for each reaction. $R^2 = 0.9267$. (C) 97 \pm 3 mg (dry weight) washed mycelia were used for each reaction. (D) The plot of the wet weight versus the dry weight of *G. trabeum* mycelia. The mycelia were dried by lyophilization. $R^2 = 0.9961$.

The ferricyanide reduction rate by *G. trabeum* mycelia increased with pH above

5. The reduction rate was 1nmol/min/mg at pH 3, 4 and 5 (Figure 3.2).

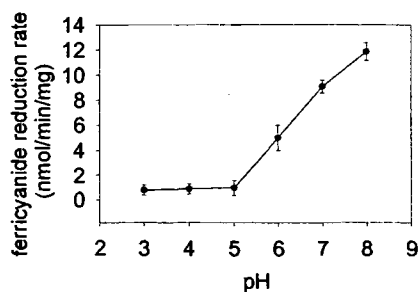


Figure 3.2. Effect of pH on ferricyanide reduction by *G. trabeum* mycelia. The reduction rate increased with pH above pH 5. 97 +/- 3 mg (dry weight) washed mycelia were used for each reaction.

The effects of inhibitors on ferricyanide reduction by *G. trabeum* were studied at the ratio of 100 nmol/mg (Table 3.2). At this ratio, ferricyanide reduction by *G. trabeum* was inhibited by sodium azide, carbonyl cyanide m-chlorophenyl hydrazone, and 2,4-dinitrophenol, but not by potassium cyanide.

Table 3.2. Effect of inhibitors on ferricyanide reduction rates by *G. trabeum*. The ratio of inhibitor / mycelia is 100 nmol/mg.

Inhibitors	Ferricyanide reduction rate (nmol/mg/min)
Water	12.1
KCN	10.7
NaN ₃	8.6
Acetone	11.8
CCCP	7.5
DNP-OH	8.7

The effect of three different pH 8.0 buffers on ferricyanide reduction in *G. trabeum* were studied. The ferricyanide reduction rate was higher in potassium phosphate buffer than in HEPES buffer (Table 3.3).

Table 3.3. Effect of buffers on ferricyanide reduction and proton excretion by the plasma membrane redox system in *G. trabeum*.

Buffer ^a	Ferricyanide reduction rate ^b (nmol/mg/min)
KH ₂ PO ₄ /K ₂ HPO ₄	9.3+/-0.7
NaH ₂ PO ₄ /Na ₂ HPO ₄	6.4+/-0.5
HEPES	4.5+/-0.6

^a. Buffers are 200 mM, pH 8.0.

^b. Washed mycelia 35 +/- 2 mg were used for each reaction.

Quinone reduction was studied by using one-week old nitrogen deficient cultures of *G. trabeum* with 1,4-benzoquinone as the substrate. The 1,4-benzoquinone was reduced by intact hyphae but not by lysed mycelia or the extracellular basal media. The intracellular enzyme extract required either NADH or NADPH for quinone – reduction (Table 3.4).

Table 3.4. Reduction of 1,4-benzoquinone by the culture filtrate, hyphae, and intracellular enzyme extract of *G. trabeum* grown in the shallow basal media.

Fraction	Rate (nmol/min/mg)*	
Culture filtrate	0	
Washed mycelia	17 +/- 4	
Lysed mycelia	0	
Intracellular enzyme extract	+NADH	+NADPH
	385 +/- 20	503 +/- 7

* The non-enzymatic reduction of 1,4-benzoquinone was subtracted.

Quinone reduction by both the plasma membrane redox system and the intracellular enzyme extract was saturable, although the K_m and V_{max} values are quite different (Figure 3.3). Reduction of 1,4-benzoquinone by the *G. trabeum* PMRS had a K_m of 59 μ M, and a V_{max} of 17.5 nmol/min/mg mycelia (dry weight). Since it required 36 mg (dry weight) of mycelia to produce 1 mg intracellular protein (data not shown), the maximum reduction rate was 630 nmol/min/mg protein. Reduction of 1,4-benzoquinone by the crude *G. trabeum* intracellular enzyme extract had a K_m of 156 μ M, and a V_{max} of 863 nmol/min/mg.

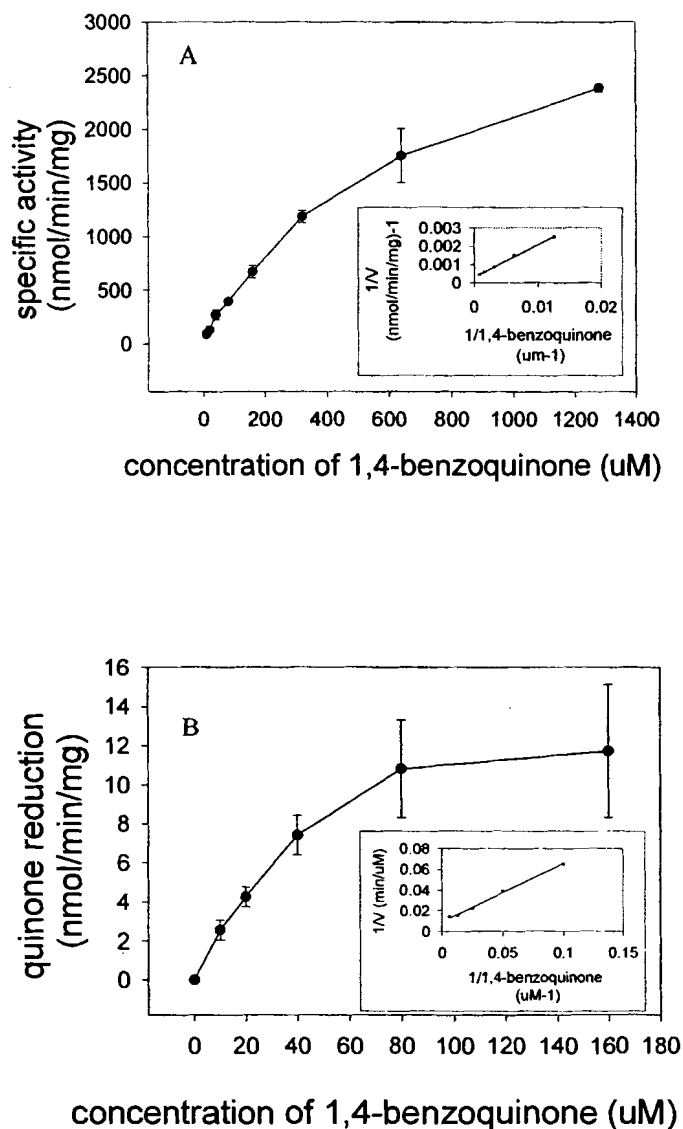


Figure 3.3. Effect of 1,4-benzoquinone concentrations on quinone reduction by *G. trabeum* intracellular enzyme extract (A) and *G. trabeum* mycelia (B). (A) The enzyme activity was based on nmole of NADH oxidized per mg of intracellular protein. In the Lineweaver - Burk plot, $R^2 = 0.9984$, $V_{max} = 863 \mu\text{M}/\text{min}$ and $K_m = 156 \mu\text{M}$. (B) The assay was performed with 30 ± 1 mg (dry weight) washed mycelia. The reduction rates were based on nmole of 1,4 -benzoquinone reduced per mg dry weight of mycelia. In the Lineweaver -Burk plot, $R^2 = 0.9964$, $K_m = 59 \mu\text{M}$, $V_{max} = 17.5 \text{ nmol}/\text{min}/\text{mg}$.

The optimum pH of the intracellular quinone - reducing activity was between pH 6.0 to 8.0. The optimal pH of the PMRS was between pH 4.0 to 7.0 (Figure 3.4).

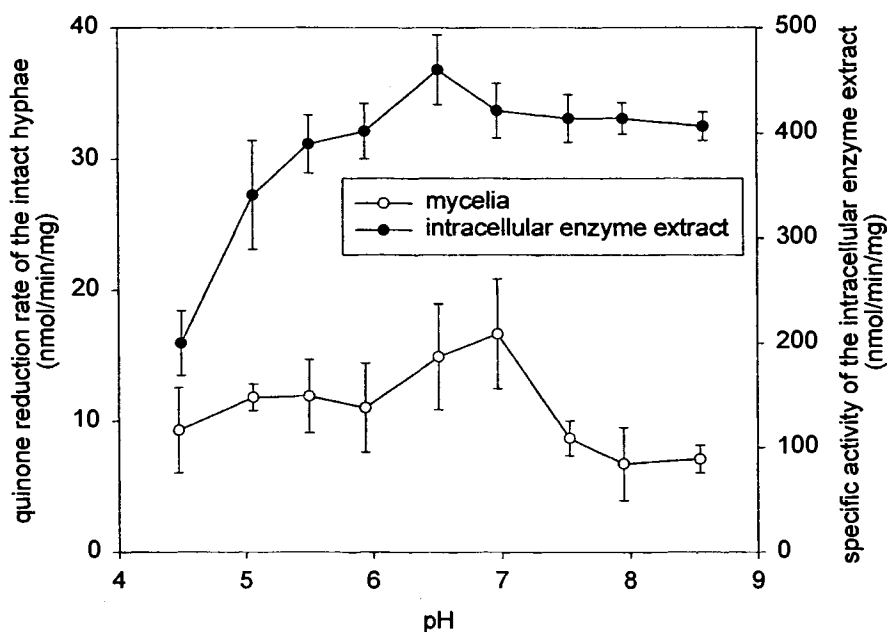


Figure 3.4. Effect of pH on 1,4-benzoquinone reduction by *G. trabeum* mycelia and the intracellular enzyme extract. The reduction was measured with 27 +/- 3 mg (dry weight) mycelia or 0.1 mL of enzyme extract in the 200 mM potassium phosphate buffer at indicated pH, with 100 mM 1,4 - benzoquinone. Reduction rates of washed mycelia were based on nmol of 1,4 - benzoquinone reduced per mg dry weight mycelia. Specific activities of enzyme extracts were based on nmol of NADH oxidized per mg intracellular protein.

Discussion

In this study a transplasma membrane redox system from the brown rot fungus *G. trabeum* was characterized by the reduction kinetics of the membrane impermeable one - electron acceptor ferricyanide. Ferricyanide reduction by intact hyphae of *G. trabeum* and *P. chrysosporium* (Stahl et al., 1995) displayed similar dependences on reaction time, mycelia mass, ferricyanide concentration, and pH, although the *G. trabeum* mycelia were obtained from nitrogen deficient basal media, while *P. chrysosporium* mycelia were from nitrogen sufficient basal media (Table 3.1, Figure 3.1, and Stahl et al., 1995). Results also showed that the ferricyanide reduction rate of the *G. trabeum* PMRS was not affected by the nitrogen level in the media (Table 3.1).

Ferricyanide reduction by *G. trabeum* and *P. chrysosporium* PMRSs was inhibited by sodium azide, carbonyl cyanide m-chlorophenyl hydrazone (CCCP), and 2,4-dinitrophenol (DNP) (Table 3.2, and Stahl et al., 1995). Potassium cyanide did not inhibit the ferricyanide reduction (Table 3.2, and Stahl et al., 1995). Azide, CCCP, and DNP are all known inhibitors of membrane redox systems and electron transport chains (Blum et al., 1993). Sodium azide and potassium cyanide have been reported to inhibit flavoproteins (Brock and Gold, 1996). DNP, a non-specific uncoupler, has been reported to inhibit the F₀F₁ ATP synthase molecule located in the inner wall of each mitochondrion (Bachs, 1999). CCCP is a protonophore and an effective uncoupler of oxidative phosphorylation (Cervinkova et al., 1998).

Ferricyanide reduction by both *G. trabeum* and *P. chrysosporium* PMRSs (Figure 3.2, and Stahl et al., 1995) was pH dependent and sensitive to the protonophore CCCP, suggesting a proton coupled reduction mechanism (Gear et al., 1999). In all the cells

tested, the functioning of PMRSs is accompanied by acidification of the media. It has been known that an important function of PMRSs is proton extrusion and control of internal and extracellular pH (Medina et al., 1997; Schafer and Buettner, 2000). Proton extrusion coupled PMRS activity has been observed for *P. chrysosporium* (Stahl et al., 1995). It is known that wood decay fungi can decrease the extracellular pH significantly during growth (Chapter 2 and 5). The mechanisms utilized by fungi to decrease the extracellular pH have not been elucidated completely. Production of organic acids such as oxalic acids by fungi has been studied widely and is considered as one of the important pH adjusting strategies. In environments with pH higher than the optimum pH for fungal growth, proton extrusion rate increases with increasing pH. This observation implies that extrusion of protons during PMRS activities may also contribute to the extracellular pH adjustment by fungi.

Effects of buffers (pH 8.0) on the ferricyanide reduction by *G. trabeum*, however, were different from those by *P. chrysosporium*. In *P. chrysosporium*, the ferricyanide reduction rate was statistically the same in phosphate buffer (pH 8.0) as in HEPES buffer (pH 8.0) (Stahl et al., 1995). In *G. trabeum*, the ferricyanide reduction rate was higher in potassium phosphate buffer than in HEPES buffer (Table 3.3). HEPES cannot cross the membrane, while phosphate can (Stahl et al., 1995). But the ferricyanide reduction rate was similar in sodium phosphate buffer and HEPES buffer (Table 3.3). Thus it is possible that the electron transport in *G. trabeum* PMRS may be coupled with potassium transport. This result is consistent with previous studies, in which the reduction of ferricyanide was coupled with potassium - proton exchange in the yeast *S. cerevisiae* (Conway & Kernan, 1955). It has also been reported that the reduction of methylene blue

by *S. cerevisiae* cells was strongly inhibited by sodium ions added to the media (Ryan, 1967).

The intact hyphae of *G. trabeum* could reduce 1,4-benzoquinone (Table 3.4), which is consistent with previous observation with 2,5-dimethoxy-1,4-benzoquinone and 2,3-dimethoxy-5-methyl-1,4-benzoquinone (Paszczynski et al., 1999; Kerem et al., 1999). The intracellular enzyme extract from *G. trabeum* also showed 1,4-quinone - reducing ability, which suggests that *G. trabeum* produces a certain level of constitutive intracellular quinone reductases (Table 3.4).

The 1,4-quinone reduction by intact hyphae of *G. trabeum* and *P. chrysosporium* showed different optimal reaction pHs and substrate saturation levels (Figure 3.3 and Figure 3.4). Reduction of 1,4-benzoquinone by *P. chrysosporium* PMRS had an optimum pH between 7.5 and 8.5, a K_m of 11 μM , and a V_{max} of 16 nmol/min/mg (dry weight mycelia) (Stahl et al., 1995). Although the maximum reaction rates with the two systems were similar, the redox system of *G. trabeum* required about 5 times more quinone to become saturated (Figure 3.3, Figure 3.4, and Stahl et al., 1995). This suggests that *P. chrysosporium* PMRS is potentially more efficient than *G. trabeum* PMRS in quinone reduction.

The intracellular enzyme extracts from *G. trabeum* and *P. chrysosporium* had similar optimal reaction pHs, substrate saturation values and maximum reaction rates (Figure 3.3, Figure 3.4, and Stahl et al., 1995). They both utilized NADH or NADPH as electron donors for quinone reduction (Table 3.4, and Stahl et al., 1995). For the intracellular enzyme extract from *P. chrysosporium*, the quinone reduction rate with NADH was approximately six times faster than that with NADPH. With NADH as the

electron donor, it had a pH optimum between 6 and 7, a K_m of 150 μM and a V_{max} of 800 nmol/min/mg (Stahl et al., 1995). For the intracellular enzyme extract from *G. trabeum*, the quinone reduction rate with NADH and NADPH was similar (Table 3.4).

The extracellular basal media after the growth of *G. trabeum* did not reduce 1,4-benzoquinone (Table 3.4). This result confirms the previous studies (Schimidhalter and Canevascini, 1993 (a) and (b); Qi and Jellison, 2000) in which it was concluded that the extracellular cellobiose dependent quinone - reducing ability was induced in the presence of cellulose but not glucose.

Both the intact hyphae and intracellular enzyme extract from *G. trabeum* could reduce 1,4-benzoquinone, but the optimum reaction pH, K_m , and V_{max} were different (Figure 3.3, and Figure 3.4). From this we conclude that two different systems both contribute to quinone reduction. Quinone reduction by the intracellular enzyme extract required added NADH or NADHP as electron donors (Table 3.4). The *G. trabeum* intracellular enzyme extract had a higher maximum reaction rate and higher kinetics constant compared with *G. trabeum* PMRS (Figure 3.3). This is consistent with what has been observed in *P. chrysosporium* (Stahl et al., 1995). It has been found that the purified *P. chrysosporium* intracellular quinone reductase has a much lower substrate saturation value than *P. chrysosporium* crude intracellular enzyme extract and *P. chrysosporium* PMRS. Thus, the intracellular quinone reductase was a much more efficient quinone - reducing mechanism (Brock et al., 1995). A *G. trabeum* intracellular quinone reductase has been purified and characterized (Chapter 4). The purified *G. trabeum* intracellular quinone reductase also has a much lower substrate saturation value than *G. trabeum* crude intracellular enzyme extract and *G. trabeum* PMRS (Chapter 4).

Although *G. trabeum* PMRS and *P. chrysosporium* PMRS could reduce quinones, the electron donors have not been identified. Quinone reaction by both PMRSs did not require added extracellular NAD(P)H and the addition of extracellular NAD(P)H did not affect the reduction rate (Stahl et al., 1995). Membrane - bound quinone reductases from plant cells utilize cytoplasmic NADH or NADPH as electrons donors (Berczi and Moller, 2000). The bacterial membrane - bound quinone reductases utilize cytoplasmic NADH as electron donors (Unemoto and Hayashi, 1993). For further biochemical and biophysical studies, the isolation of the plasma membrane and the purification of the membrane-bound quinone reductase will be necessary. Isolation of membrane fractions from filamentous wood decay fungus is underway (Chapter 5).

Catechols and hydroquinones have been proposed to drive the extracellular Fenton reaction in brown rot decay (Goodell et al., 1997 (a) and (b), 2001; Paszczynski et al., 1999; Kerem et al., 1999; Jensen et al., 2001). Catechols and hydroquinones are oxidized to quinones by reducing ferric iron and molecular oxygen. The quinone - reducing ability of the PMRS suggests it could be capable of playing a role in the regeneration of catechols/hydroquinones that drive the Fenton reaction. But there are several unsolved difficulties for this mechanism to be significant *in vivo*. First, in the brown rot wood, the degree of polymerization of cellulose is decreased rapidly at the very early stage of decay, when little weight loss can be observed. In addition, the reaction is not associated with hyphae. Since hydroxyl radicals are destructive within a very limited spatial distance, the hydroxyl radical generating Fenton reaction has been proposed to occur inside the wood cell wall and initiate the attack on lignocelluloses *in situ*. Thus it is not likely that the mycelia in the wood cell lumen could directly participate in the

quinone reduction happening within the wood cell wall. It has also been observed that the optimum pHs for ferricyanide reduction and quinone reduction by *G. trabeum* PMRS are higher than pH 5, while it is known that the pH in the *G. trabeum* hyphal vicinity is lower than pH 4 *in vivo*. The low pH also inhibits the iron reduction by catechols and hydroquinones (Jensen et al., 2001). The quinone reduction should also be inhibited.

In summary, a better understanding of the plasma membrane redox system of *G. trabeum* has been obtained by examining the ferricyanide reduction kinetics. The proton extrusion ability associated with the PMRS activity might play a role in the ability of fungi to quickly adjust the environmental pH and to maintain the cytoplasmic pH. Although the relationship between *G. trabeum* PMRS activity and alkali ions, such as K^+ and Na^+ , is not clear, ferricyanide reduction by the PMRS was affected by the alkali ions in the media (Table 3.4). *Gloeophyllum trabeum* and some other wood decay fungi have been found to play important roles in ion translocation in forest ecosystems and in bioremediation of heavy metals (Jellison et al., 1993; Connolly et al., 1996; Connolly and Jellison, 1995 and 1997; Doyle and Jellison, 1996; Fuller et al., 2000.) PMRS activity might be also associated with the pathway of some ion uptake by *G. trabeum*. Quinone reducing ability of the PMRS implies that the system might play a role in regeneration of components of the biochelator - driven Fenton reaction. However, spatial separation of the mycelia and the extracellular quinone reduction would pose difficulties for the proposed mechanism to function *in vivo*. More research is needed to fully understand the functions of PMRS in fungal physiology and brown rot mechanisms.

Chapter 4

**PURIFICATION AND CHARACTERIZATION OF AN
INTRACELLULAR 1,4-QUINONE REDUCTASE FROM THE BROWN ROT
BASIDIOMYCETE *GLOEOPHYLLUM TRABEUM***

Abstract

The roles quinone - reducing enzymes may play in fungal physiology and biodegradative mechanisms have not been completely elucidated, but they may be involved in hyphal protection and in the quinone metabolism of brown rot fungi. An intracellular 1,4-quinone reductase was purified from stationary shallow cultures of the brown rot fungus *Gloeophyllum trabeum* by ammonium sulfate precipitation, followed by hydrophobic interaction, ion exchange, and dye ligand affinity chromatographies. The native enzyme is a flavin protein with a molecular weight of 66 KD and a pI value of 4.2. Flavin mononucleotide (FMN) is the coenzyme. The ratio of the enzyme to the FMN is 1:2.8. The subunit molecular weight is 22 KD. The enzyme is inducible by 2,6-dimethoxy-1,4-benzoquinone and 4-hydroxy-3-methoxybenzoic acid in both low nitrogen and nitrogen sufficient media at either 24 or 30 °C. The quinone reductase purified utilizes NADH as an electron donor and catalyzes the reduction of multiple quinones and other electron acceptors such as 2,6-dichloro-indophenol and potassium ferricyanide. For enzyme catalyzed 2,6-dimethoxy-1,4-benzoquinone reduction, the apparent K_m is 6.8 μM and the K_{cat} is $1.0 \times 10^3 \text{ S}^{-1}$. The pH optimum is between 5.5 and 7. The optimal temperature is between 24 and 40 °C. The stoichiometry of NADH oxidation versus 2,6-dimethoxy-1,4-benzoquinone is 1:1. Inhibition of 2,6-dimethoxy-1,4-benzoquinone

reduction occurs at low NADH concentration. Dicumarol and cibacron blue are competitive inhibitors with K_i values of 0.5 and 0.2 μM , respectively. The relevance of this intracellular quinone reduction system to hyphal protection mechanisms and extracellular lignocellulose biodegradation processes has not yet been determined.

Introduction

Intracellular NAD(P)H dependent quinone reductases in mammals have been widely studied relative to their ability to protect against the toxicity of quinones, oxidizing agents, and reactive forms of oxygen (Lind et al., 1982; Wefers et al., 1984; Prochaska and Talalay, 1986; Prochaska et al., 1987; Schlaget and Powis, 1990; Foster et al., 1999; Dinkova-Kostova and Talalay, 2000), as well as their possible roles in cancer chemotherapy and carcinogenesis (Benson et al., 1980; Talalay and Benson, 1982; Talalay, 1989; Murphy et al., 1991; Li et al., 1995; Rauth et al., 1997). The most widely studied quinone reductase in mammals is the quinone reductase type 1 (DT-diaphorase), a highly inducible flavoprotein that can utilize both NADH and NADPH as electron donors and reduce multiple quinones. DT-diaphorase protects cells against quinone and semiquinone toxicity by mediating a two-electron reduction that results in the formation of hydroquinones instead of semiquinones (Lind et al., 1982; Horie, 1990; Merk and Jugert, 1991; Hasspieler et al., 1996; Beyer et al., 1996 and 1997; Galkin et al., 1999; Foster et al., 2000).

Cytosolic quinone reductases from the white rot basidiomycete *Phanerochaete chrysosporium* have also been well studied. This fungus produces several intracellular quinone reductases (Buswell et al., 1979; Schoemaker et al., 1989), two of which have

been purified and characterized (Constam et al., 1991; Brock et al., 1995). Production of both enzymes is highly inducible by vanillic acid and 2-methoxy-1,4-benzoquinone. The NADH dependent enzyme purified by Constam (1991) is a polypeptide with a molecular weight of 69 KD. The pI values are 5.7, 5.9, 6.0 and 6.3. The NAD(P)H dependent quinone reductase purified by Brock (1995) has a molecular weight of 44 KD, subunit molecular weight of 22 KD, and pI of 4.3. It is a flavin mononucleotide (FMN) containing dimer, which is similar to the DT-diaphorase (Lind et al., 1982; Horie, 1990; Chen et al., 1994; Li et al., 1995; Foster et al., 2000). The cDNA clone encoding the NAD(P)H dependent quinone reductase has also been isolated and sequenced (Akileswaran et al., 1999). Both of the enzymes from *P. chrysosporium* can reduce multiple 1,4-benzoquinones and 1,2-benzoquinones (Constam et al., 1991; Brock et al., 1995).

Cytosolic quinone reductases from *P. chrysosporium* have been proposed to have several physiological functions. They may participate in the metabolism of vanillic acid, which is an important metabolite produced during lignin biodegradation (Ander et al., 1980). Quinones are also lignin biodegradation products released by ligninolytic enzymes (Schoemaker et al., 1989). The uptake of quinones by cells and the subsequent reduction of those quinones can shift the ligninolytic reactions toward the direction of continuous degradation. Consequently, cytosolic quinone reductases from *P. chrysosporium* may play a role in complete lignin degradation (Schoemaker et al., 1989; Brock et al., 1995; Brock and Gold, 1996; Akileswaran et al., 1999). Since quinones and semiquinones are toxic to cells, cytosolic quinone reductases from *P. chrysosporium* may protect mycelia against quinone and semiquinone toxicity, as well (Wefers et al., 1984; Brock et al.,

1995; Brock and Gold, 1996; Akileswaran et al., 1999; Dinkova-Kostova and Talalay, 2000).

Catechol iron chelators, such as hydroxylated phenylacetic acids, hydroxylated benzoic acids, hydroxylated benzene derivatives and dihydroxyphenyl pentanediol, have been isolated from *G. trabeum* cultures (Jellison et al., 1991 (a) and (b); Easwaran, 1994; Goodell et al., 1996, 1997 (a) and (b)). Phenolate type compounds, 4,5-dimethoxy-1,2-benzenediol and 2,5-dimethoxyhydroquinone, as well as 2,5-dimethoxy-1,4-benzoquinone, have also been isolated and identified from the stationary cultures of *G. trabeum* (Paszczynski et al., 1999; Kerem et al., 1999). It has been found that phenolate iron chelators can play a role in brown rot non-enzymatic degradation of wood by mediating the extracellular hydroxyl radical generating Fenton reaction through the reduction of ferric iron (Goodell et al., 1996, 1997 (a) and (b), 1999 (a) and (b), 2001; Goodell and Jellison, 1997, 1998 and 1999; Lu et al., 1994; Qian and Goodell, 1999).

In the phenolate biochelator - driven Fenton reaction observed in brown rot fungi, an interesting phenomenon is the ability of one equivalent of phenolate compound to reduce multiple equivalents of iron (Goodell et al., 1996, 1997 (a) and (b), 1999 (a) and (b), 2001; Qian and Goodell, 1999). Two different theories have been proposed to explain the non-stoichiometric iron reduction (Goodell et al., 1996, 1997 (a) and (b), 2001; Pracht et al. 2001; Kerem et al., 1999; Jensen et al., 2001). A redox cycle had been initially suggested by Goodell (Goodell et al., 1996, 1997 (a) and (b), Qian and Goodell, 1999), through which oxidized phenolate biochelators could be regenerated. A quinone redox cycle driven by quinone - reducing enzymes was then proposed (Kerem et al., 1999; Paszczynski et al., 1999; Jensen et al., 2001). An alternative pathway proposed by Goodell

(Goodell et al., 2001; Pracht et al., 2001) is complete or partial mineralization of catechol chelators when reducing multiple equivalents of ferric iron. The two pathways are not mutually exclusive and the relative importance of recycling versus mineralization may depend upon the microenvironment and metabolite inquisition.

Gloeophyllum trabeum mycelia can reduce 2,5-dimethoxy-1,4-benzoquinone to 2,5-dimethoxy hydroquinone in sodium phosphate buffer (50mM, pH 4.1) (Kerem et al., 1999). *Gloeophyllum trabeum* has also been found to reduce 2,3-dimethoxy-5-methyl-1,4-benzoquinone (coenzyme Q₀) added into the media (Paszczynski et al., 1999). Studies in our laboratory have demonstrated that *G. trabeum* can produce constitutive intracellular quinone reductases. The *in vivo* relevance of these enzymes has not been established. The crude intracellular enzyme extract from *G. trabeum* can reduce 1,4-benzoquinone with NADH or NADPH as electron donors. The preliminary research indicated that the reaction had a pH optimum of 6.5, a K_m of 156 μM, and a V_{max} of 863 nmol/min/mg (Chapter 3).

We report here the purification and characterization of an intracellular NADH dependent quinone reductase from *G. trabeum*.

Materials and Methods

Organism and Culture Conditions

Stock cultures of *Gloeophyllum trabeum* ATCC 11539 were maintained on Difco® malt extract agar slants at 4 °C. The fungus was grown on BBL® potato dextrose agar plates (PDA) (20 mL media/plate) at 30 °C for one week. The PDA with the fungus was homogenized with distilled water at the ratio of 1 : 4 (weight ratio) in an Osterizer®

blender, three times in 15-second bursts with one minute between each burst. The homogenate was used to inoculate stationary 500 mL PYREX® flasks containing 9 mL of basal growth media (Tien and Kirk, 1988; Appendix B). One mL of the homogenized agar culture was inoculated into each flask (Kerem et al., 1999). Cultures were grown at 24 °C and 30 °C for one week. The inducer, vanillic acid (2 mM) or 2,6-dimethoxy-1,4-benzoquinone (100 µM), was added to the cultures 3 days after inoculation (Brock et al., 1995).

Enzyme Extraction

Mycelia were collected by vacuum filtration through Whatman® glass micro-fiber filters, washed with an equal volume of 4 °C deionized distilled water, and stored at -70 °C. Frozen cells (15 gram) in 100 mL of 4 °C extraction buffer (50 mM sodium phosphate buffer, pH 7.0) were broken in a pre-chilled Osterizer® blender (Brock et al., 1995). Fresh protease inhibitor cocktail (Bollag et al., 1996) was added into the extraction buffer before homogenization. The final concentrations of the protease inhibitors were 35 µg/mL phenylmethylsulfonyl fluoride (PMSF), 0.3 mg/mL EDTA, 0.7 µg/mL pepstatin A, and 0.5 µg/mL Leupeptin. Cells were homogenized 3 times in 20-second bursts with 1 minute between each burst. The homogenate was transferred to a VWR brand® tissue grinder and further homogenized three times in an ice-air bath. The final homogenate was centrifuged at $17,418 \times g$ for 20 minutes (Beckman J2-21 centrifuge with a JA-20 rotor). The supernatant was further centrifuged at $105,000 \times g$ for 30 minutes (Beckman L8-70M ultracentrifuge with a SW28 rotor).

Enzyme Purification

The protocol was modified from the one described by Brock (Brock et al., 1995) and those described by Bollag (Bollag, 1996). All the following chromatographies were carried out using an ISCO chromatographic system. An ISCO Tris pump controlled flow rates, and created the linear buffer gradient with a gradient maker (C.B.S. Scientific Co). An ISCO Retriever 500 was used to collect column elution every 0.5 minute unless otherwise stated. The absorbance of column elution at 280 nm was monitored using an ISCO UA-6 UV-VIS absorbance detector. Ten volumes of the corresponding equilibrium buffer were run through each column after the column was packed unless otherwise stated.

Ammonium Sulfate Precipitation. The enzyme extract was fractionated by ammonium sulfate precipitation (at 40% then 70% saturation), followed by centrifugation at 10,000 × g for 10 minutes (Beckman J2-21 centrifuge with a JA-20 rotor). The precipitate was re-dissolved in 10 mL of extraction buffer containing the protease inhibitor cocktail and 20% glycerol. The resuspended ammonium sulfate precipitated fraction was stored at -70 °C.

Hydrophobic Interaction. Phenyl sepharose CL-4B (3.9 mL) was equilibrated in equilibration buffer (50 mM sodium phosphate buffer containing 0.5 M ammonium sulfate, pH 7.0) and packed into a 0.7 cm × 10 cm Flex column at the rate of 1 mL/min. All the buffers used in the hydrophobic interaction chromatography contained 0.7 µg/mL pepstatin A, and 0.5 µg/mL Leupeptin. The ammonium sulfate fraction was thawed and diluted in the equilibration buffer at a 1:4 ratio and applied to the CL-4B column at the rate of 0.75 mL/min. The proteins were eluted with a step reverse ammonium sulfate

gradient and a step reverse sodium phosphate gradient (0.75 mL/min). Active fractions were pooled and concentrated by Amicon Centricon plus-20 centrifugal filter units with PL-10 membranes. The procedure was according to the manufacturer's recommendations.

Ion Exchange. The resin Q sepharose fast flow (3.9 mL) was equilibrated in 20 mM piperazine buffer (pH 5.2) and packed into a 0.7 cm × 10 cm Flex column using a pump speed of 2.5 mL/min. The concentrated CL-4B column elution was diluted in 20 mM piperazine buffer (pH 5.2) at a 1:1 ratio before being loaded onto the column. The proteins were eluted with a linear sodium chloride gradient (1 mL/min). Active fractions were pooled and concentrated by Amicon Centricon plus-20 centrifugal filter units with PM-10 membranes.

Dye Ligand Affinity. Blue-agarose (3.0 mL) was equilibrated in 10 mM sodium phosphate buffer containing 5 mM MgSO₄ (equilibration buffer) and packed into a 0.7 cm × 10 cm Flex column at a rate of 1 mL/min. The concentrated ion-exchange column elution was loaded onto the column. The proteins were eluted using the equilibration buffer followed by the equilibration buffer containing 0.5 mM NADH (0.75 mL/min). The active fractions were pooled, concentrated by Amicon Centricon plus-20 centrifugal filter units with PM-10 membranes, freeze-dried using a VirTis lyophilizer and stored at 0 °C, or pooled and stored in the equilibration buffer containing 20% glycerol at -70 °C.

Standard Enzyme Assays

Quinone reductase activity was determined by monitoring the oxidation of 200 μM NADH at 340 nm in 1 mL 50 mM sodium citrate buffer (pH 6.0) containing 100 μM

2,6-dimethoxy-1,4-benzoquinone (Buswell and Eriksson, 1979; Brock et al., 1995). Reactions were initiated by the addition of 1 to 10 μ l of the enzyme solution. Assays were performed at room temperature with a Spectronic GeneSys™ 2 spectrophotometer. The extinction coefficient for NADH at 340 nm is $6.22 \text{ mM}^{-1}\text{cm}^{-1}$. One unit of enzyme activity was defined as the amount of enzyme that oxidizes 1 μ mol of NADH per minute. Non-enzymatic oxidization of NADH was recorded as the control and was deducted from sample measurements.

Protein Measurements

Protein concentrations were measured by Bradford (Sigma) micro-assay with triplicate samples for each measurement. Bovine serum albumin was used as the protein standard.

Gel Filtration

Sephacryl S-300 (16 mL) was equilibrated in gel filtration buffer (30 mM Tris-HCl, pH 7.0, containing 100 mM NaCl and 2% glycerol) and was packed into a CONTES Flex-column (0.7 \times 40 cm) (1 mL/min for 2 hours, 2.3 mL/min for 1 hour). The purified quinone reductase (0.5 mg), and 2 mg of each protein standard (bovine serum albumin, ovalbumin and carbonic anhydrase) were dissolved in 1 mL gel filtration buffer and loaded onto the column. The proteins were eluted with gel filtration buffer at the rate of 0.5 mL/min. Fractions were collected every 2 minutes. The elution profile was monitored and recorded by the ISCO UA-6 UV-VIS absorbance detector. Quinone reductase

activity analysis and SDS-polyacrylamide gel electrophoresis analysis were performed for the peak fractions to identify the eluted proteins.

Electrophoresis

All experiments were carried out with the Sturdier vertical slab gel system (Hoefer Scientific Instrument). Procedures were according to "Protein Methods" (Bollag et al., 1996). Sodium dodecyl sulfate - polyacrylamide gel electrophoresis was performed with 15% gel. Proteins were visualized using Coomassie Blue stain. Native isoelectric focusing in the range of pH 3 to 10 was performed with polyacrylamide gel (5% T and 3.3% C). Proteins were visualized using Coomassie Blue stain followed by silver stain (Bollag et al., 1996). The low pI marker proteins kit (pI 3.6 to 6.6, Sigma) was used to determine pI values.

Flavin Identification

The assay used for flavin identification followed Faeder and Siegel's protocol (1973). Flavin adenine dinucleotide (FAD) and flavin mononucleotide (FMN) (Sigma) were used without further purification. All the solutions were prepared in 0.1 M potassium phosphate buffer (pH 7.7) containing 0.1 mM of EDTA. An excitation wavelength of 490 nm was used. The emission wavelength used was 535 nm. The fluorometer was blanked with phosphate buffer and was set at 1000 with 80 nM of FMN. The purified enzyme (6 µg/mL) was diluted with phosphate buffer at a 1:3 ratio. Aliquots of 3.0 mL of the diluted sample were immersed in a boiling water bath for 3 minutes, cooled rapidly in an ice-water bath, and centrifuged at 10,000×g for 10 minutes. The

supernatant (2 mL) was transferred to the cuvette for reading. The pH of the samples was adjusted from 7.7 to 2.6 with 0.1 N HCl.

Steady-State Kinetics Measurements

The one-electron acceptors ferricyanide and 2,6-dichloro-indophenol (DCPIP), and all of the quinones except 2,5-dimethoxy-1,4-benzoquinone (2,5-DMBQ) were obtained from Sigma. The 2,5-DMBQ was obtained from TCI America. All the compounds were used without further purification. All solutions were prepared in deionized distilled water. Measurements were carried out at room temperature in 1 mL 50 mM sodium citrate buffer (pH 6.0) with 6 μ g of enzyme. Velocities were measured by monitoring the decrease of absorbance at 340 nm and calculated as described above (standard enzyme assay). Non-enzymatic oxidization of NADH was recorded as the control and was deducted from sample measurements. Experiments were carried out in triplicate. All kinetic constants were determined by Lineweaver-Burk plots (Appendix C).

Stoichiometry of 2,6-DMBQ Reduction

Reaction mixtures contained 400 μ M 2,6-DMBQ and 4 μ g enzyme in 1 mL of 50 mM pH 6.0 sodium citrate buffer. The reduction of 2,6-DMBQ was measured by monitoring absorbance decrease at 390 nm with a fixed amount of NADH (50, 100, 150, 200 μ M, respectively). The extinction coefficient for 2,6-DMBQ is 0.5 $\text{cm}^{-1}\text{mM}^{-1}$. Reactions were initiated by the addition of the enzyme.

Temperature and pH Dependency of the Purified Enzyme

The temperature dependence of the purified enzyme was determined in 50 mM sodium citrate buffer (pH 6.0) with the presence of 200 μ M NADH, 100 μ M 2,6-DMBQ and 1 μ l purified enzyme solution at temperatures of 0 to 50 °C. Non-enzymatic oxidization of NADH was recorded as the control and was deducted from sample measurements.

The pH dependence of the purified enzyme was determined in 50 mM sodium citrate buffer (pH 3 to 6.3) and 50 mM sodium phosphate buffer (pH 6.5 to 8) in the presence of 200 μ M NADH, 100 μ M 2,6-DMBQ and 1 μ l purified enzyme solution at room temperature (24 °C). Non-enzymatic oxidization of NADH was recorded as the control and was deducted from sample measurements.

Inhibition of the Purified Enzyme

Inhibition of the purified quinone reductase by ZnSO₄, MgSO₄, CuSO₄, MnSO₄, EDTA, Na₃N, and KCN was studied (Brock et al., 1995). Experiments were carried out in triplicate. Oxidization of NADH (200 μ M) in the presence of 100 μ M 2,6-DMBQ and 1 mM inhibitor was monitored.

Inhibition constants of cibacron blue 3GA and dicumarol were also determined (Brock and Gold, 1996). Experiments were carried out in triplicate. Oxidization of NADH (6.25 to 100 μ M) was monitored in the presence of 12.5 μ M 2,6-DMBQ and cibacron blue 3GA (0.25, 0.5 and 1 μ M) or Dicumol (1, 2, and 4 μ M).

Results

Induction and Production of Intracellular Quinone Reductases

The effects of inducers, nitrogen levels, and temperatures on intracellular enzyme expression are summarized in Table 4.1. Both vanillic acid and 2,6-DMBQ increased intracellular quinone reductase production. After 7 days of incubation at either 24 or 30 °C, intracellular quinone reductase activity was detected in both nitrogen sufficient and nitrogen deficient liquid media. When 2 mM vanillic acid was added into the liquid cultures on the fourth day of incubation, specific activities of intracellular quinone reductases at the end of one-week incubation increased 1.52 to 3.85 fold, depending on the nitrogen level and growth temperature. When 100 µM 2,6-DMBQ was added, specific activities of intracellular quinone reductases increased 6.16 to 11.14 fold.

Table 4.1. The effects of inducers, nitrogen levels, and temperatures on intracellular quinone reductase activity in *G. trabeum*^a.

Culture condition	Inducer	Activity (U ^b /mL)	Protein conc. (mg/mL)	Sp. Activity (U/mg)	Induction (fold)	Temp. (fold)	Nitr. (fold)
Low nitrogen 24°C	Control	0.490±/0.193	0.52±/0.06	0.950±/0.374			
	Vanillic acid	0.225±/0.023	0.15±/0.00	1.531±/0.154	1.61		
	2,6-DMBQ ^c	1.334±/0.182	0.23±/0.02	5.853±/0.798	6.16		
Low nitrogen 30°C	Control	0.800±/0.058	0.66±/0.01	1.218±/0.879		1.28	
	Vanillic acid	0.525±/0.102	0.28±/0.02	1.849±/0.360	1.52	1.21	
	2,6-DMBQ	3.516±/0.643	0.26±/0.02	13.574±/2.484	11.14	2.32	
High nitrogen 30°C	Control	0.123±/0.033	0.10±/0.00	1.128±/0.035			1.38
	Vanillic acid	0.573±/0.226	0.12±/0.00	4.943±/1.947	3.85		2.67
	2,6-DMBQ	0.698±/0.098	0.07±/0.01	9.415±/1.327	7.33		0.69

^a Fungal cultures were harvested 3 days after the addition of the inducers. The activities were measured with 0.01 mL of each enzyme extract. The induction fold was calculated based on specific activities.

^b 1 U = 1 µmol of NADH oxidized min⁻¹.

^c 2,6-dimethoxy-1,4-benzoquinone

Nitrogen levels in media affected the intracellular enzyme production in different ways. When enzyme production at 30 °C was compared, without inducers or with vanillic acid as the inducer, cultures grown in high nitrogen media produced higher (1.38 and 2.67 fold, respectively) quinone reductase activity than did cultures grown in low nitrogen media. In contrast, if 2,6-DMBQ was added as the inducer, cultures grown in low nitrogen media produced higher (1.45 fold) quinone reductase activity than those growth under similar conditions in high nitrogen media.

Temperature also affected the intracellular enzyme production. Cultures grown in low nitrogen media at 30 °C produced higher enzyme specific activities than did cultures grown in low nitrogen media at 24 °C (1.21 to 2.32 fold, depending on the inducers). The temperature effect was most evident for cultures induced by 2,6-DMBQ.

A time study of intracellular quinone reductase induction by 2,6-DMBQ in low nitrogen media is shown in Figure 4.1. The specific activity increased little by day one after the inducer addition, but increased rapidly by day 2 and day 3, reaching a maximum at day 3. At incubation times greater than 3 days the specific activity decreased.

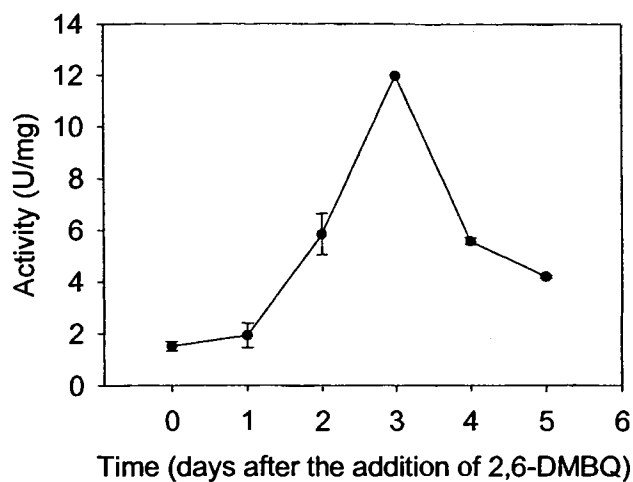


Figure 4.1. Induction of intracellular quinone reductase activity by 2,6-DMBQ in low nitrogen media at 30 °C. The inducer, 2,6-DMBQ was added 3 days after the inoculation. The enzyme specific activity reached the maximum (11.966 U/mg) 3 days after the addition of 2,6-DMBQ, and 6 days after the inoculation.

Total quinone reductase activity was greatest in 2,6-DMBQ induced, low nitrogen, 7-day cultures incubated at 30 °C. These conditions were used for enzyme preparation, with 2,6-DMBQ added on the fourth day of incubation.

Purification of Quinone Reductase

The purification of quinone reductase from 15 g of mycelia is summarized in the purification table (Table 4.2). The protein profiles from each purification step were visualized by SDS-page (Figure 4.2). The overall yield and the purification fold were 14% and 79 fold, respectively.

Table 4.2. Purification of the intracellular quinone reductase from *G. trabeum* grown in nitrogen limited liquid media.

Purification stage	Tot. vol. (mL)	Protein conc. (mg/mL)	Tot. protein (mg)	Activity (U/mL)	Tot. activity (U)	Sp activity (U/mg)	Yield (%)	Purification (fold)
Mycelial extract	100	0.65	65.20	7.702	770.200	11.813	100	1.00
40-70% (NH ₄) ₂ SO ₄ precipitation	10	3.90	39.00	56.720	567.200	14.544	74	1.23
Phenyl Sepharose hydrophobic interaction	20	0.20	40.00	11.552	231.040	57.760	30	4.90
Q Sepharose Fast flow Ion-exchange	7	0.23	1.62	27.369	191.583	118.481	25	10.00
Cibacron Blue 3GA agarose	9	0.013	0.11	12.130	109.170	933.070	14	79.00

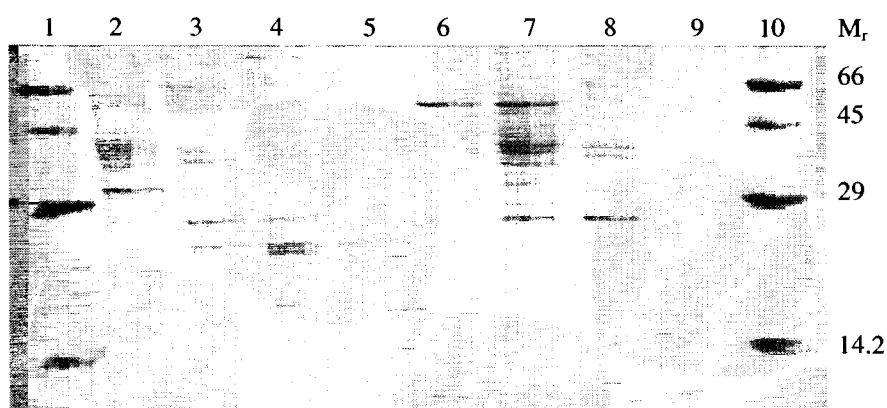


Figure 4.2. SDS-PAGE of the protein profiles from *G. trabeum*. The purified enzyme is shown in lane 5. Lanes 1 and 10, molecular weight marker; lane 2, crude intracellular enzyme extract; lane 3, after CL-4B hydrophobic interaction; lane 4, after Q Sepharose Fast Flow ion-exchange; lane 5, after Cibacron Blue 3GA agarose, which is the purified product; lanes 6 and 7, other protein fractions after the hydrophobic interaction column showing low level of quinone - reducing activities; lanes 8 and 9, other ion-exchange eluted fractions. Protein standards (2 μg of each), chromatography fractions (10 μg of each) and the purified quinone reductase (0.5 μg) were loaded. The experiment was performed with a 0.75 mm 15% polyacrylamide gel (16 \times 18 cm) subjected to the constant voltage (200 V) for 2 hours. The gel was stained with Coomassie Blue. The photo was taken by the ChemiImager low light digital imaging system.

As shown in the phenyl Sepharose CL-4B hydrophobic interaction chromatographic profile (Figure 4.3), 30% of quinone reductase activity was eluted in the 4 mM sodium phosphate buffer fraction with a 5-fold purification (Table 4.2). Part of the activity was also eluted in the 50 mM sodium phosphate buffer fraction and water fraction (Figure 4.2 and 4.3). The enzyme specific activities of these two fractions were much lower than that of the ammonium sulfate fraction (data not shown).

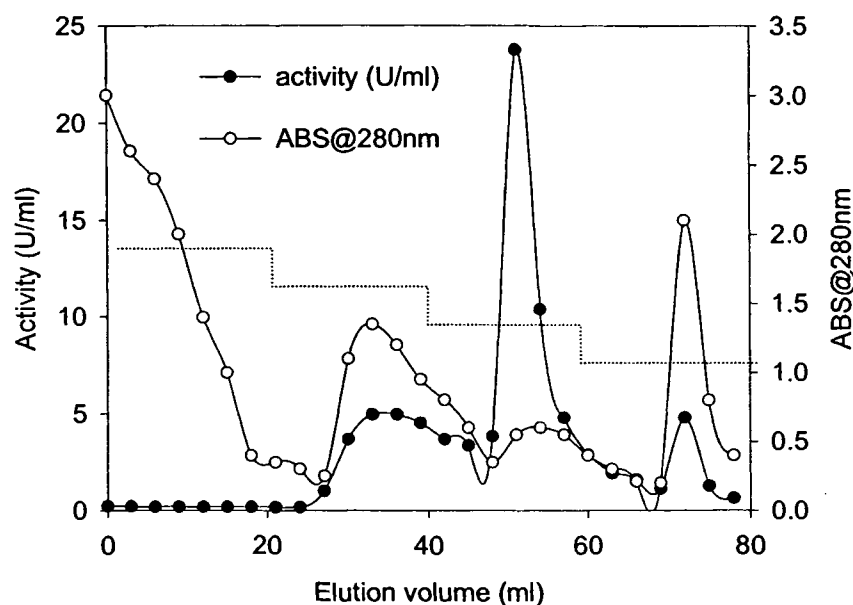


Figure 4.3. Phenyl Sepharose CL-4B hydrophobic interaction affinity chromatography of the quinone reductase from *G. trabeum*. The first, second and third activity peak corresponds to lane 6, 3, and 7 of figure 4.2, respectively. The sample was eluted with a step reverse ammonium sulfate gradient and a step reverse sodium phosphate gradient. 0-20 mL, 0.5 M ammonium sulfate in 50 mM sodium phosphate buffer (pH 7.0); 21-40 mL, 50 mM sodium phosphate buffer (pH 7.0); 41-60 mL, 4 mM sodium phosphate buffer (pH 7.0); 61-80 mL, water.

Quinone reductase activity was eluted as a single peak in both Q Sepharose Fast Flow ion-exchange (Figure 4.4) and Cibacron Blue 3GA agarose dye ligand affinity (Figure 4.5) chromatographies.

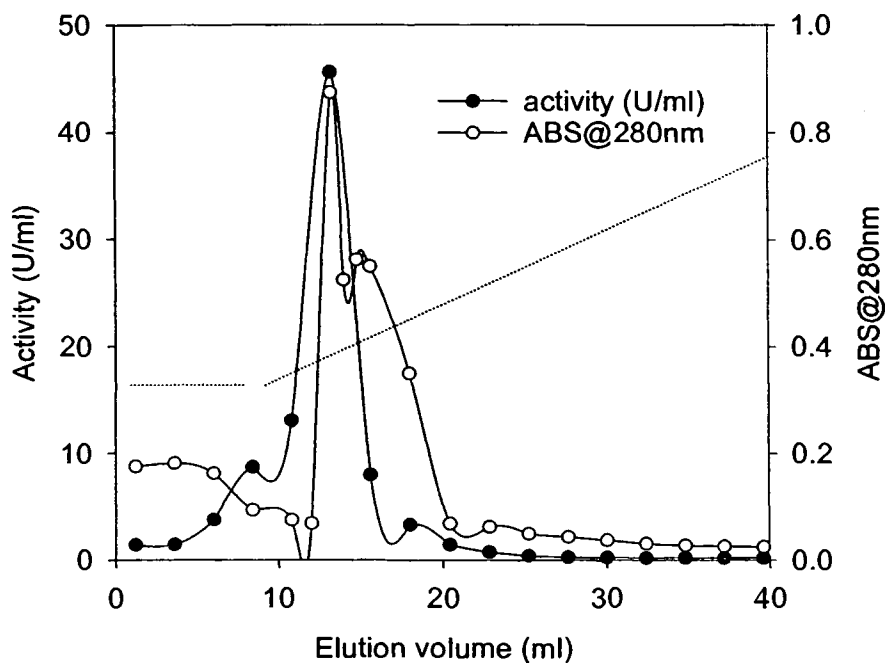


Figure 4.4. Q Sepharose Fast Flow ion-exchange chromatography of the quinone reductase from *G. trabeum*. The sample was eluted with a linear gradient of NaCl. 0-8 mL, equilibrium buffer (20 mM pH 5.2 piperazine buffer); 9-40 mL, the linear gradient (0 to 0.8 M) of sodium chloride in 20 mM piperazine buffer (pH 5.2).

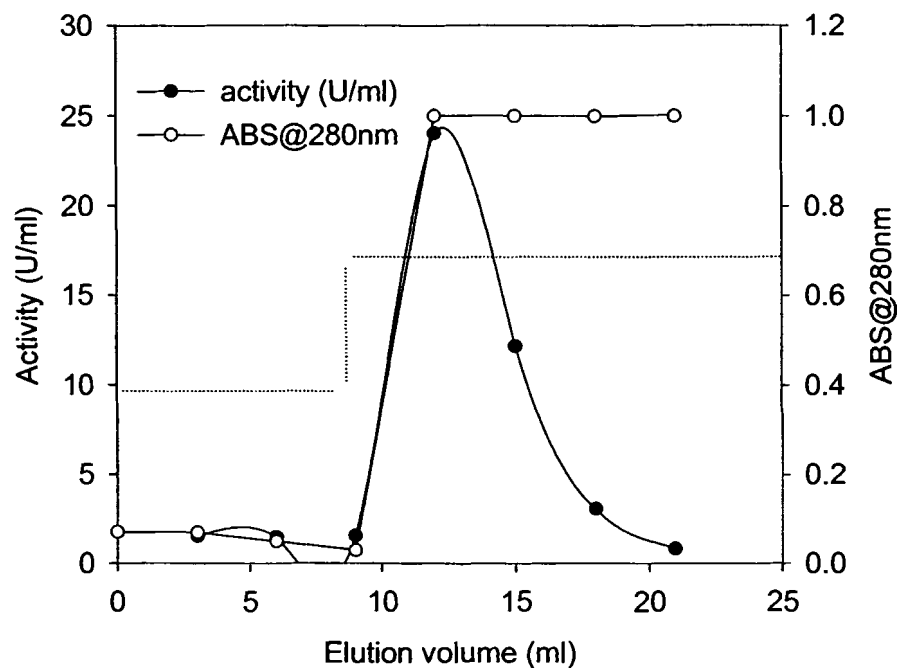


Figure 4.5 Cibacron Blue 3GA agarose dye ligand affinity chromatography of the quinone reductase from *G. trabeum*. 0-8 mL: 10 mM sodium phosphate buffer containing 5 mM MgSO₄; 9-25 mL: 10 mM sodium phosphate buffer containing 5 mM MgSO₄ and 0.5 mM NADH. Both the eluted protein and the NADH in elution buffer contributed to the high absorbance at 280 nm.

Physical Properties

The molecular weight of the native enzyme was 66 KD determined by Sephacryl S-300 gel filtration (Figure 4.6). The subunit molecular weight estimated by SDS-PAGE was 22 KD (Figure 4.7). The purified enzyme had a pI value of 4.2 (Figure 4.8).

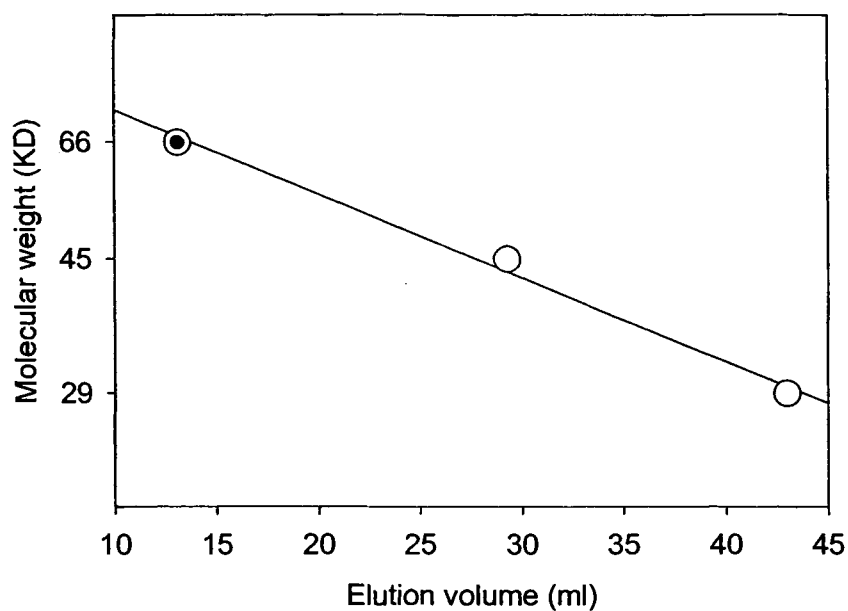
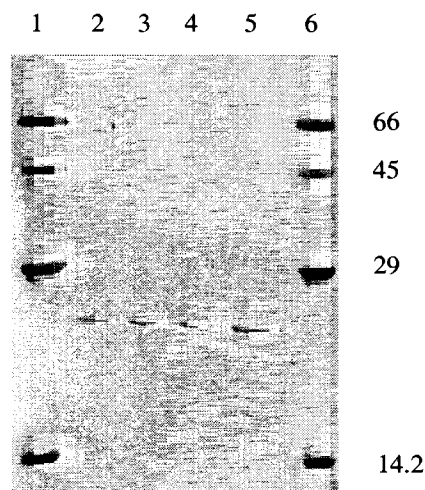
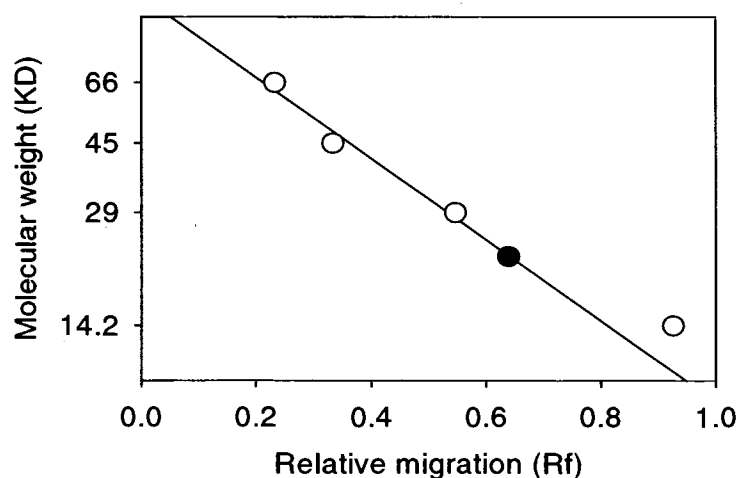


Figure 4.6 The molecular weight of the quinone reductase (●) determined by the gel filtration chromatography is 66 KD. The molecular weight standards (○) were bovine serum albumin (66 KD), ovalbumin (45 KD), and carbonic anhydrase (29 KD). The sample (1 mL) which contained 2 mg/mL of each protein standard and 0.5 mg/mL quinone reductase was loaded, and was eluted with gel filtration buffer at 0.37 mL/min flow rate.



(A)



(B)

Figure 4.7. (A) Purity confirmation of the quinone reductase by the SDS- PAGE. Lanes 2, 3, and 4, Blue agarose fraction (the purified enzyme) from different purification batches; lane 5, blue agarose fraction recovered from the gel filtration experiment and concentrated by centrifugal filtration; lanes 1 and 6; molecular weight standards, bovine serum albumin (66 KD), ovalbumin (45 KD), carbonic anhydrase (29 KD) and α -lactalbumin (14.2 KD). Protein standards (2 μ g of each) and 0.5 μ g of the purified quinone reductase were loaded. The experiment was performed with a 0.75 mm 15% polyacrylamide gel (16 \times 18 cm) subjected to the constant voltage (200 V) for 2 hours. The gel was stained with Coomassie Blue. The photo was taken with the ChemiImager digital imaging system. (B) Subunit molecular weight of the quinone reductase (\bullet) was 22 KD, determined by SDS-PAGE. The molecular weight standards (o) were as listed in (A).

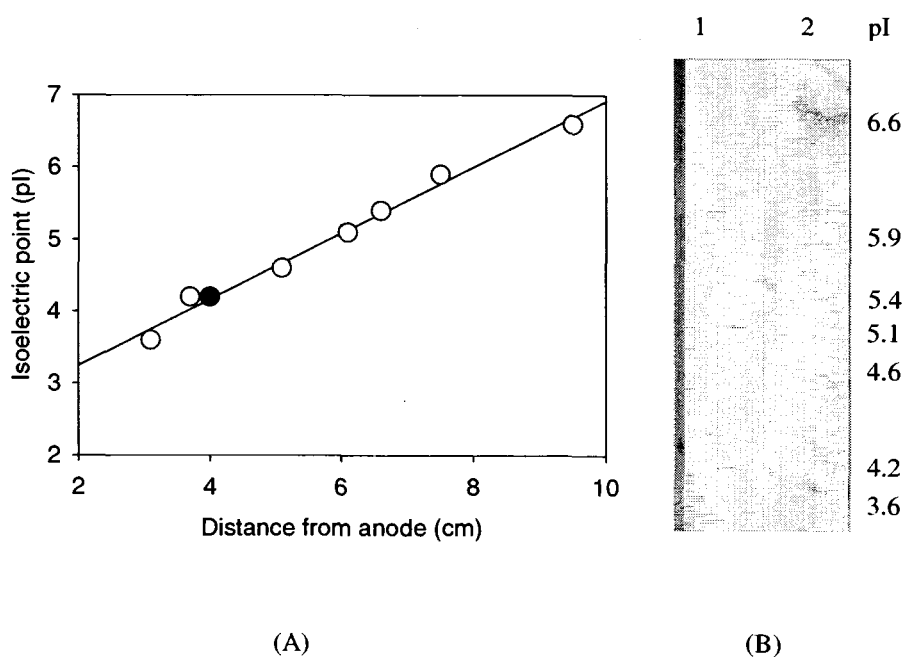


Figure 4.8. (A) The quinone reductase (●) displayed a pI value of 4.2 determined by the isoelectric focusing with pI markers (○): Amyloglucosidase (3.6), Glucose oxidase (4.2), Trypsin Inhibitor (4.6), β -Lactoglobulin A (5.1), Carbonic anhydrase II (5.4 and 5.9), Carbonic anhydrase (6.6). (B) Purity confirmation of the quinone reductase by the native polyacrylamide gel isoelectric focusing. Protein standards (6 μ g of each) and the purified quinone reductase (1.5 μ g) were loaded. The experiment was performed with a 5% T, 3.3% C polyacrylamide gel (16 \times 18 cm) subjected to the constant voltage (200 V for 1.5 hours, followed by 400 V for 1.5 hours). The proteins were visualized with Coomassie Blue followed by silver stain. The photo was taken with the ChemiImager low light digital imaging system.

The purified enzyme showed an oxidized flavin spectrum with maximal absorbance at 375 nm and 450 nm. The flavin spectrum was changed by reduction with NADH (Figure 4.9). The enzyme bound flavin was determined by the fluorescence of the flavin extracted from the enzyme. The enzyme bound flavin showed a pH dependence similar to that of flavin mononucleotide (FMN) but very different from that of flavin adenine dinucleotide (FAD) (Table 4.3). Using a molecular weight of 66 KD, a 1:2.8 ratio of native enzyme to FMN was obtained.

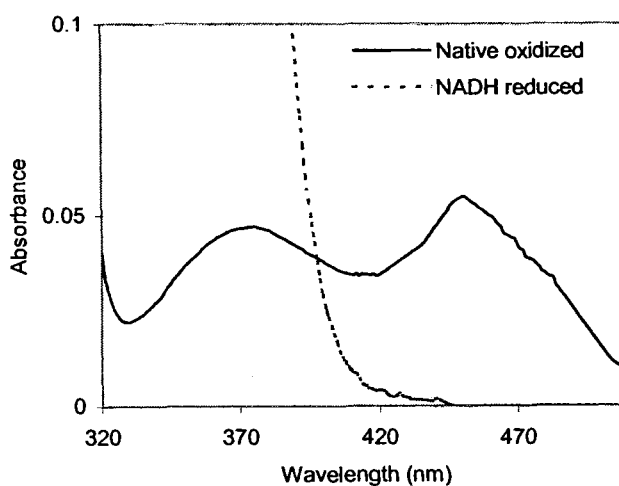


Figure 4.9. Wavelength scan of the native oxidized *G. trabeum* quinone reductase and NADH reduced enzyme. The oxidized enzyme showed maximum absorbance at 375 nm and 450 nm, which is a typical flavin spectrum.

Table 4.3. Determination of the nature of the enzyme-bound flavin by the pH dependency of the fluorescence.

Flavin source	Enzyme (nM) ^a	Actual		Fluorescence ^b		
		FMN (nM)	FAD (nM)	pH 7.7	pH 2.6	ratio
Standard solution	-	80	-	1000	664	0.664
Standard solution	-	40	-	462	284	0.615
Standard solution	-	20	-	218	124	0.569
Standard solution	-	-	60	82	462	5.634
Standard solution	-	-	30	36	235	6.528
Standard solution	-	-	20	12	105	8.75
		Measured				
Quinone reductase flavin	23	64	0	793	458	0.578

^a Protein concentration was determined by Bradford assay.

^b Fluorescence was monitored at 23 °C with a Turner 450 spectrophotofluorometer. Excitation wavelength was 490 nm, and the emission wavelength was 535 nm. Enzyme extract flavin concentration was calculated from the standard curve prepared from standard solution (std. sol.). Solutions were in 0.1 M potassium phosphate buffer containing 0.1 mM EDTA.

Catalytic Properties

The quinone reductase utilized NADH as the electron donor and catalyzed the reduction of several quinones, such as 1,4-benzoquinone, 2,5-dimethoxy-1,4-benzoquinone (2,5-DMBQ), 2,6-DMBQ, and 2,3-dimethoxy-5-methyl-1,4-benzoquinone (coenzyme Q₀). It also reduced electron acceptors such as 2,6-dichloro-indophenol and potassium ferricyanide (Table 4.4). The turn over number (K_{cat}) ranged from $5.3 \times 10^2 \text{ S}^{-1}$ for coenzyme Q₀ to $2.2 \times 10^4 \text{ S}^{-1}$ for DCPIP. NADPH oxidization was not detected when 2,6-DMBQ was used as the electron acceptor. Of the several quinones tested, the highest quinone reductase activity was observed with 1,4-benzoquinone. The rate of NADH oxidization by the enzyme in the presence of ferricyanide was 25% of that for 2,6-DMBQ (Table 4.5).

Table 4.4. Kinetic constants ^a for the quinone reductase from *G. trabeum*.

Compound	Apparent K_m (μM)	Apparent K_{cat} (S^{-1})	K_{cat} / K_m
1,4-benzoquinone ^b	3.8	4.0×10^3	1.1×10^3
2,5-DMBQ ^c	5.8	1.1×10^3	1.9×10^2
2,6-DMBQ ^d	6.8	1.0×10^3	1.5×10^2
Coenzyme Q_0 ^e	16.2	5.3×10^2	3.3×10
DCPIP ^f	17.2	2.2×10^4	1.3×10^3
$\text{K}_3\text{Fe}(\text{CN})_6$ ^g	215.8	2.6×10^3	1.2×10
NADH ^h	46.4	1.2×10^3	2.6×10

^a Enzyme assays were performed as described in materials and methods unless otherwise stated. 200 μM of NADH was used in determining the K_m for the electron receptors. 100 μM of 2,6-DMBQ was used in determining the K_m for the electron donor NADH. Experiments were performed in triplicate. Raw data is listed in Appendix C.

^b Concentration ranged from 3.13 to 100 μM . Prepared from 2 mM stock.

^c 2,5-dimethoxy-1,4-benzoquinone. Concentrations ranged from 1.25 to 40 μM . Prepared from 200 μM stock.

^d Concentrations ranged from 6.25 to 50 μM . Prepared from 2 mM stock.

^e 2,3-dimethoxy-5-methyl-1,4-benzoquinone. Concentration range from 6.25 to 200 μM . Prepared from 2 mM stock.

^f 2,6-dichloro-indophenol. Concentrations ranged from 3.13 to 200 μM . Prepared from 2 mM stock.

^g Concentrations ranged from 100 to 1600 μM . Prepared from 10 mM stock.

^h Concentrations ranged from 6.25 to 100 μM . Prepared from 1 mM stock.

Table 4.5 Relative efficiencies of electron acceptors in the quinone reductase reaction.

Electron acceptors	Specific activity (U ^a /mg)	Relative activity
1,4-benzoquinone	3638	388%
2,5-DMBQ	1014	108%
2,6-DMBQ	938	100%
Coenzyme Q ₀	483	51%
Ferricyanide	235	25%
DCPIP	2034	217%

^a 1 unit = 1 μmol of NADH oxidized min^{-1} . The NADH concentration was 200 μM in all experiments. Acceptor concentrations were 100 μM (1,4-benzoquinone, 2,5-DMBQ, 2,6-DMBQ, Coenzyme Q₀, DCPIP) and 500 μM (ferricyanide).

The stoichiometry of NADH oxidation versus 2,6-DMBQ reduction was determined spectrophotometrically (Figure 4.10). The plot of NADH added versus 2,6-DMBQ reduction has a slope of 1. The spectral analysis indicated one equivalent of 2,6-DMBQ was reduced for each equivalent of NADH oxidized.

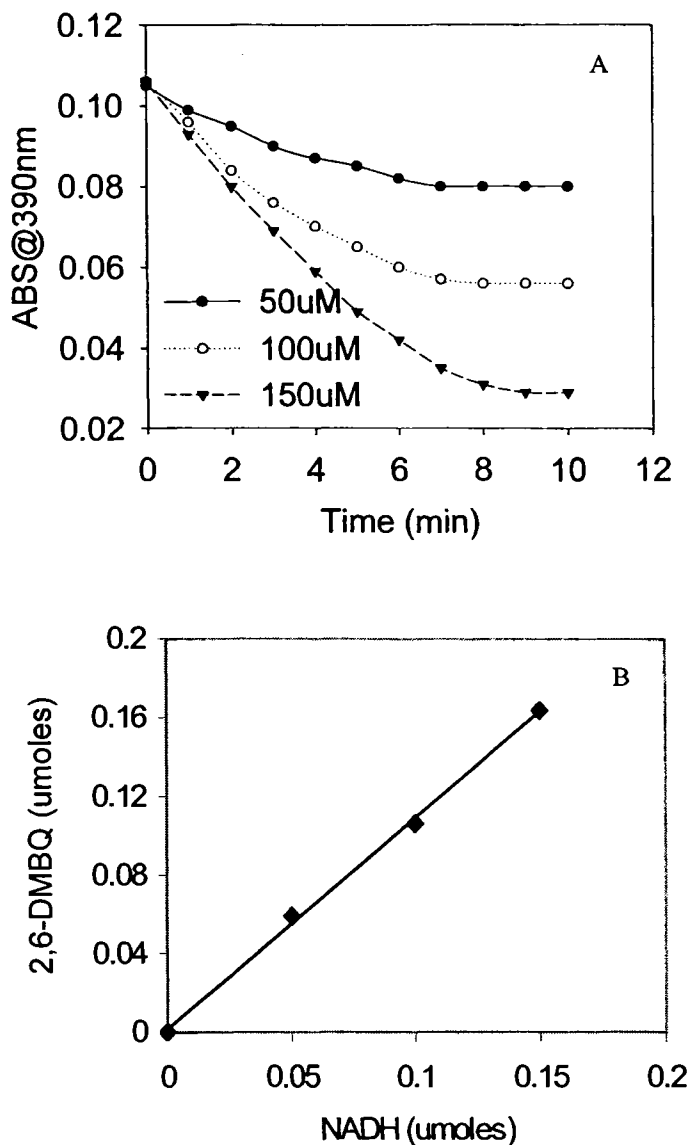


Figure 4.10. The stoichiometry of the quinone reductase catalyzed reduction of 2,6-DMBQ. (A) Reduction of 100 μM 2,6-DMBQ was monitored in the presence of indicated concentration of NADH. 4 μg enzyme was used for each assay. (B) The stoichiometry of NADH added versus 2,6-DMBQ reduction. The plot of the moles of 2,6-DMBQ reduced versus the moles of NADH added (0, 50, 100, and 150 μM) has a slope of 1. The concentration of 2,6-DMBQ reduced was calculated using the Beer-Lambert equation: $\text{Abs} = \text{ECl}$, in which Abs is the absorbance at 390nm, E is the extinction coefficient (see materials and methods), l is the cuvette pathlength (1cm in this study). The total volume of the reaction system was 1mL. Based on the concentration and the volume, the amount of 2,6-DMBQ reduced could be obtained.

pH and Temperature Dependency

The pH optimum was between 5.5 and 7 (Figure 4.11). The optimal temperature was between 24 and 40 °C (Figure 4.12). Enzyme activity decreased sharply above pH 7 or 40 °C (Figure 4.11 and 4.12 A). The activation energy for the NADH oxidization was 43.7 kJ/mol calculated from the Arrhenius plot (Figure 4.12 B).

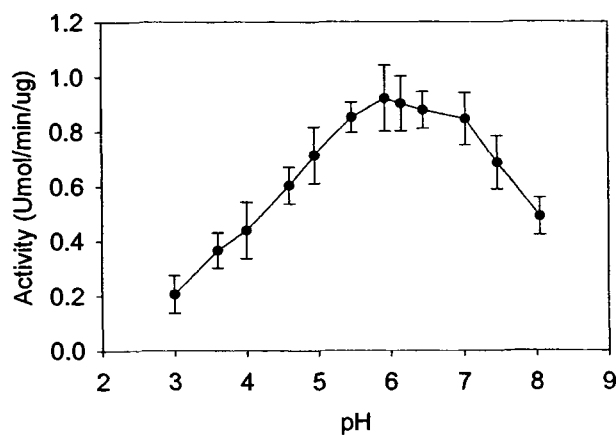


Figure 4.11. The optimum reaction pH for the quinone reductase from *G. trabeum* is between 5.5 to 7. The effect of pH on activity was measured with sodium citrate-citric acid buffer (pH 3 to 6.3) and sodium phosphate buffer (pH 6.5 to 8). Data represents the average and standard deviation of 5 samples.

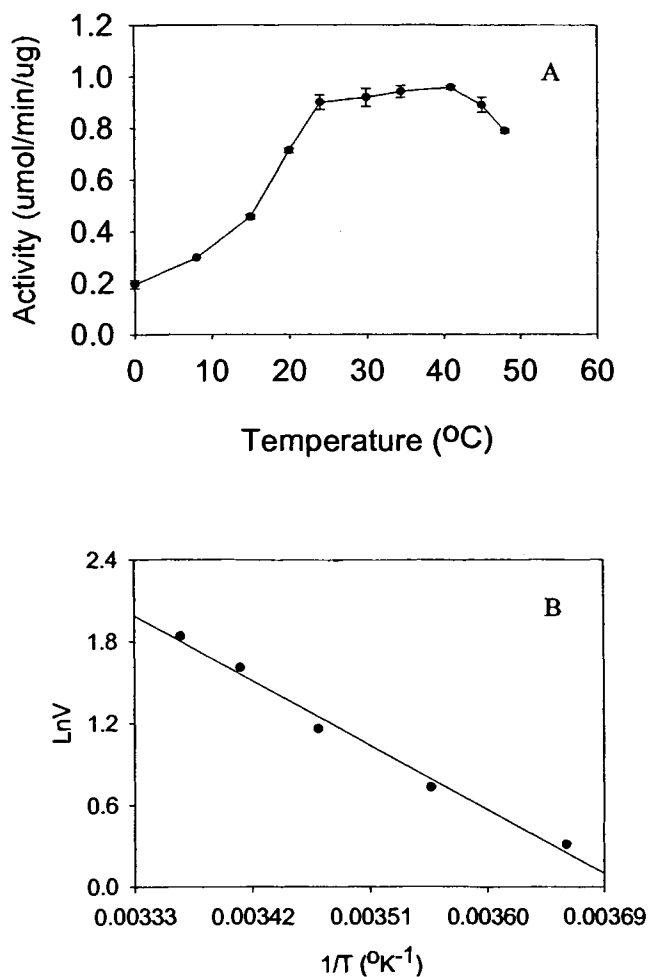


Figure 4.12. (A) The optimum reaction temperature for the quinone reductase from *G. trabeum* is between 24 to 40 °C. Data represents the average and standard deviation of 5 samples. (B) The activation energy for the oxidation of NADH was 43.7 kJ/mol calculated by the Arrhenius plot. It was based on the Arrhenius equation: $k=Ae^{-E_a/RT}$, in which A is Arrhenius constant, k is the rate constant ($k=V/[\text{substrate}]$), E_a is the activation energy, R is the gas constant (8.317J/Kelvin.mol), T is the temperature in Kelvin degree (°K, °K = °C+273.15). Since [substrate] is constant during the initial rate period, the equation can be written as $V=[\text{substrate}] Ae^{-E_a/RT}$ or $\text{Ln}V=\text{Ln}A[\text{substrate}]-E_a/RT$. Consequently the slope of a plot of LnV versus 1/T gives $-E_a/R$.

Inhibition of Quinone Reductase

The enzyme was not inhibited by 1mM of ZnSO₄, MgSO₄, CuSO₄, MnSO₄, EDTA, or Na₃N, but was inhibited by 1mM KCN (Table 4.6).

Table 4.6. Enzyme activity levels in the presence of potential quinone reductase inhibitors ^a.

Potential inhibitor	Activity ^b
Control	0.906+/-0.090
KCN	0.647+/-0.073
Na ₃ N	0.802+/-0.090
ZnSO ₄	1.087+/-0.127
MgSO ₄	0.88+/-0.073
CuSO ₄	0.906+/-0.073
MnSO ₄	0.828+/-0.037
EDTA	0.802+/-0.097

^a. Values which are statistically different from the control at P < 0.05 (based upon T-test analysis) are shown in bold.

^b. Data represent the average and standard deviation of triplicate samples.

Dicumarol and cibacron blue competitively inhibited the reduction. The re-plots of Lineweaver-Burk slopes versus inhibitor concentrations give K_i values of 0.5 and 0.2 μM, respectively (Figure 4.13).

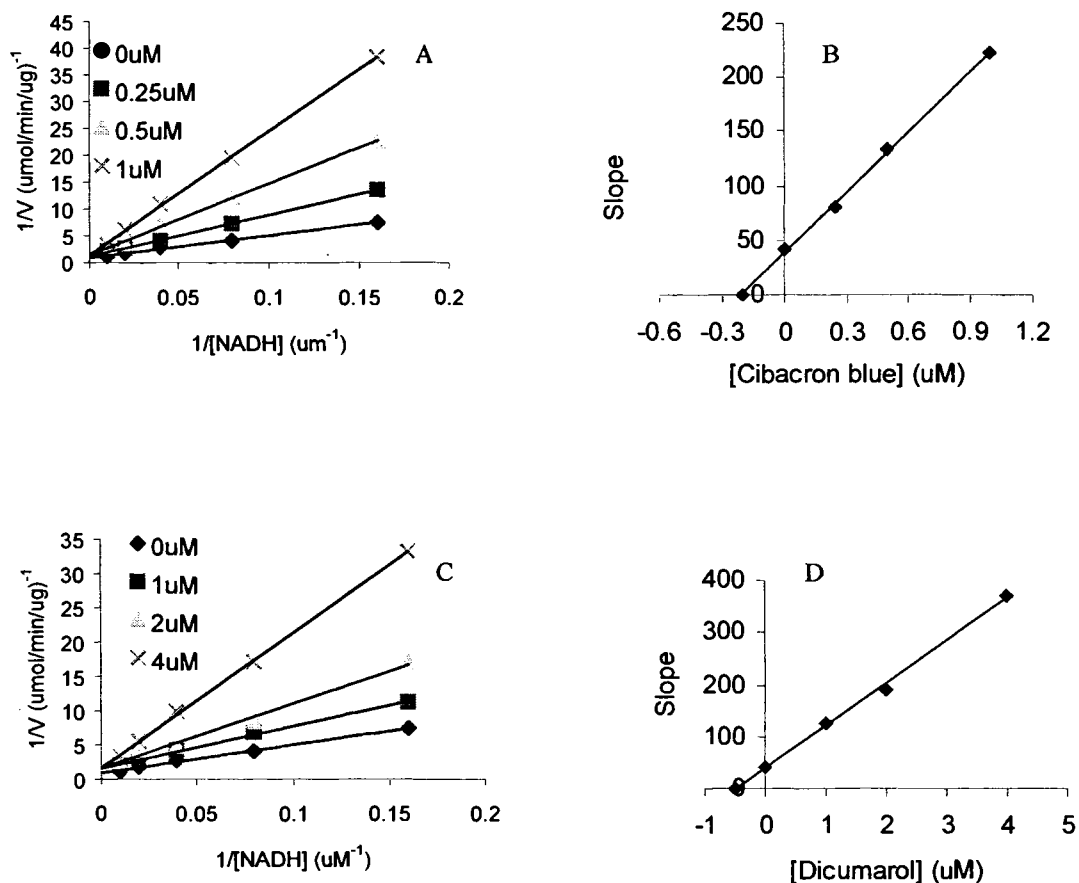


Figure 4.13. Inhibition of *G. trabeum* quinone reductase by cibacron blue (A) and dicumarol (C). Experiments were carried out in triplicate. (A) Oxidization of NADH (6.25 to 100 μM) was monitored in the presence of 12.5 μM 2,6-DMBQ and Cibacron blue 3GA (0.25, 0.5 and 1 μM). (B) The replot of slope versus Cibacron blue 3GA concentration indicates the K_i value as 0.2 μM . (C) Oxidization of NADH (6.25 to 100 μM) was monitored in the presence of 12.5 μM 2,6-DMBQ and Dicumarol (1, 2, and 4 μM). (D) The replot of slope versus Dicumarol indicates the K_i value as 0.5 μM .

In the Lineweaver-Burk plot of 2,6-DMBQ reduction catalyzed by quinone reductase under various concentrations of NADH (Figure 4.14), parallel lines were obtained when the NADH concentration was between 50 and 200 μM . The slope of the plot increased for the reaction in the presence of 25 μM NADH, indicating that inhibition of enzyme catalyzed 2,6-DMBQ reduction occurred at low NADH concentration.

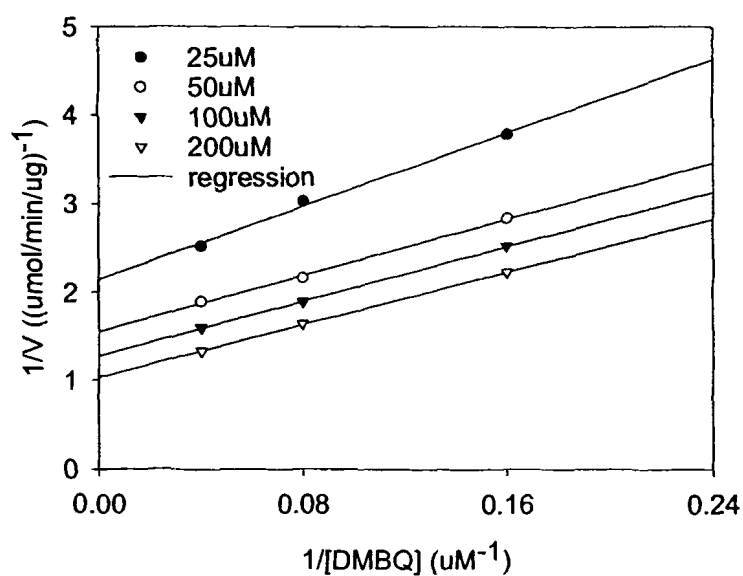


Figure 4.14. Enzyme inhibition at 25 μM NADH was observed in the steady state kinetic analysis of *G. trabeum* quinone reductase. 2,6-DMBQ concentrations ranged from 6.25 to 25 μM . Experiments were carried out with triplicate samples.

Discussion

Expression of intracellular 1,4-quinone reductase activity in the brown rot fungus *G. trabeum* was studied. An inducible, NADH-dependent 1,4-quinone reductase has been isolated from low-nitrogen cultures of *G. trabeum*. Physical and catalytic properties of this enzyme were determined.

Vanillic acid increased the intracellular quinone reductase activity in *G. trabeum* by 1.5 fold in low-nitrogen media, and 3.85 fold in high-nitrogen media 3 days after the addition of the inducer. Vanillic acid is a lignin decomposition model compound. It is an inducer of the ligninolytic enzyme system in the white rot fungi, and had been used to induce quinone reductase activity in the white rot fungus *Phanerochaete chrysosporium* (*Sporotrichum pulverulentum*). NAD(P)H : quinone oxidoreductase activity increased 5 fold in *S. pulverulentum* when grown in the presence of vanillate (Buswell et al., 1979). Two and a half days after the addition of 1.5 mM vanillic acid, the quinone reductase activity increased by 4.1 to 4.5 fold in *P. chrysosporium* low-nitrogen cultures (Constam et al., 1991). Twenty hours after the addition of 1 mM vanillic acid into the high-nitrogen culture of *P. chrysosporium*, the intracellular quinone reductase activity had increased by 13.9 fold (Brock et al., 1995).

The intracellular quinone reductase activity in *G. trabeum* increased by 11.14 fold in low-nitrogen media, and 7.33 fold in high-nitrogen media 3 days after the addition of 100 μ M 2,6-DMBQ. The significant response of *G. trabeum* cells to added quinones implies that *G. trabeum* has a sensitive intracellular mechanism for quinone metabolism. Similar phenolate compounds, 4,5-dimethoxy-1,2-benzenediol, 2,5-dimethoxy-1,4-hydroquinone, and 2,5-dimethoxy-1,4-benzoquinone, have been identified as metabolites

produced by *G. trabeum* in liquid cultures (Paszczynski et al., 1999; Kerem et al., 1999). The compound 2,6-DMBQ was chosen as the inducer in this study for its relative stability and water solubility. The compound is also a product found in fungal wood degradation (Brock et al., 1995). It has been reported that in *P. chrysosporium*, the intracellular quinone reductase activity was increased 6.18 fold in high-nitrogen cultures 20 hours after the addition of 100 μ M 2-methoxy-1,4-benzoquinone (Brock et al., 1995).

Both vanillic acid and 1,4-benzoquinone increased the intracellular quinone reductase activity in *G. trabeum*. This is consistent with observations with *P. chrysosporium*. For *P. chrysosporium*, vanillic acid was a more effective quinone reductase inducer (Brock et al., 1995). For *G. trabeum*, 1,4-benzoquinone was a much more effective inducer. The difference might imply that the enzymes play different roles in the white rot fungi and the brown rot fungi. The quinone reductases in *P. chrysosporium* were not only significantly induced by vanillic acid, the regulation of the quinone reductases was also similar to that of vanillate hydroxylase (Buswell, et al., 1981; Yajima et al., 1979). The *P. chrysosporium* quinone reductases were likely involved in vanillate metabolism (Ander et al., 1980; Brock, et al., 1995). Brown rot fungi do not produce ligninolytic peroxidases (Freitag and Morrell, 1992; Milstein et al., 1992); it is not likely that the enzyme is naturally involved in vanillic acid metabolism. The significant induction of *G. trabeum* cytosolic quinone reductases by quinones indicates the quinone reductases may act as an efficient type of electron source for quinone redox cycles and/or a protective mechanism against bioactive quinones.

The time study on enzyme production showed *G. trabeum* quinone reductase activity reached the maximum 3 days after the addition of 2,6-DMBQ. This result is in

accordance with Constam's study on *P. chrysosporium* (Constam et al., 1991). Brock's study with *P. chrysosporium* showed that significant specific activity increases occurred 20 hours after the addition of either vanillic acid or 2-methoxy-1,4-benzoquinone (Brock et al., 1995; Akileswaran et al., 1999).

The quinone reductase activity was eluted irregularly as 3 different peaks (Figure 4.2 and 4.3) during the phenyl sepharose CL-4B hydrophobic interaction chromatography. This indicated the enzyme was adsorbed to the matrix at several sites. This is probably because hydrophobic interactions are relatively nonspecific (Bollag et al., 1996). Although phenyl sepharose is a less hydrophobic matrix, at some sites very strong hydrophobic interaction with the quinone reductase occurs, causing irrecoverable binding and lowering the recovery rate. Because the hydrophobic interaction becomes stronger as the salt concentration increases, the ammonium sulfate precipitated quinone reductase was diluted with loading buffer in our study to increase the recovery rate as well as the purification fold.

The homogeneous enzyme has a molecular weight of 66 KD, a subunit molecular weight of 22 KD, and a pI value of 4.2. During the isoelectric electrophoresis, another very weak band at pH 5.1 was also observed. Whether this was an impurity or another protein with quinone - reducing ability has yet to be determined. The quinone reductase from *P. chrysosporium* isolated by Brock et al. (1995) had a molecular mass of 44 KD and was composed of two similar 22 KD subunits. The pI value was 4.3. The quinone reductase from *P. chrysosporium* isolated by Constam et al. (1991) was a single polypeptide chain of 69 KD with pI values of 5.7, 5.9, 6.0, and 6.3.

The *G. trabeum* quinone reductase contained FMN as the co-enzyme. This is consistent with studies of *P. chrysosporium* quinone reductase (Brock et al., 1995) and DT-diaphorase (Chen et al., 1994; Li et al., 1995; Foster et al., 2000). Using the molecular weight of 66 KD, the ratio of native enzyme to FMN determined by fluorescence was 1:2.8.

The purified quinone reductase utilizes NADH as the electron donor, as does the enzyme purified by Constam and colleagues (1991). The enzyme purified by Brock et al. (1995 and 1996) utilized both NADH and NADPH. Studies have shown that *P. chrysosporium* produced several intracellular quinone reductases (Shoemaker et al., 1989; Constam et al., 1991). In our previous studies, the crude intracellular enzyme extract from *G. trabeum* could reduce 1,4-benzoquinone with either NADH or NADPH as the electron donor (Chapter 3). This suggests that *G. trabeum* may produce other quinone reductases that utilize NADPH or both NADH and NADPH as electron donors.

The purified quinone reductase catalyzed the reduction of several 1,4-benzoquinones. The broad substrate specificity is consistent with *P. chrysosporium* quinone reductases and DT-diaphorase. The compound 2,5-DMBQ has been identified as a potentially key *G. trabeum* metabolite (Paszczynski et al., 1999; Kerem et al., 1999). The purified quinone reductase had a high turn over number ($K_{cat} = 1.0 \times 10^3 \text{ S}^{-1}$) for this compound, which indicates that the fungus has an efficient mechanism for conversion of this metabolite. It has been reported that 50% of added coenzyme Q_0 is reduced within 1 day by *G. trabeum*, even though extracellular cellobiose dehydrogenase (cellobiose dependent quinone reductase) has not been detected in this type of medium (Paszczynski et al., 1999; Kerem et al., 1999). The purified quinone reductase also had a high turn over

number ($K_{\text{cat}} = 0.5 \times 10^3 \text{ S}^{-1}$) for coenzyme Q_0 . The highest quinone reductase activity was observed with 1,4-benzoquinone. This is consistent with the observation with the quinone reductase extract from *P. chrysosporium* (Buswell et al., 1979). The greatest activity of the partially purified quinone reductases from *P. chrysosporium* was observed with 2-methoxy-5-methoxymethyl-2,5-cyclohexadiene (Constam et al., 1991). The greatest activity of the quinone reductase from *P. chrysosporium* purified by Brock was observed with 2,6-dichloro-1,4-benzoquinone (Brock and Gold, 1996). The quinone reductases from *P. chrysosporium* can reduce both 1,4-benzoquinone and 1,2-benzoquinone, forming hydroquinones and catechols, respectively (Buswell, 1979; Constam et al., 1991; Brock et al., 1995; Brock and Gold, 1996). The ability of the purified quinone reductase from *G. trabeum* to reduce 1,2-benzoquinone has not been studied. It has been reported that *G. trabeum* reduces 2,5-dimethoxy-1,4-benzoquinone to 2,5-dimethoxy hydroquinone much more rapidly than it reduces 4,5-dimethoxy-1,2-benzoquinone to 4,5-dimethoxy catechol (Jensen et al., 2001).

As reported in Chapter 3, the reduction of 1,4-benzoquinone by the plasma membrane redox system of *G. trabeum* had a K_m of 59 μM , and a V_{max} of 17.5 nmol/min/mg (dry weight mycelia), which was 630 nmol/min/mg (protein). While the reduction of 1,4-benzoquinone by the purified intracellular quinone reductase had a K_m of 3.8 μM and a V_{max} of 3638 $\mu\text{mol}/\text{min}/\text{mg}$. This suggests that the intracellular enzyme may be responsible for the majority of the cell-associated 1,4-benzoquinone reduction.

As seen with the *P. chrysosporium* quinone reductase, purified *G. trabeum* quinone reductase could also reduce the non-physiological electron acceptors DCPIP and ferricyanide. The turn over numbers were $2.2 \times 10^4 \text{ S}^{-1}$ and $2.6 \times 10^3 \text{ S}^{-1}$, respectively.

The stoichiometry of the 2,6-DMBQ reduction catalyzed by *G. trabeum* quinone reductase was similar to that catalyzed by *P. chrysosporium* quinone reductase. One equivalent of the two-electron acceptor 2,6-DMBQ was reduced for each equivalent of NADH oxidized. The strict adherence to the 1:1 ratio suggested a two-electron transfer mechanism (Li et al., 1995; Brock et al., 1995; Brock and Gold, 1996; Galkin et al., 1999).

Enzyme inhibition at low NADH concentrations was observed with *G. trabeum* quinone reductase. This is similar to results observed for *P. chrysosporium* quinone reductase (Brock et al., 1995; Brock and Gold, 1996) and DT-diaphorase (Hories, 1990). This indicates that the mechanism of the *G. trabeum* quinone reductase may be similar to that of *P. chrysosporium* quinone reductase and DT-diaphorase, in which quinones were reduced directly to hydroquinones by two-electron reduction and the semiquinones were not released from the enzyme active site (Hories, 1990; Li, et al., 1995; Brock and Gold, 1996; Galkin et al., 1999).

Dicumarol and cibacron blue were efficient inhibitors for the purified *G. trabeum* quinone reductase, as is true for the *P. chrysosporium* quinone reductase (Brock and Gold, 1996) and DT-diaphorase (Roberts et al., 1989; Prestera et al., 1992). This further suggests that the three quinone reductases have similar two-electron reduction mechanisms. The inhibition is competitive with respect to NADH. The competition constants K_i were 0.5 and 0.2 μM for dicumarol and cibacron blue, respectively. The corresponding K_i values for the enzyme from *P. chrysosporium* were 2.1 and 0.3 μM (Brock and Gold, 1996). *Gloeophyllum trabeum* quinone reductase is more sensitive to both inhibitors than is the *P. chrysosporium* quinone reductase. These inhibitors could be

used *in vivo* to study the role the enzyme plays in both fungal physiology and fungal biodegradation.

Gloeophyllum trabeum quinone reductase was not inhibited by 1 mM of ZnSO₄, MgSO₄, CuSO₄, MnSO₄, or EDTA. This implies that quinone reductase activity does not require transition metals (Brock et al., 1995). Na₃N and KCN have been reported to inhibit the activities of other flavoproteins. The enzyme was not inhibited by 1 mM Na₃N, but was inhibited by 1 mM KCN. The quinone reductase from *P. chrysosporium* was slightly inhibited by 1 mM MnSO₄ and 1 mM EDTA. But it was not inhibited by either 1 mM Na₃N or 1 mM KCN (Brock et al., 1995).

As it is true for *P. chrysosporium* quinone reductases and DT-diaphorase, a significant function of *G. trabeum* quinone reductase may be to protect the cells from quinone and semiquinone toxicity in the brown rot fungi. Quinones behave as electrophiles and represent one source of oxidative stress in cells (Lind et al., 1982; Wefers et al., 1984; Murphy et al., 1991; Hasspieler et al., 1996; Brock and Gold, 1996; Dinkova-Kostova and Talalay, 2000). Quinones can react deleteriously with proteins and nucleic acids. They readily form semiquinones enzymatically or non-enzymatically via one-electron reduction. Semiquinones can then react with molecular oxygen yielding reactive superoxide anion radicals that participate in the generation of hydrogen peroxide. Meanwhile, toxic quinones are regenerated spontaneously. The ability of the enzyme to reduce quinones directly to hydroquinones in the cell can function to prevent the release of semiquinones into the cytoplasm.

The high induction of *G. trabeum* intracellular quinone reductase activity by benzoquinones and the low apparent K_m values of the enzyme to benzoquinones indicates

that the quinone reductase has critical physiological functions in quinone metabolism and may play a potentially important role in brown rot degradation. A possible function for the enzyme in the brown rot fungi could be that the hydroquinones produced drive the extracellular Fenton reaction. The hydroquinones generated could be released extracellularly and react with ferric iron directly, producing ferrous iron and semiquinones. The semiquinones could react with molecular oxygen and participate in hydrogen peroxide generation, or also react with ferric iron. Quinones would be generated at the same time. Ferrous iron would then react with hydrogen peroxide to generate destructive hydroxyl radicals that could participate directly in fungal lignocellulose biodegradation (Jellison et al., 1991(a); Goodell et al., 1997 (a) and (b), 2001; Paszcynski et al., 1999; Kerem et al., 1999; Jensen et al., 2001). By releasing the hydroquinones extracellularly, the quinone reductase could function to transport the electrons from an intracellular NADH pool to the extracellular Fenton reaction. The generated quinones might be taken up by cells and be reduced to hydroquinones by the cytosolic quinone reductase. Hydroquinones could then again be released and mediate the Fenton reaction extracellularly. It has also been demonstrated that 2,5-demethoxy hydroquinone produced by *G. trabeum* can reduce 4,5-dimethoxy-1,2-benzoquinone to 4,5-dimethoxy catechol extracellularly (Jensen et al., 2001). Thus, the catechol chelators produced by the brown rot fungi can also be regenerated extracellularly and non-enzymatically in the presence of hydroquinones.

The intracellular location of this quinone reductase however, is inconsistent with current theories, which indicate that non-enzymatic biodegradation of wood is an extracellular process spatially separated from the fungal hyphae. Thus, the role that the

quinone redox cycle mediated by the cytosolic quinone reductase may play in continuous production of Fenton reagents is significantly limited by the spatial separation.

Recent research has shown catechols can be partially or completely mediated to carbon dioxide by reducing multiple equivalents of ferric iron (Pracht et al., 2001). The catechol biochelators produced by brown rot fungi may undergo a similar pathway extracellularly to generate multiple equivalents of Fenton reagents (Goodell et al., 2001).

The extracellular pathway for the regeneration of hydroquinone chelators remains unknown. Mineralization to carbon dioxide by reducing ferric iron has not been observed with hydroquinones (*p*-diol) (Pracht et al., 2001).

In summary, an intracellular quinone reductase was purified and characterized from the brown rot fungus *G. trabeum*. Although previously studies in white rot fungi, this is the first biochemical characterization of a brown rot intracellular quinone reductase. This enzyme represents an efficient mechanism in quinone metabolism and may be important in the generation of cytosolic hydroquinones. By mediating a two-electron quinone reduction, the enzyme prevents the production of cytosolic semiquinones and protects cells against quinone and semiquinone toxicity. Via releasing hydroquinones out of cells, the enzyme may also function in part, as a type of electron carrier that transports electrons from an intracellular NADH pool to the extracellular biochelator - driven Fenton reaction. However, because of the spatial separation of fungal mycelia and the extracellular Fenton reaction, the role that the quinone redox cycle mediated by the quinone reductase could play in fungal wood degradation may be spatially limited.

Chapter 5

ISOLATION AND CHARACTERIZATION OF PLASMA MEMBRANES FROM THE WOOD DECAY FUNGUS *PHANEROCHAETE CHRYSOSPORIUM*

Abstract

Plasma membrane isolation is a prerequisite step for characterization of membrane proteins. Four membrane fractions were isolated from the filamentous white rot fungus *Phanerochaete chrysosporium* grown in shaking malt extract liquid media for 24 hours. Snail digestive enzyme (β -glucuronidase type H-1) was used to weaken the cell wall and form the protoplasts. Membrane fractions were obtained by homogenization, followed by sequential centrifugation and ultra centrifugation. Each fraction was characterized based upon the activities of plasma membrane ATPase and mitochondrial ATPase. The fraction with relatively high plasma membrane ATPase activity and the lowest mitochondria ATPase activity was observed under the transmission electron microscope by negative staining. Plasma membranes were isolated in this study, although the yield was low and there was some contamination by mitochondria membranes.

Introduction

A range of wood decay fungi produce both hydroxamic acid derived and phenolate derived low molecular weight siderophore-like iron chelating compounds (Fekete et al., 1989; Jellison et al., 1991 (a) and (b); Qi and Jellison, 2000; chapter 2). The phenolate-derived biochelators are postulated to be an integral part of the non-enzymatic brown rot mechanism. They have been shown to drive the degradation-

associated Fenton reaction by participating in iron reduction and hydrogen peroxide generation (Goodell et al., 1997 (a) and (b), 2001; Paszczynski et al., 1999).

Siderophores are low molecular weight iron chelating compounds produced by microorganisms grown under iron deficient conditions. Their primary function is to acquire iron for cells. Most knowledge about fungal iron acquisition has been derived primarily from studies using the yeast *Saccharomyces cerevisiae* and the smut *Ustilago* (Burgstaller, 1997). Studies on *Ustilago* mainly concentrated on the synthesis of siderophores and the regulation of siderophore production (Leong and Winkelmann, 1998). *Saccharomyces cerevisiae* did not produce siderophores and sequestered iron via the ferric iron reductase in the plasma membrane redox system (Askwith et al., 1996).

Specific membrane receptors are produced by bacteria for the uptake of the iron-siderophore complex (Barton and Hemming, 1992). Comparison of outer membrane proteins in bacteria grown under iron sufficient and iron deficient conditions by using SDS-PAGE has been the traditional method used to identify bacterial siderophore receptors (Crosa and Hodges, 1981; Weger et al., 1986; Cody and Gross, 1987; Enard et al., 1988; Abash and Ferreira, 1990; Ishimaru and Lopper, 1992 (b); Rabsch et al., 1999). However, no siderophore receptors have thus far been detected in any fungi (Huschka and Winkelmann, 1989). Studies on putative siderophore receptors in wood decay fungi could contribute to the understanding of the iron uptake process.

An understanding of the plasma membrane redox system (PMRS) of the white rot fungus *Phanerochaete chrysosporium* and the brown rot fungus *Gloeophyllum trabeum* has been obtained by ferricyanide reduction kinetics (Stahl and Aust, 1993; Stahl et al., 1995; Chapter 3). The PMRS of *P. chrysosporium* has been found to be able to reduce

several quinones and free radicals (Stahl et al., 1995). It has been proposed that the PMRS of *P. chrysosporium* plays important roles in regulating extracellular pH, bioremediation of highly oxidized contaminants, and cell protection against the extracellular free radicals generated by ligninolytic systems. The PMRS of *G. trabeum* can reduce quinones and has been proposed to play important roles in adjusting extracellular and cytoplasmic pH, and in ion translocation. It may also under some circumstances be a component of fungal degradative mechanisms by driving an extracellular quinone redox cycle (Chapter 3), although special constraints may limit this function in vivo. For better biophysical and biochemical understanding of the PMRS, isolation of the plasma membrane and purification of specific oxidoreductases are required.

Intrinsic difficulties in isolating membrane fractions and membrane proteins from filamentous fungi explain the scarcity of studies of siderophore receptors and the PMRS. Few studies have been carried out on the isolation of plasma membranes from fungi, and most of the work has involved the yeast form of fungi (Labarere and Bonneau, 1982). Although plasma membrane fractions have been isolated from the filamentous fungus *Neurospora crassa* Shear et Dodge (Bowman and Slayman, 1981), reports on plasma membrane isolation from filamentous wood decay fungi are scarce. *Phanerochaete chrysosporium* is the only wood rot fungus from which membrane vesicles have been obtained; cross-membrane transportation of glucose and protons has been studied by using these vesicles (Green et al., 1984).

Here we report a preliminary study on the plasma membrane isolation and characterization from the filamentous wood decay fungus *P. chrysosporium*. The

protocols used to isolate vesicles from *P. chrysosporium* (Green et al., 1984) and to isolate plasma membrane from *N. crassa* (Bowman and Slayman, 1981) were modified as noted and utilized. Plasma membrane ATPase was used as the plasma membrane marker. Mitochondrial ATPase was used as the marker indicating the contamination caused by mitochondrial membrane fractions. Previous studies have shown that plasma membrane ATPase and mitochondrial ATPase have different optimum pH values and different specific inhibitors (Bowman et al., 1978; Bowman and Slayman, 1979). The optimum pH of plasma membrane ATPase from *N. crassa* is 6.8. The specific inhibitors are vanadate and diethylstilbestrol. The optimum pH of mitochondrial ATPase is 8.2. The specific inhibitors are azide, oligomycin, venturicidin, and leucinostatin.

Materials and Methods

Organism and Culture Conditions

Stock cultures of the white rot fungus *Phanerochaete chrysosporium* were maintained on Difco® malt extract agar plates at 24 °C. The spores and mycelia on the surface of a one-week-old *P. chrysosporium* malt extract agar plate were collected and inoculated into 250 mL liquid Difco® malt extract broth. Cultures were grown with 200 rpm aeration at room temperature for 24 hours.

Cell Collection

The cells were collected by filtration through Whatman® No. 2 filters, and were washed by ice cold distilled water and ice cold media A (0.59 M sucrose, 5 mM EDTA, 50 mM NaH₂PO₄, pH 6.5).

Cell Lysis

After harvesting, cells were treated with snail digestive enzyme (Sigma β -glucuronidase type H-1). Two grams (wet weight) cells were suspended by gentle shaking in 20 mL media A, 70 μ l Mercaptoethanol and 200 mg powdered snail enzyme for 16 hours at 30 °C. Microscopic phase contrast observation (Leitz LABORLUX S Microscope system) was used to detect the formation of the protoplasts.

Plasma Membrane Isolation

The protocol was modified from Bowman's procedure (Bowman and Slayman, 1981). The enzyme treated suspension was centrifuged at $4354 \times g$ for 10 minutes. The pellets were washed with 20 mL of 0.68 M sucrose and centrifuged at $4354 \times g$ for 10 minutes. The pellets were suspended in 20 mL media B (0.33 M sucrose, 1 mM EGTA, 0.3% bovine serum albumin, pH 7.1), homogenized once, and centrifuged at $1,088 \times g$ for 10 minutes. The pellets were suspended in 20 mL of media B for a second homogenization and serial centrifugations (producing mito-2 and mem-2 fractions). The supernatant was centrifuged at $14,636 \times g$ for 30 minutes. The pellets were fractions containing mainly mitochondrial membrane fractions (mito-1) and were suspended in a small volume of media C (1 mM EGTA, pH 7.5). The supernatant was centrifuged sequentially at $12,096 \times g$ for 30 minutes, $39,191 \times g$ for 40 minutes, and $100,000 \times g$ for 60 minutes. The 12 k pellets, 40 k pellets and 100 k pellets were washed by suspension in 40 mL of media C and centrifuged at $39,191 \times g$ (12 k and 40 k pellets) or $100,000 \times g$ (100 k pellets). The washed pellets were pooled and suspended in a small volume of media C. The pellets contained mainly plasma membranes (mem-1).

Protein Determination

Protein concentrations of the membrane fractions were determined by the Lowry assay (Lowry et al., 1951), with bovine serum albumin as the protein standard.

Enzyme Assays

ATPase activity was assayed at 30 °C by the liberation of inorganic phosphate (Dryer et al., 1957; Bowman et al., 1978; Bowman and Slayman, 1979). Plasma membrane ATPase activity was assayed in 0.5 mL of the following reaction mixture: 5 mM Na₂ATP, 5 mM MgCl₂, 5 mM phosphoenolpyruvate, 2.5 µl of pyruvate kinase, 5 mM sodium azide, and 10 mM PIPES (pH 6.7). The reaction was started by the addition of membrane fractions and stopped after 10 minutes by the addition of 0.1 mL of 50% trichloroacetic acid. The mixture was centrifuged at 2000 × g for 5 minutes. The inorganic phosphate was measured by Dryer's assay (Dryer et al., 1957). The clear supernatant (0.5 mL) was mixed with 0.1 mL of 0.008 M ammonium molybdate solution. One mL of semidine hydrochloride (50mg in 100 mL of 0.1% NaHSO₄) was added. After 10 minutes, absorbance was read at 350 or 770 nm. A trichloroacetic acid solution of KH₂PO₄ was run as a standard. Mitochondrial ATPase was assayed in the same reaction mixture except sodium azide was omitted.

Transmission Electron Microscope Observation

The membrane fraction mem-1 was negatively stained with 1% phosphotungstate acid and observed by a Philips EM201 transmission electron microscope.

Effects of pH on ATPase Activities of Isolated Membrane Fractions

Effects of pH on plasma membrane ATPase activity were measured with membrane fraction mem - 1 in potassium phosphate buffer (5.5 to 7.5) as described previously.

Effects of pH on mitochondrial ATPase activity were measured with membrane fraction mito - 2 in potassium phosphate buffer (8 to 8.8) as described previously.

Results

When *P. chrysosporium* was grown in malt extract liquid media for 4 weeks, the iron concentration before and after fungal growth was 1 μ M. The pH of the media was decreased by fungal growth from 4.6 to 2.4. The concentrations of phenolate type and hydroxamic acid type chelators were 35.7 and 16.5 μ M as measured by the Arnow assay and the Csaky assay, respectively. Liquid malt extract media was used for the growth of *P. chrysosporium* for membrane isolation, because of the relatively fast fungal growth rate and relatively high production of biochelators in this media.

After the snail digestive enzyme treatment, swelling spores and hyphae were observed by phase contrast microscopy (Figure 5.1).



Figure 5.1. Phase contrast photograph of hyphae and spores of *P. chrysosporium* after the treatment of snail digestive enzyme (β - glucuronidase type H-1, EC 3.2.1.31, 200 mg were used for 2 g of cells), taken under the Leitz Laborlux S microscope. Swelling spores and hyphae can be observed. Magnification: $\times 800$. The fungal conidia and hyphae (2 g) from MEA plates were inoculated in MEA liquid media (200 mL), grown for 24 hours on Thermolyne type 72000 orbital shaker (200 rpm, room temperature), and were collected by vacuum filtration through Whatman 2 filter paper. Enzyme treatment was performed under 37 °C for 6 hours in 20 mL of 50mM sodium phosphate buffer (pH 6.5, with 5 mM EDTA and 0.59 M sucrose) (Bowman and Slayman, 1981).

Two mitochondrial fractions, mito-1 and mito-2, and two membrane fractions, mem-1 and mem-2, were isolated from 2 gram (wet weight) of a 24-hour culture of *P. chrysosporium*. The yield of the membrane fraction was 0.5874 mg of protein per gram of wet weight cells. Both of the mitochondrial fractions showed higher mitochondria ATPase activity than plasma membrane ATPase activity. Both of the membrane fractions showed higher plasma membrane ATPase activity (Table 5.1). The optimum pH of each fraction was the same as the reported values (Figure 5.2).

Table 5.1. Protein concentrations and ATPase activities of membrane fractions from a 24-hour culture of *Phanerochaete chrysosporium*.

Fraction	Protein concentration (mg/mL)	Plasma membrane ATPase activity ^a (μmol/min/mg)	Mitochondria ATPase activity ^a (μmol/min/mg)
Mito-1 ^b	1.854	0.624	1.341
Mito-2	2.141	0.439	1.177
Mem-1 ^c	1.061	0.722	0.397
Mem-2	0.326	1.494	0.795

^a Plasma membrane ATPase and mitochondrial ATPase were used as the marker of plasma membranes and the marker of intracellular mitochondria membranes, respectively. ATPase activity was measured at 30 °C by the liberation of inorganic phosphate (Bowman et al., 1978).

^b Mito: fractions mainly consisting of mitochondrial membranes, isolated by sequential centrifugation by using Beckman J2-21 centrifuge with a JA-20 rotor (3 times at 4,000 × g, once at 1,000 × g, once at 12,000 × g).

^c Mem: fractions mainly consisting of plasma membranes, isolated by sequential centrifugation as described above, followed by sequential ultra-centrifugation by using Beckman L8-70M ultracentrifuge with a SW48Ti rotor (Once at 40,000 × g and once at 100,000 × g).

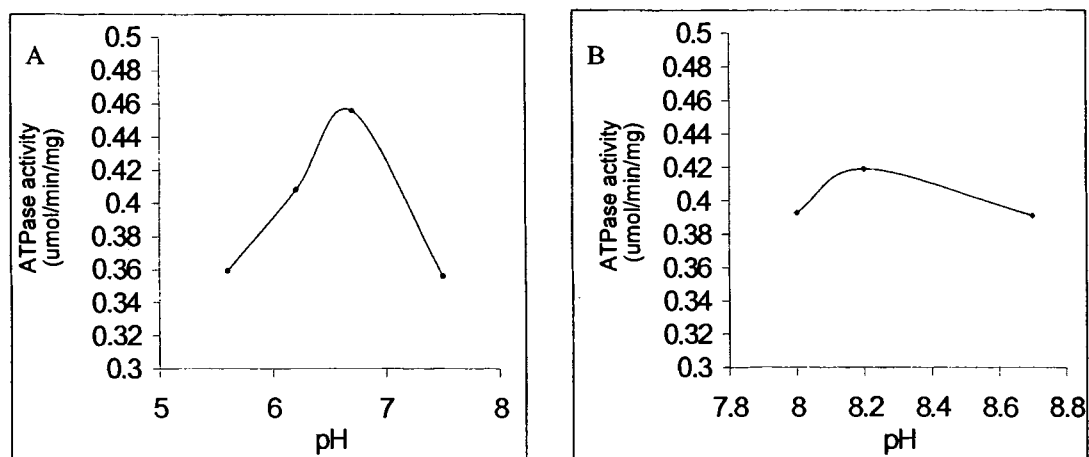


Figure 5.2. (A). The effect of pH on ATPase activity of the membrane fraction mem-1 from *Phanerochaete chrysosporium*. The optimum pH 6.7 was similar to the reported optimum pH of plasma membrane ATPase (pH 6.8). (B). The effect of pH on ATPase activity of the membrane fraction mito-2. The optimum pH 8.2 was the same as the reported optimum pH of mitochondrial membrane ATPase.

Membrane fragments could be observed in the membrane fraction under electron microscope (Figure 5.3).

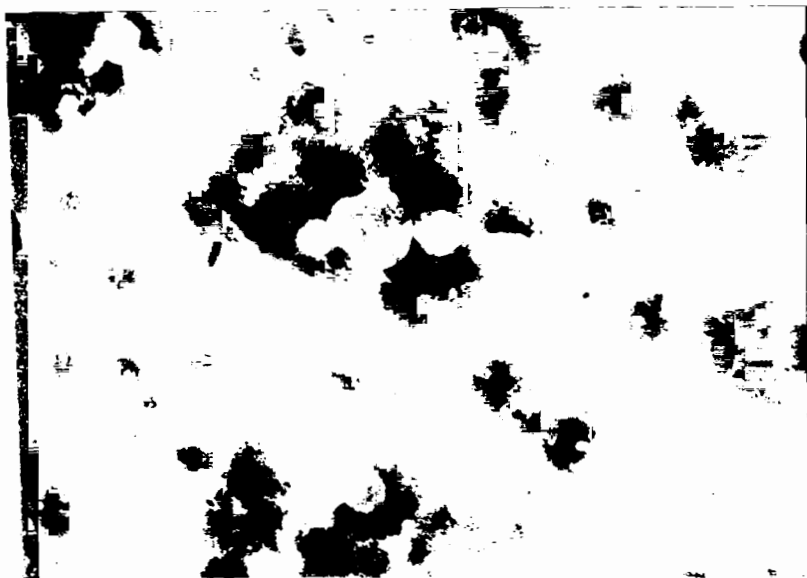


Figure 5.3. *Phanerochaete chrysosporium* membrane fraction mem-1 was negatively stained with 1% phosphotungstate acid and observed by transmission electron microscope Philips EM201. Magnification: $\times 45K$. The round/irregular structures lighter in color were membrane fragments.

Discussion

Plasma membranes were isolated from the wood decay fungus *P. chrysosporium*. The yield of the plasma membrane fractions was 0.587 mg protein/g cell (wet weight). The plasma membrane fractions still contained some intracellular mitochondrial membranes. Modifying the current method may increase the yield and the purification of the membrane fraction.

The inoculum for the liquid media included spores and old hyphae. Enzyme treatment was not effective on the old hyphae. The hyphae also stuck together, preventing exposure of germinated spores in the clump to the enzyme (Photos were not shown here).

Clumps of hyphae also made it difficult to separate the protoplasts, since the protoplasts have a tendency to adhere to them (Wiley, 1974). In future studies, the inoculum should be filtered to remove the old hyphae before use (Seanna Annis, private communication).

Twenty-four hours after inoculation is too short a time for the growth of *P. chrysosporium*. Most spores did not germinate in this time period (Photo was not shown here). Seven-day cultures have been used to isolate membrane vesicles from *P. chrysosporium* (Green et al., 1984). It was reported that protoplast yield was highest from mycelia in the exponential growth phase (Smith and Berry, 1975).

The malt extract liquid media was reported as a nitrogen sufficient media and the adding of the malt extract into the liquid media decreased the yield of protoplasts from *Aspergillus niger*. Low nitrogen glucose-salts-asparagine liquid media was reported to give the highest yield of protoplasts from *A. niger* (Smith and Berry, 1975). The low nitrogen liquid media used for *P. chrysosporium* culture in membrane vesicle isolation contained 0.6mM asparagine and 0.6 mM NH_4NO_3 as the nitrogen source (Green et al., 1984).

Gradient ultra - centrifugation can increase the purity of the plasma membrane fractions (Bowman and Slayman, 1981; Labarere and Bonneu, 1982).

Another approach for studying the siderophore receptors in wood decay fungi would be identifying the receptor genes directly. The sequences of 23 outer membrane ferric siderophore receptors from gram-negative bacteria have been published and a phylogenetic study has been performed for 21 receptors. Some amino acid sequences of receptors are highly conserved (Helm, 1998; Baumler et al., 1998). At least 3 sets of different primers have been designed for PCR studies of siderophore receptor genes in

bacteria (Koster et al., 1995; Levier and Guerinot, 1996; Baumler et al., 1997). This background information would be very helpful for studying the siderophore receptors of wood decay fungi.

Developing methods to isolate and purify membrane fractions from wood decay fungi will contribute to research on the physiology of wood decay fungi, which will also help to elucidate the wood biodegradation process as utilized by these organisms.

Chapter 6

CONCLUSIONS

Phenolate biochelators are believed to mediate a Fenton reaction responsible for wood biodegradation by brown rot fungi (Jellison et al., 1991 (a); Goodell et al., 1997 (a) and (b), 2001). Brown rot biodegradation of wood is characterized by rapid strength losses and diffused patterns of degradation (Zabel and Morel, 1992; Eaton, 2000). The brown rot fungi have been shown to produce iron - reducing phenolate biochelators (Jellison et al., 1991 (a) and (b)). In the presence of ferric iron, the biochelators can reduce ferric iron to ferrous iron. The ferrous iron reacts with hydrogen peroxide, leading to the generation of destructive hydroxyl radicals (Fenton reaction) (Koenigs, 1974 and 1975; Jellison et al., 1991 (a) and (b), 1993, 1996, 1997; Goodell et al., 1997 (a) and (b), 2001). The phenolate biochelators produced by the brown rot fungus *Gloeophyllum trabeum* have been isolated and identified as hydroxylated phenylacetic acids, hydroxylated benzoic acids, hydroxylated benzene derivatives and dihydroxyphenyl pentanediol (Easwaran, 1994; Goodell et al., 1997 (a)). Phenolate compounds 4,5-dimethoxy catechol (4,5-DMC) and 2,5-dimethoxy hydroquinone (2,5-DMHQ) have also been identified as key metabolites with iron - reducing activity produced by *G. trabeum* (Paszczynski et al., 1999; Jensen et al., 2001).

It has been demonstrated that brown rot, white rot, and wood-inhabiting non-decay fungi all produce biochelators (Charlang et al., 1981; Fekete et al., 1989). To elucidate the effects of biochelators on the ability of a fungus to degrade lignocellulose, biochelators produced by brown rot fungi *G. trabeum*, *Postia placenta*, *Fomitopsis pinicola*, white rot fungi *Phanerochaete chrysosporium*, *Trametes versicolor*, *Trichaptum*

abietinum, and wood-inhabiting non-decay fungi *Trichoderma viride*, *Phialocephala fusca*, *Phialophora mutabilis* were characterized based on the main chelating groups and iron reducing ability. As reported previously, all fungal species tested produced biochelators. The ubiquitous production of siderophore-like iron-chelating compounds by these fungi suggests that biochelators may play a role in general fungal physiology such as iron acquisition.

The patterns of biochelator production by tested fungi varied. All species tested produced hydroxamic acid type biochelators. All three brown rot fungi and all three non-decay fungi produced phenolate type compounds that were distributed in both the organic phase and the aqueous phase. The white rot fungus *P. chrysosporium* produced very low levels of phenolate type compounds. The white rot fungi *T. versicolor* and *T. abietinum* produced phenolate type or mixed type compounds that were only distributed in the aqueous phase. HPLC analysis indicated that the brown rot fungus *G. trabeum* produced DHBA like phenolate compounds, which were not observed with the white rot fungus *P. chrysosporium*. *Phanerochaete chrysosporium* produced higher amount of hydroxamic acid type chelators than phenolate type chelators. The reverse was seen for *G. trabeum*. Among the fungi tested, *P. chrysosporium* produced the highest amount of hydroxamic acid type chelators, while *G. trabeum* produced the highest amount of phenolate type chelators.

The iron - reducing ability of biochelators produced by tested fungi also varied. Biochelators from the brown rot fungi showed higher iron - reducing ability than did comparable amounts of biochelators from the white rot fungi. Of the fungi examined, the brown rot fungus *F. pinicola* produced biochelators with the highest iron - reducing

ability. The high iron - reducing ability of biochelators produced by the brown rot fungi supports previous observations. That is, the brown rot fungi, unlike the white rot fungi, utilize a non-enzymatic, FeII dependent, free radical based process in lignocellulose breakdown (Koenigs, 1974 and 1975; Kirk et al., 1991; Backa et al., 1992; Wood, 1993; Hirano et al., 1997). The brown rot fungi would therefore need not only siderophore-like compounds for iron acquisition, but also additional iron-chelating compounds capable of catalyzing extracellular iron reduction.

An extracellular cellobiose dependent quinone - reducing enzyme, cellobiose dehydrogenase (CDH), has been proposed to mediate the Fenton reaction in white rot fungi and in the brown rot fungus *Coniophora puteana* by reducing ferric iron and molecular oxygen (Schimidhalter and Canevascini, 1993 (a) and (b); Cameron and Aust, 1999). CDH has been purified from various white rot and soft rot fungi (Ayers et al., 1978; Dekker, 1980; Fahnrich and Irrgang, 1982; Coudray et al., 1982; Canevascini et al., 1991; Bao et al., 1993; Schou et al., 1993 and 1998; Fang et al., 1998; Dumonceaux et al., 1998; Temp and Eggert, 1999; Moukha et al., 1999; Subramaniam et al., 1999; Igarashi et al., 1999; Hallerg et al., 2000; Baminger et al., 2001). To our knowledge, *Coniophora puteana* is the only brown rot fungus from which CDH has been purified and characterized (Schimidhalter and Canevascini, 1993 (a) and (b)). Production of CDH by *G. trabeum* in glucose mineral media has been studied and no CDH activity was detected (Kerem et al., 1999).

In this study, the production of CDH by the white rot fungus *P. chrysosporium*, the brown rot fungus *G. trabeum*, and the non-decay fungus *T. viride* grown under cellulolytic conditions was monitored. In the presence of cellulose, all the fungi tested

produced low levels of CDH activity in the media. The results are consistent with the observations that the enzyme is induced by cellulose, but little of the activity is released into the media because the enzyme is bound to cellulose strongly via a cellulose - binding site (Henriksson et al., 1997). Cellobiose dehydrogenase has been purified from *P. chrysosporium* (Bao et al., 1993; Higham et al., 1994; Raices et al., 1995; Lehner et al., 1996; Li et al., 1996 and 1997; Igarashi et al., 1996, 1998 and 1999; Cohen et al., 1997; Henriksson et al., 1997 and 1998; Habu et al., 1993 and 1997; Vallim et al., 1998; Cameron and Aust, 1999). Production of CDH by *G. trabeum* and *T. viride* has not been previously reported. To efficiently purify CDH from *G. trabeum* and *T. viride*, increasing the release of CDH into liquid media would be required. Shake cultures have been shown to increase the production and release of the CDH into liquid media (Igarashi et al., 1996). It has also been reported that supplementing the liquid media with bovine calf serum increases the CDH production in *P. chrysosporium* (Habu et al., 1997). Genes encoding CDH in *P. chrysosporium*, *P. cinnabarinus*, *T. versicolor*, and *S. thermophile* have been cloned and characterized. The enzymes from different fungi showed high protein sequence identity (Raices et al., 1995; Li et al., 1996 and 1997; Vallim et al., 1998; Moukha et al., 1999; Dumonceaux et al., 1998; Subramaniam et al., 1999). This suggests that it will be possible to characterize the CDH in *G. trabeum* and *T. viride* directly at the gene level.

A new role played by CDH was proposed in our study. It has been shown that CDH oxidizes cellobiose to cellobionolactone, determined to be a hydroxamic acid derivative (Westermarck and Eriksson, 1975; Higham et al., 1994). Increased production of hydroxamic acid biochelators in the media containing cellulose was observed in our

study. We suggest that CDH may be involved in the pathway generating hydroxamic acid biochelators.

The non-decay fungi examined in this work produced moderate levels of both phenolate type and hydroxamic acid type chelators. The biochelators produced also showed iron reduction ability, which was usually higher than the ability of the chelators from the white rot fungi and from some of the brown rot fungi. The non-decay fungus *Trichoderma viride* also produced detectable CDH activity. However, *T. viride* did not degrade the spruce wood blocks in the soil block decay test. The ability of a non-decay fungus such as *Trichoderma* to produce many of the components postulated to be involved in wood biodegradation but still not decay wood has not been explained, and clearly has implications for understanding wood degradation and preservation.

The presence of extracellular, membrane - bound, or intracellular quinone - reducing enzymes in *G. trabeum*, has been first proposed by Paszczynski and colleagues (1999). The enzymes have been suggested to play a role in the generation of phenolate compounds, such as 2,5-DMHQ and 4,5-DMC (Paszczynski et al., 1999). In the proposed phenolate biochelator mediated Fenton reaction, the biochelators are oxidized to quinones by reducing ferric iron and/or molecular oxygen. Through in vitro studies, it has been found that one equivalent of biochelator can reduce multiple equivalents of ferric iron (Goodell et al., 1997 (a) and (b)). Possible biochelator regeneration via a redox cycle was first proposed by Goodell and colleagues (1997). A quinone redox cycle mediated by either extracellular, or membrane-bound, or intracellular quinone - reducing enzymes was proposed subsequently (Paszczynski et al., 1999; Kerem et al., 1999; Jensen et al., 2001).

Spatial and other constraints suggest that the utility of such a redox system in vivo may be limited. Recent research highlights the role mineralization may play in the ability of biochelators to reduce multiple iron equivalents (Goodell et al., 2001; Pracht et al., 2001). To determine the role of reductive systems in the physiology of decay organisms, quinone – reducing systems of *G. trabeum*, such as the extracellular cellobiose dependent quinone - reducing activity, the plasma membrane redox system (PMRS), and the intracellular quinone - reducing enzymes, were studied.

The *G. trabeum* PMRS was characterized based upon ferricyanide reduction kinetics and 1,4-quinone reduction. For comparison, 1,4-quinone reduction by the crude intracellular enzyme extract from *G. trabeum* was also characterized.

For *G. trabeum*, the ferricyanide reduction rates depended on initial ferricyanide concentration and initial mycelial mass. The reduction rates were within linear range when the ferricyanide concentration was up to 20 mM and when the mycelia mass was up to 120 mg (dry weight) in 200 mM potassium phosphate buffer (pH 8.0). Specific activity of 12 nmol/min/mg (mycelia dry weight) was obtained in pH 8.0 potassium phosphate buffer (200 mM) with 10 mM ferricyanide and 97 +/- 3mg dry weight of mycelia. The rates increased with pH above the physiological pH. Ferricyanide reduction was inhibited by carbonyl cyanide m-chloromethoxyphenyl hydrazone, 2,4-dinitrophenol and sodium azide, all of which are known inhibitors for membrane redox systems, at 100 nmol/mg (dry weight) mycelia. Ferricyanide reduction was not inhibited by potassium cyanide.

Reduction of 1,4-benzoquinone by the *G. trabeum* PMRS had an optimum pH between 5.0 and 7.0, a K_m of 59 μ M, and a V_{max} of 17.5 nmol/min/mg (dry weight mycelia). The intracellular enzyme extract from *G. trabeum* utilized NADH or NADPH

as the electron donor for quinone reduction. The quinone reduction rates with NADH and NADPH were similar. With NADH as the electron donor, it had a pH optimum of 6.5, a K_m of 156 μM , and a V_{max} of 863 nmol/min/mg.

Both the intact hyphae and the intracellular enzyme extract from *G. trabeum* could reduce 1,4-benzoquinone. The optimum reaction pH, K_m , and V_{max} were different, from which we conclude that *G. trabeum* produces a certain level of constitutive intracellular quinone reductases, and both of the PMRS and intracellular quinone reductases contribute to quinone reduction in *G. trabeum*. An intracellular quinone reductase from *G. trabeum* was purified and characterized.

The native enzyme purified from *G. trabeum* was a flavin protein with a molecular weight of 66 KD and a pI value of 4.2. The subunit molecular weight was 22 KD. The coenzyme determined by visible spectrum and fluorescence was flavin mononucleotide. The ratio of the enzyme to the FMN was 1:2.8. The enzyme was inducible by 2,6-dimethoxy-1,4-benzoquinone and 4-hydroxy-3-methoxybenzoic acid in both low nitrogen and nitrogen sufficient media at either 24 or 30 °C. It utilized NADH as an electron donor and catalyzes the reduction of multiple quinones and electron acceptors such as 2,6-dichloro-indophenol, and potassium ferricyanide. For enzyme catalyzed 2,6-dimethoxy-1,4-benzoquinone reduction, the apparent K_m was 6.8 μM and the K_{cat} was $1.0 \times 10^3 \text{ S}^{-1}$; the pH optimum was between 5.5 and 7; the optimal temperature was between 24 and 40 °C. The stoichiometry of NADH oxidation versus 2,6-dimethoxy-1,4-benzoquinone was 1:1. Inhibition of 2,6-dimethoxy-1,4-benzoquinone reduction occurred at low NADH concentration. Dicumarol and cibacron blue were competitive inhibitors with K_i values of 0.5 and 0.2 μM , respectively.

CDH, the PMRS and the intracellular quinone reductase from *G. trabeum* all showed quinone-reducing ability. They may participate in the production of phenolate compounds. However, they are spatially separated from the biochelator driven Fenton reaction occurring in the wood cell wall. Consequently it may be difficult for these enzymes to mediate the proposed quinone redox cycle *in vivo*.

CDH catalyzes cellobiose dependent quinone reduction, but the electron donor, cellobiose, is a product from enzymatic degradation of cellulose. It will not exist at the early stage of brown rot decay, which is believed to be a non-enzymatic oxidation process. As an enzyme, the ability of CDH to diffuse in the intact wood cell wall would also be limited at the early stage of degradation. As a result, CDH would not be expected to contribute much to the quinone redox cycle at initial degradation stages.

Spatial separation of the mycelia and the extracellular quinone redox cycle would prohibit the mycelial quinone - reducing systems, such as the plasma membrane redox system and the intracellular quinone reductase, from functioning directly. In brown rotted wood, the degree of polymerization of cellulose decreases rapidly at a very early stage of decay, when little weight loss has been observed. The reaction is not associated with hyphae and is highly diffusible. Since hydroxyl radicals are highly destructive but short lived within very limited spatial distances, the hydroxyl radical generating Fenton reaction has been proposed to occur inside the wood cell wall and to initiate attack of lignocellulose *in situ*. As a result, it is not likely for the hyphae in the wood cell lumen to participate directly in a quinone redox cycle that is expected to occur inside the wood cell wall. For the intracellular quinone reductase to function, quinones produced by catalyzing the extracellular Fenton reaction would have to be taken up by the fungal cells for

reduction. Then the hydroquinones would be released out of the cells and diffuse away into the wood cell wall. For the membrane redox system, the low pH conditions in the hyphal vicinity also need to be considered. It has been observed that the optimum pHs for ferricyanide reduction and quinone reduction by the PMRS are higher than pH 5, while it has been known that the pH in the *G. trabeum* hyphal vicinity is often lower than pH 4 *in vivo*. Thus the reduction of ferricyanide and quinones, as well as associated activities, are expected to be inhibited at least at later stages of wood colonization and degradation. The low pH also inhibits the iron reduction by catechols and hydroquinones. Thus, if the quinone reduction by PMRS did play a role in the quinone redox cycle in the biochelator - driven Fenton reaction brown rot mechanism, it is more likely to occur at the very early stage when the fungus is decreasing the environmental pH. The reduction would also be expected to occur near the hyphae.

Recent research has shown that catechols can be partially or completely mediated to carbon dioxide by reducing multiple equivalents of ferric iron, while such mineralization was not observed with hydroquinones (*p*-diol) (Pracht et al., 2001). It has also been demonstrated that 2,5-demethoxy hydroquinone produced by *G. trabeum* can reduce 4,5-dimethoxy-1,2-benzoquinone to 4,5-dimethoxy catechol extracellularly (Jensen et al., 2001). As a result, the catechol chelators produced by the brown rot fungi could be either mediated to carbon dioxide or regenerated by a hydroquinone mediated quinone redox cycle extracellularly, while the extracellular pathway for the regeneration of hydroquinone chelators remains unknown.

Although there exist spatial difficulties limiting the mycelial quinone - reducing system ability to participate in the extracellular quinone redox cycle, it has been found

that *G. trabeum* mycelia are necessary for the depolymerization of polyethylene glycol by the extracellular Fenton reaction system containing 2,5-dimethoxy-1,4-benzoquinone, ferric iron and hydrogen peroxide (Kerem et al., 1998). It has also been found that 2,5-dimethoxyl hydroquinone is more effective than 4,5-dimethoxy catechol in driving the extracellular Fenton reaction to degrade polyethylene glycol. The rate of 2,5-DMBQ reduction by *G. trabeum* mycelia is much higher than the rate of 4,5-DMBQ reduction, as well (Jensen et al., 2001). Consequently, 2,5-dimethoxy-1,4-benzoquinone would be more likely to be reduced to 2,5-dimethoxy hydroquinone by mycelial quinone - reducing activities (Jensen et al., 2001). Both redox cycling pathways and mineralization pathways may exist in *G. trabeum*. The relative importance of 2,5-DMBQ and 4,5-DMBQ versus other more ubiquitous phenolates has not been established.

Gloeophyllum trabeum PMRS and intracellular quinone reductase have been proposed to have other functions. The proton extrusion ability associated with the PMRS activity might play a role in the ability of fungi to both quickly adjust the environmental pH and to maintain the cytoplasmic pH. PMRS activity might be also associated with the pathway of some ion uptake pathways in *G. trabeum*. The high induction of *G. trabeum* intracellular quinone reductase activity by benzoquinones and the low apparent K_m values to benzoquinones indicate that quinone reductase may play critical roles in the quinone metabolism of brown rot fungi. A significant function of the intracellular quinone reductase from *G. trabeum* may be protecting the cells from quinone and semiquinone toxicity.

Although the PMRS can reduce 1,4-benzoquinone, the electron donors have not been identified. For further biochemical and biophysical studies, isolation of the plasma

membrane and purification of the membrane-bound quinone reductase will be necessary. Isolation of the plasma membrane is also important to many other studies of fungal physiology, such as studies on siderophore receptors. Isolation and characterization of membrane fractions from *P. chrysosporium* were performed but additional work is required. The study is meaningful for further studies of the physiology and biochemistry of wood decay fungi.

In summary, the present research has characterized the production of biochelator and CDH by different fungi. All the tested fungi (white rot, brown rot and wood-inhabiting non-decay) produced iron-chelating compounds. The brown rot fungi produced more phenolate biochelators than hydroxamic acid type biochelators. Biochelators produced by the brown rot fungi also show higher iron - reducing activity. The results support the theory that a biochelator mediated Fenton reaction is involved in brown rot biodegradation. Biochelators were ubiquitous in the tested fungi indicating they may also play roles in general fungal physiology such as in iron acquisition.

All fungi tested also produced detectable level of CDH in the presence of cellulose. Previous reports on the lack of CDH production by *G. trabeum* (Kerem et al., 1999) may have been due to inappropriate culture conditions. Cellobiose dehydrogenase has been reported to oxidize cellobiose and drive the Fenton reaction enzymatically. Cellobiose dehydrogenase may participate in the pathway that generates hydroxamic acid biochelators. The quinone - reducing activity of CDH suggests it might play a role in the phenolate biochelator mediated Fenton reaction. But limited by the availability of cellobiose and by the diffusibility of the enzyme at the initial decay stage, a CDH mediated quinone reduction is not likely to occur *in vivo* at the initial decay stages.

An intracellular NADH dependent quinone reductase from *G. trabeum* has been purified and characterized. The enzyme is a constitutive enzyme, but the expression is highly induced by methoxy benzoquinone. It is also induced by vanillic acid at a lower induction fold. The quinone reductase has low substrate saturation values toward 1,4-benzoquinones. It reduces multiple quinones by a two-electron reduction. The characteristics of the enzyme indicate that *G. trabeum* has a sensitive mechanism for quinone metabolism. An important function of the enzyme would be to protect cells from quinone and semiquinone toxicity. As an important enzyme in the pathway generating catechols, hydroquinones and other phenolate compounds, the intracellular quinone reductase may also play an indirect role in the biochelator - driven Fenton reaction brown rot mechanism. By mediating the intracellular quinone reduction and releasing the catechols/hydroquinones produced externally, the intracellular quinone reductase would act as a type of electron carrier that transports the electrons from the intracellular NADH pool to the extracellular environment. The spatial separation of fungal hyphae from the extracellular Fenton reaction however, limits the role the PMRS and intracellular quinone reductase could potentially play in the brown rot degradation process. And as noted earlier, mineralization of catechol biochelators may be a significant pathway in some cases for continuous production of Fenton reagents.

A method to isolate and characterize the plasma membrane fractions from wood decay fungi has been developed. It will be helpful for further study of fungal physiology and biochemistry.

The present study contributes to the understanding of the brown rot decay mechanism and to some aspects of the physiology and biochemistry of wood decay fungi.

Significant questions still remain encompassing the role of biochelators and reductive enzymes in physiological and biodegradative processes ranging from pH regulation, to hyphal protection, ion uptake and quinone recycling. Studies on the decay mechanisms and the physiology of wood decay fungi will eventually help in the development of environmentally - friendly wood preservation methods and the utilization of biodegradative mechanisms for remediation and bioprocesses.

REFERENCES

- Abash, F. G. C., and L. C. D. S. Ferreira. 1990. Comparative studies of *Perinea pest*'s outer membrane isolation techniques and their potential use in plague epidemiology. *Rev. Inst. Med. Trop. Sao. Paulo.* 32(2): 78-83.
- Akileswaran, L., B. J. Brock, J. L. Cereghino, and M. H. Gold. 1999. 1,4-Benzoquinone reductase from *Phanerochaete chrysosporium*: cDNA cloning and regulation of expression. *App. Environ. Microbiol.* 65(2): 415-421.
- American Society for Testing and Materials. 1994. Standard method of accelerated laboratory test of natural decay resistance of woods. (D1413-76). In: 1994 Annual Book of ASTM Standards, Set 4, Vol. 04. 10. American Society for Testing and Materials, Philadelphia, PA.
- Ander, P. 1994. The cellobiose-oxidizing enzymes CBQ and CBO as related to lignin and cellulose degradation - a review. *FEMS Microbiology Reviews.* 13: 297-312.
- Ander, P., A. Hatakka, and K. E. Eriksson. 1980. Vanillic acid metabolism by the white rot fungus *Sporotrichum pulverulentum*. *Archives of Microbiology.* 125: 189-202.
- Ander, P., and L. Marzullo. 1997. Sugar oxidoreductases and veratryl alcohol oxidase as related to lignin degradation. *J. Biotechnol.* 53: 115-131.
- Arnow, L. E. 1937. Colorimetric determination of the components of 3,4-Dihydroxyphenylalanine - tyrosine mixtures. *J. Biol. Chem.* 118: 531-537.
- Askwith, C. C., D. D. Silva, and J. Kaplan. 1996. Molecular biology of iron acquisition in *Saccharomyces cerevisiae*. *Molecular Microbiology.* 20(1): 27-34.
- Aust, S. D. 1995. Mechanisms of degradation by white rot fungi. *Environ. Health Perspect.* 103(Suppl 5): 59-61.
- Avron, M., and N. Shavit. 1963. A sensitive and simple method for determination of ferrocyanide. *Analytical Biochemistry.* 6: 549-554.
- Ayers, A. P., S. B. Ayers, and K. E. Eriksson. 1978. Cellobiose oxidase, purification and partial characterization of a hemoprotein from *Sporotrichum pulverulentum*. *Eur. J. Biochem.* 90: 171-181.
- Bachs, D. 1999. DNP (2,4-Dinitrophenol) getting leaner through chemistry. *Pharma Group.* 2: 1-13.
- Backa, S., J. Gierer, T. Reitberger, and T. Nilsson. 1992. Hydroxyl radical activity in brown rot fungi studied by a new chemiluminescence method. *Holzforschung.* 46: 61-67.

- Baminger, U., S. S. Subramaniam, V. Renganathan, and D. Haltrich. 2001. Purification and characterization of cellobiose dehydrogenase from the plant pathogen *sclerotium (Athelia) rolfsii*. *App. Environ. Microbiol.* 67(4): 1766-1774.
- Bao, W., S. N. Usha, and V. Renganathan. 1993. Purification and characterization of cellobiose dehydrogenase, a novel extracellular hemoflavoenzyme from the white rot fungus *Phanerochaete chrysosporium*. *Arch. Biochem. Biophys.* 300(2): 705-713.
- Bardage, S. L., and D. Geoffrey. 1998. The ability of fungi to penetrate micropores: Implications for wood surface coating. *Materials and Organisms.* 31(4): 233-245.
- Barr, R., A. Brightman, D. J. Morre, and F. L. Crane. 1990. Modulation of plasma membrane electron transport reactions and associated proton excretion by vitamin K1 and related naphthoquinones. *J. Cell. Biol.* 111: 389.
- Barton, L. L., and B. C. Hemming. 1992. Iron Chelation in Plants and Soil Microorganisms. Academic Press, Inc., San Diego, California.
- Baumler, A. J., F. Heffron, and R. Reissbrodt. 1997. Rapid detection of *Salmonella enterica* with primers specific for ironB. *Journal of Clinical Microbiology.* 35(5): 1224-1230.
- Baumler, A. J., T. L. Norris, T. Lasco, W. Voight, R. Reissbrodt, W. Rabsch, and F. Heffron. 1998. IronN, a novel outer membrane siderophore receptor characteristic of *Salmonella enterica*. *Journal of Bacteriology.* 180(6): 1446-1453.
- Benson, A. M., M. J. Hunkeler, and P. Talalay. 1980. Increase of NAD(P)H : quinone reductase by dietary antioxidants: possible role in protection against carcinogenesis and toxicity. *Proceedings of the National Academy of Sciences of the United States of America.* 77: 5216-5220.
- Berczi, A., and M. Moller. 2000. Redox enzymes in the plant plasma membrane and their possible roles. *Plant, Cell and Environment.* 23(12): 1287-1302.
- Beyer, R. E., J. Segura-Aguilar, S. Di Bernardo, M. Cavazzoni, R. Fato, D. Fiorentini, M. C. Galli, M. Setti, L. Landi, and G. Lenaz. 1996. The role of DT-diaphorase in the maintenance of the reduced antioxidant form of coenzyme Q in membrane systems. *Proceedings of the National Academy of Sciences of the United States of America.* 93: 2528-2532.
- Beyer, R. E., J. Segura-Aguilar, S. Di Bernardo, M. Cavazzoni, R. Fato, D. Fiorentini, M. C. Galli, M. Setti, L. Landi, and G. Lenaz. 1997. The two-electron quinone reductase DT-diaphorase generates and maintains the antioxidant (reduced) form of coenzyme Q in membranes. *Molecular Aspect of Medicine.* 18 Suppl: S15-S23.

- Bienfait, H. F. 1985. Regulated redox processes at the plasmalemma of plant root cells and their function in iron uptake. *J. Bioenerg. Biomembr.* 17: 73-83.
- Blanchette, R. A. 1994. Degradation of the lignocellulose complex in wood. *Can. J. Bot.* 73(Suppl. 1): S999-S1010.
- Blum, J. S., C. W. Culbertson, and R. S. Oremland. 1993. Anaerobic growth of bacterial strain ses#3 with selenate as the electron acceptor. Colorado Springs Proceedings. Section J. Colorado Springs, Colorado.
- Bollag, D. M., M. D. Rozycki, and S. J. Edelstein. 1996. Protein Methods. Wiley-Liss, Inc., New York.
- Bourbonnais, R., and M. G. Paice. 1990. Oxidation of non-phenolic substrates. An expanded role for laccase in lignin biodegradation. *FEBS Letters.* 267: 99-102.
- Bourbonnais, R., D. Leech, and M. G. Paice. 1998. Electrochemical analysis of the interactions of laccase mediators with lignin model compounds. *Biochimica et Biophysica Acta.* 1379: 381-390.
- Bowman, B. J., and C. W. Slayman. 1979. The effect of vanadate on the plasma membrane ATPase of *Neurospora crassa*. *J. Biol. Chem.* 254: 2928-2934.
- Bowman, B. J., and C. W. Slayman. 1981. Isolation and characterization of plasma membranes from wild type *Neurospora crassa*. *J. Biol. Chem.* 256: 12336-12342.
- Bowman, B. J., S. E. Mainzer, K. E. Allen, and C. W. Slayman. 1978. Effects of inhibitors on the plasma membrane and mitochondria adenosine triphosphatases of *Neurospora crassa*. *Biochimica et Biophysica Acta*, 512: 13-28.
- Brock, B. J., S. Rieble, and M. H. Gold. 1995. Purification and characterization of a 1,4-benzoquinone reductase from the basidiomycete *Phanerochaete chrysosporium*. *App. Environ. Microbiol.* 61(8): 3076-3081.
- Brock, B. J., and M. H. Gold. 1996. 1,4-benzoquinone reductase from the basidiomycete *Phanerochaete chrysosporium*: spectral and kinetic analysis. *Arch. Biochem. Biophys.* 331(1): 31-40.
- Burgstaller, W. 1997. Transport of small ions and molecules through the plasma membrane of filamentous fungi. *Critical Reviews in Microbiology.* 23(1): 1-46.
- Buswell, J. A., K. E. Eriksson, and B. Petterson. 1981. Purification and partial characterization of vanillate hydroxylase (decarboxylating) from *Sporotrichum pulverulentum*. *J. Chromatogr.* 215: 99-108.

- Buswell, J. A., S. Hamp, and K. E. Eriksson. 1979. Intracellular quinone reduction in *Sporotrichum pulverulentum* by an NAD(P)H:quinone oxidoreductase. FEBS Letter. 108(1): 229-232.
- Cameron, M. D., and S. D. Aust. 1999. Degradation of chemicals by reactive radicals produced by cellobiose dehydrogenase from *Phanerochaete chrysosporium*. Arch. Biochem. Biophys. 367: 115-121.
- Canevascini, G., P. Borer, and J. Dreyer. 1991. Cellobiose dehydrogenase of *Sporotrichum (Chrysosporium) thermophile*. Eur. J. Biochem. 198: 43-52.
- Cervinkova, Z., Z. Drahota, H. Lotkova, R. Svatkova, and M. Cervinka. 1998. Mitochondrial membrane potential as an indicator of hepatocyte injury. Vedecka Konferenc. Simkova, Hradec Kralove.
- Charlang, G., B. Ng, N. H. Horowitz, and R. M. Horowitz. 1981. Cellular and extracellular siderophores of *Aspergillus nidulans* and *Penicillium chrysogenum*. Mol. Cell Biol. 1(2): 94-100.
- Chen, Y. 1994. Regulation of Hyphal Sheath Formation and Biochelator Production by the Brown Rot Fungi *Gloeophyllum trabeum* and *Postia placenta*. MS Thesis. University of Maine at Orono.
- Chen, S., P. S. Deng, J. M. Bailey, and K. M. Swiderek. 1994. A two-domain structure for the two subunits of NAD(P)H : quinone acceptor oxidoreductase. Protein Science. 3: 51-57.
- Cody, Y. S., and D. C. Gross. 1987. Outer membrane protein mediating iron uptake via Pyoverdinps, the fluorescent siderophore produced by *Pseudomonas syringae pv. syringae*. Journal of Bacteriology. 169(5): 2207-2214.
- Cohen, J. D., W. Bao, V. Renganathan, S. S. Subramaniam, and T. M. Loehr. 1997. Resonance raman spectroscopic studies of cellobiose dehydrogenase from *Phanerochaete chrysosporium*. Archives of Biochemistry and Biophysics. 341(2): 321-328.
- Connolly, J. H., and J. Jellison. 1995. Enhanced oxalate production by the brown rot fungus *Gloeophyllum trabeum* upon exposure to TCA cycle acids. Phytopathology. 85(10): 1161.
- Connolly, J. H., and J. Jellison. 1997. Two-way translocation of cations by the brown rot fungus *Gloeophyllum trabeum*. International Biodeterioration & Biodegradation. 39(2-3): 181-188.

- Connolly, J. H., H. J. Arnott, and J. Jellison. 1996. Patterns of calcium oxalate crystal production by three species of wood decay fungi. *Scanning Microscopy*. 10(2): 385-400.
- Constam, A., A. Muheim, W. Zimmermann, and A. Fiechter. 1991. Purification and characterization of an intracellular NADH : quinone oxidoreductase from *Phanerochaete chrysosporium*. *J. Gen. Microbiol.* 137: 2209-2214.
- Conway, E. J., and R. P. Kernan. 1955. The effect of redox dyes on the active transport of hydrogen, potassium and sodium ions across the yeast cell wall. *Biochemical Journal*. 61: 32-36.
- Cotoras, M., and E. Agosin. 1992. Regulatory aspects of endoglucanase production by the brown rot fungus *Gloeophyllum trabeum*. *Experimental Mycology*. 16(4): 253-260.
- Coudray, M., G. Canevascini, and H. Meier. 1982. Characterization of a cellobiose dehydrogenase in the cellulolytic fungus *Sporotrichum(Chrysosporium) thermophile*. *Biochemistry Journal*. 203: 277-284.
- Crane, F. L., H. Roberts, A. W. Linnane, and H. Low. 1982. Transmembrane ferricyanide reduction by cells of the yeast *Saccharomyces cerevisiae*. *Journal of Bioenergetics & Biomembranes*. 14: 191-205.
- Crestini, C., and D. S. Argyropoulos. 1998. The early oxidative biodegradation steps of residual kraft lignin models with laccase. *Bioorganic & Medicinal Chemistry*. 6: 2161-2169.
- Crosa, J. H., and L. L. Hodges. 1981. Outer membrane proteins induced under conditions of iron limitation in the marine fish pathogen *Vibrio anguillarum* 755. *Infection and Immunity*. 31(1): 223-227.
- Csaky, T. Z. 1948. On the estimation of bound hydroxylamine in biological materials. *Acta Chem. Scand.* 2: 450-454.
- Dekker, R. F. H. 1980. Induction and characterization of a cellobiose dehydrogenase produced by a species of *Monilia*. *J. Gen. Microbiol.* 120: 309-316.
- Dinkova-Kostova, A. T., and P. Talalay. 2000. Persuasive evidence that quinone reductase type 1 (DT-diaphorase) protects cells against the toxicity of electrophiles and reactive forms of oxygen. *Free Radical Biology & Medicine*. 29(3-4): 231-240.
- Doyle, B., and J. Jellison. 1996. Arsenic, chromium, and copper toxicity in four species of brown rot fungi. *Phytopathology*. 86(11 supplement): S102.

- Dryer, R. L., A. R. Tammes, and J. I. Routh. 1957. The determination of phosphorus and phosphatase with N-phenyl-p-phenylenediamine. *J. Biol. Chem.* 225: 177-183.
- D'Souza, T. M., K. Boominathan, and C. A. Reddy. 1996. Isolation of laccase gene-specific sequences from white rot and brown rot fungi by PCR. *Appl. Environ. Microbiol.* 62(10): 3739-3744.
- Dumonceaux, T. J., K. A. Bartholomew, T. C. Charles, S. M. Moukha, and F. S. Archibald. 1998. Cloning and sequencing of a gene encoding cellobiose dehydrogenase from *Trametes versicolor*. *Gene.* 210: 211-219.
- Easwaran, V. 1994. The purification and partial characterization of iron-binding compounds produced by *Gloeophyllum trabeum*. MS Thesis. University of Maine at Orono.
- Eaton, R. 2000. A breakthrough for wood decay fungi. *New Phytologist.* 146(1): 3-4.
- Enard, C., A. Dioloz, and D. Expert. 1988. Systematic virulence of *Erwinia chrysanthemi* 3937 requires a functional iron assimilation system. *Journal of Bacteriology.* 170(6): 2419-2426.
- Enoki, A., H. Tanaka, and G. Fuse. 1989. Relationship between degradation of wood and production of hydrogen peroxide producing or one electron oxidases by brown rot fungi. *Wood Sci. Technol.* 23: 1-12.
- Enoki, A., S. Itakura, and H. Tanaka. 1997. The involvement of extracellular substances for reducing molecular oxygen to hydroxyl radical and ferric iron to ferrous iron in wood degradation by wood decay fungi. *J. Biotechnol.* 53: 265-272.
- Enoki, A., T. Hirano, and H. Tanaka. 1992. Extracellular substance from the brown rot basidiomycete *Gloeophyllum trabeum* that produces and reduces hydrogen peroxide. *Mater. Org.* 27: 247-261.
- Eriksson, K. E. L., R. A. Blanchette, and P. Ander. 1990. Biodegradation of lignin. *Microbial & Enzymatic Degradation of Wood and Wood Components.* Springer-Verlag K G, Berlin.
- Faeder, E. J., and L. M. Siegel. 1973. A rapid micromethod for determination of FMN and FAD in mixtures. *Analytical Biochemistry.* 53: 332-336.
- Fahnrich, P., and K. Irrgang. 1982. Conversion of cellulose to sugars and cellobionic acid by the extracellular enzyme system of *Chaetomium cellulolyticum*. *Biotechnol. Lett.* 4: 775-780.

- Fahr, K., H. Wetzstein, R. Grey, and D. Schlosser. 1999. Degradation of 2,4-dichlorophenol and pentachlorophenol by two brown rot fungi. *FEMS Microbiology Letters*. 175(1): 127-132.
- Fang, J., W. Liu, and P. Gao. 1998. Cellobiose dehydrogenase from *Schizophyllum commune*: purification and study of some catalytic, inactivation, and cellulose binding properties. *Arch. Biochem. Biophys.* 353(1): 37-46.
- Fekete, A. F. 1992. Assays for microbial siderophores. P. 399 - 417. In Barton, L. L., and B. C. Hemming. Iron Chelation in Plants and Soil Microorganisms. Academic Press Inc., San Diego, California.
- Fekete, A. F., V. Chandhoke, and J. Jellison. 1989. Iron binding compounds produced by wood decaying basidiomycetes. *Appl. Environ. Microbiol.* 55: 2720-2722.
- Fernando, T., J. A. Bumpus, and S. D. Aust. 1990. Biodegradation of TNT (2,4,6-Trinitrotoluene) by *Phanerochaete chrysosporium*. *Appl. Environ. Microbiol.* 56(6): 1666-1671.
- Flournoy, D. S., T. K. Kirk, and T. Highley. 1991. Wood decay by brown rot fungi: changes in pore structure and cell wall volume. *Holzforschung*. 45: 383-388.
- Foster, C. E., M. A. Bianchet, P. Talalay, M. Faig, and L. M. Amzel. 2000. Structures of mammalian cytosolic quinone reductases. *Free Radical Biology & Medicine*. 29: 241-245.
- Foster, C. E., M. A. Bianchet, P. Talalay, Q. Zhao, and L. M. Amzel. 1999. Crystal structure of human quinone reductase type 2, a metalloflavoprotein. *Biochemistry*. 38: 9881-9886.
- Freitag, M., and J. J. Morrell. 1992. Changes in selected enzyme activities during growth of pure and mixed cultures of the white rot decay fungus *Trametes versicolor* and the potential biocontrol fungus *Trichoderma harzianum*. *Can. J. Microbiol.* 38(4): 317-323.
- Fuller, K., A. Ostrofsky, and J. Jellison. 2000. Uptake and translocation of calcium, cobalt, zinc, and copper by wood decay fungi. *Phytopathology*. 90(6 Supplement): S25.
- Galkin, A. S., V. G. Grivennikova, A. D. Vinogradov. 1999. $H^+/2e^-$ stoichiometry in NADH-quinone reductase reactions catalyzed by bovine heart submitochondrial particles. *FEBS Letters*. 451: 157-161.
- Gear, M. L., D. W. McCurdy, and J. W. Patrick. 1999. Molecular characterization of a hexose transporter gene family in tomato. *International Conference on Assimilate Transport and Partitioning*. Session 5. Newcastle, Australia.

- Goodell, B. 2002. Brown rot fungal degradation of wood: our changing view. In press.
- Goodell, B., and J. Jellison. 1997. Wood degradation mechanisms by the brown rot fungus *Gloeophyllum trabeum*. International Research Group on Wood Preservation. IRG Secretariat, Box 5607 S-114 86 Stockholm, Sweden.
- Goodell, B., and J. Jellison. 1998. Role of biological metal chelators in wood biodeterioration. In A. Bruce and J. Palfreyman (Eds.). Forest Products Biotechnology. Taylor and Francis Publishers. London.
- Goodell, B., and J. Jellison. 1999. Brown rot biodegradation of wood. International Society of Biodegradation and Biodeterioration. Washington, D.C.
- Goodell, B., J. Jellison, G. Daniel, and Y. Qian. 1997 (a). Redox cycling chelators isolated from *Gloeophyllum trabeum* and their effect on wood fibers. TAPPI Proceedings. TAPPI Biological Sciences Symposium and Pulping Symposium. San Francisco, California.
- Goodell, B., J. Jellison, J. Liu, G. Daniel, A. Paszczynski, F. Fekete, S. Krishnamurthy, L. Jun, and G. Xu. 1997 (b). Low molecular weight chelators and phenolic compounds isolated from wood decay fungi and their role in the fungal biodegradation of wood. *Journal of Biotechnology*. 53: 133-162.
- Goodell, B., J. Jellison, Y. Qian, and J. Connolly. 1999 (a). Understanding how structural timbers decay: Mechanisms involved in the brown rot decay process. 1st International Conference on Advanced Engineered Wood Composites. July 5-8, 1999. Bar Harbor, Maine.
- Goodell, B., J. Jellison, Y. Qian, J. Connolly, and A. Paszczynski. 1999 (b). Chelating phenolates and the generation of oxygen radicals in brown rot wood decay. FPS 1999 Annual Meeting. June 27-30, 1999. Boise, Idaho.
- Goodell, B., J. Liu, J. Jellison, L. Jun, A. Pazchynski, and F. Fekete. 1996. Chelation activity and hydroxyl radical production mediated by low molecular weight phenolate compounds isolated from *Gloeophyllum trabeum*. In E. Srebotnik and K. Messner (Eds.) Biotechnology in the Pulp and Paper Industry. TAPPI Sixth Intrnl. Conf. On Biotech. in Pulp and Paper. Facultas-Universit Stsverlag, Berggasse 5, A-1090 Wien.
- Goodell, B., Y. Qian, J. Jellison, M. Richard, and W. Qi. 2001. Lignocellulose oxidation by low molecular weight metal binding compounds isolated from wood degrading fungi: A potential application of chelator-mediated Fenton reactions. In Press.
- Green, F. I., C. A. Clausen, T. A. Kuster, and T. L. Highley. 1995. Induction of polygalacturonase and the formation of oxalic acid by pectin in brown rot fungi. *World Journal of Microbiology & Biotechnology*. 11(5): 519-524.

- Green, R. V., and J. M. Gould. 1984. Electrogenic symport of glucose and protons in membrane vesicles of *Phanerochaete chrysosporium*. Arch. Biochem. Biophys. 228: 97-104.
- Guebitz, G. M., S. D. Mansfield, B. Boehm, and J. N. Saddler. 1998. Effect of endoglucanases and hemicellulases in magnetic and flotation deinking of xerographic and laser-printed papers. Journal of Biotechnology. 65(2-3): 209-215.
- Habu, N., K. Igarashi, M. Samejima, B. Pettersson, and K. Eriksson. 1997. Enhanced production of cellobiose dehydrogenase in cultures of *Phanerochaete chrysosporium* supplemented with bovine calf serum. Biotech. Appl. Biochem. 26: 97-102.
- Habu, N., M. Samejima, J. F. D. Dean, and K. L. Eriksson. 1993. Release of the FAD domain from cellobiose oxidase by proteases from cellulolytic cultures of *Phanerochaete chrysosporium*. FEBS. 327(2): 161-164.
- Hallerg, B. M., T. Bergfors, K. Backbro, G. Pettersson, G. Henriksson, and C. Divne. 2000. A new scaffold for binding haem in the cytochrome domain of the extracellular flavocytochrome c cellobiose dehydrogenase. Structure with Folding and Design. 8(1): 79-88.
- Hasspieler, B. M., G. D. Haffner, and K. Adeli. 1996. Influence of DT diaphorase on quinone-mediated genotoxicity in human and fish cell lines. Mutation Research. 360: 43-49.
- Helm, V. D. 1998. The physical chemistry of bacterial outer membrane siderophore receptor protein. Metal Ions in Biological Systems. 35: 355-401.
- Henriksson, G., A. Salumets, C. Divine, and G. Pettersson. 1997. Studies of cellulose binding by cellobiose dehydrogenase and a comparison with cellobiohydrolase 1. Biochem. J. 324: 833-838.
- Henriksson, G., V. Sild, I. J. Szabo, G. Pettersson, and G. Johansson. 1998. Substrate specificity of cellobiose dehydrogenase from *Phanerochaete chrysosporium*. Biochemica et Biophysica Acta. 1383: 48-54.
- Higham, C. W., D. Gordon-Smith, C. E. Dempsey, and P. M. Wood. 1994. Direct ¹H NMR evidence for conversion of β-D-cellobiose to cellobionolactone by cellobiose dehydrogenase from *Phanerochaete chrysosporium*. FEBS Letters. 351: 128-132.
- Highley, T. L. 1973. Influence of carbon source on cellulase activity of white-and brown-rot fungi. Wood Fiber. 5: 50-58.

- Highley, T. L. 1977. Requirements for cellulose degradation by a brown rot fungus. *Material and Organisms*. 12: 25-36.
- Highley, T. L. 1987. Biochemical aspects of brown rot and white rot. Stockholm. Int. Res. Group on Wood Pres. Doc. No: IRG/WP 1319. IRG Secretariat, Box 5607, S-115 86, Stockholm, Sweden.
- Highley, T. L. 1997. Control of wood decay by *Trichoderma (Gliocladium) virens*: I. Antagonistic properties. *Material and Organisms*. 31(2): 79-89.
- Highley, T. L., H. S. Padmanabha, and C. R. Howell. 1997. Control of wood decay by *Trichoderma (Gliocladium) virens*: II. Antibiosis. *Material and Organisms*. 31(3): 157-166.
- Hirano, S. M., H. Tanaka, and A. Enoki. 1997. Relationship between production of hydroxyl radicals and degradation of wood by the brown rot fungus *Tyromyces palustris*. *Holzforschung*. 51: 389-395.
- Hirano, T., H. Tanaka, and A. Enoki. 1995. Extracellular substance from the brown rot basidiomycete *Tyromyces palustris* that reduces molecular oxygen to hydroxyl radicals and ferric iron to ferrous iron. *Mokuzai Gakkaishi*. 41: 334-341.
- Hofte, M. 1992. Classes of microbial siderophores. In L. L. Barton and B. C. Hemming (ed.), Iron Chelation in Plants and Soil Microorganisms. Academic Press. Inc., San Diego, California.
- Horie, S. 1990. Advances in research on DT-diaphorase - catalytic properties, regulation of activity and significance in the detoxification of foreign compounds. *Kitasato Archives of Experimental Medicine*. 63(1): 11-30.
- Huschka, H., and G. Winkelmann. 1989. Iron limitation and its effect on membrane proteins and siderophore transport in *Neurospora crassa*. *Biol. Metals*. 2: 108-113.
- Hyde, S. M., and P. M. Wood. 1997. A mechanism for production of hydroxyl radicals by the brown rot fungus *Coniophora puteana*: Fe(III) reduction by cellobiose dehydrogenase and Fe(II) oxidation at a distance from the hyphae. *Microbiology*. 143: 259-266.
- Igarashi, K., M. F. J. M. Verhagen, M. Samejima, M. Schulein, K. L. Eriksson, and T. Nishino. 1999. Cellobiose dehydrogenase from the fungi *Phanerochaete chrysosporium* and *Humicola insolens*. *J. Biol. Chem.* . 274(6): 3338-3344.
- Igarashi, K., M. Samejima, and K. L. Eriksson. 1998. Cellobiose dehydrogenase enhances *Phanerochaete chrysosporium* cellobiohydrolase I activity by relieving product inhibition. *Eur. J. Biochem*. 253: 101-106.

- Igarashi, K., M. Samejima, Y. Saburi, N. Habu, and K. L. Eriksson. 1996. Localization of cellobiose dehydrogenase in cellulose grown cultures of *Phanerochaete chrysosporium*. *Fungal Genetics and Biology*. 21: 214-222.
- Ishimaru, C. A., and J. E. Loper. 1992 (a). Biochemical and genetic analysis of siderophores produced by plant-associated *Pseudomonas* and *Erwinia* species. In Barton, L. L. and B. C. Hemming (eds.) Iron Chelation in Plants and Soil Microorganisms. 27-73. Academic Press, Inc., San Diego, California.
- Ishimaru, C. A., and J. E. Loper. 1992 (b). High-affinity iron uptake systems present in *Erwinia carotovora* subsp. *carotovora* include the hydroxamate siderophore aerobactin. *Journal of Bacteriology*. 174(9): 2993-3003.
- Jellison, J., A. Enoki, B. Goodell, M. Ishihara, N. Hayashi, and H. Tanaku. 1993. Iron II and Iron III chelators produced by the brown rot fungus *Gloeophyllum trabeum*. *Phytopathology*. 83(12): 1410-1411.
- Jellison, J., B. Goodell, F. Fekete and V. Chandhoke. 1990 (a). Fungal siderophores and their role in wood biodeterioration. The International Research Group on Wood Preservation. IRG Secretariat, Box 5607, S-115 86, Stockholm, Sweden. Twenty-first Annual Meeting. Rotorua, New Zealand.
- Jellison, J., J. H. Connolly, and B. Goodell. 1997. Non-enzymatic degradation of wood by the brown rot fungus *Gloeophyllum trabeum*. *Phytopathology*. 87(6 supplement): S48.
- Jellison, J., J. Liu, B. Goodell, N. Hayashi, and M. Ishihara. 1996. Non-enzymatic biodegradation of cellulose by the brown rot fungus *Gloeophyllum trabeum*. *Phytopathology*. 86(11 supplement): S87.
- Jellison, J., V. Chandhoke, B. Goodell, and F. Fekete. 1990 (b). Biological chelators produced by wood decay fungi. Proceedings of the 8th International Biodeterioration and Biodegradation Symposium, Windsor, Canada.
- Jellison, J., V. Chandhoke, B. Goodell, and F. Fekete. 1991 (a). The isolation and immunolocalization of iron binding compounds produced by *Gloeophyllum trabeum*. *Appl. Microbiol. Biotechnol.* 35: 805-809.
- Jellison, J., V. Chandhoke, B. Goodell, F. Fekete, N. Hayashi, M. Ishihara, and K. Yamamoto. 1991 (b). The action of siderophores isolated from *Gloeophyllum trabeum* on the structure and crystallinity of cellulose. International Research Group on Wood Preservation Series. Box 5607. S-114 86. Stockholm, Sweden. Document IRG/WP 1479.

- Jensen, Jr., K. A., C. J. Houtman, Z. C. Ryan, and K. E. Hammel. 2001. Pathways for extracellular Fenton chemistry in the brown rot basidiomycete *Gloeophyllum trabeum*. *App. Environ. Microbiol.* 67: 2705-2711.
- Job-Cei, C., J. Keller, and D. Job. 1996. Degradation of unbleached pulp paper treated in solid state conditions with five species of the brown rot *Gloeophyllum*. *Material and Organisms (Berlin)*. 30(2): 105-116.
- Johannes, C., and A. Majcherczyk. 2000. Natural mediators in the oxidation of polycyclic aromatic hydrocarbons by laccase mediator systems. *App. Environ. Microbiol.* 66: 524-528.
- Johannes, C., A. Majcherczyk, and A. Huttermann. 1996. Degradation of anthracene by laccase of *Trametes versicolor* in the presence of different mediator compounds. *App. Environ. Microbiol.* 46: 313-317.
- Jones, H. L., and J. J. Worrall. 1993. Errors in wood decay studies attributable to fungal biomass. *Phytopathology*. 83(12): 1364.
- Jones, H. L., and J. J. Worrall. 1995. Fungal biomass in decayed wood. *Mycologia*. 87(4): 459-466.
- Kerem, Z., K. A. Jensen, and K. E. Hammel. 1999. Biodegradative mechanism of the brown rot basidiomycete *Gloeophyllum trabeum*: evidence for an extracellular hydroquinone-driven Fenton reaction. *FEBS Letters*. 446: 49-54.
- Kerem, Z., W. Bao, and K. E. Hammel. 1998. Rapid polyether cleavage via extracellular one-electron oxidation by a brown rot basidiomycete. *Proceedings of the National Academy of Sciences of the United States of America*. 95(18): 10373-10377.
- Keyser, P., T. K. Kirk, and J. G. Zeikus. 1978. Ligninolytic enzyme system of *Phanerochaete chrysosporium*: synthesized in the absence of lignin in response to nitrogen starvation. *J. Bacteriol.* 135: 790-797.
- Kirk, T. K. 1987. Enzymatic combustion: the microbial degradation of lignin. *Ann. Rev. Microbiol.* 41: 465-505.
- Kirk, T. K., R. Ibach, M. D. Mozuch, A. H. Conner, and T. L. Highley. 1991. Characterization of cotton cellulose depolymerized by a brown rot fungus, by acid, or by chemical oxidants. *Holzforschung*. 45: 239-244.
- Kirk, T. K., S. Croan, and M. Tien. 1986. Production of multiple ligninases by *Phanerochaete chrysosporium*: effect of selected growth conditions and use of a mutant strain. *Enzyme Microb. Technol.* 8: 27-32.

- Koenigs, J. W. 1974. Hydrogen peroxide and iron: a proposed system for decomposition of wood by brown rot basidiomycetes. *Wood Fiber*. 6: 66-79.
- Koenigs, J. W. 1975. Hydrogen peroxide and iron: a microbial cellulolytic system? *Biotechnology and Bioengineering Symposium*. 5: 151-159.
- Koster, M., W. Ovaas, W. Bitter, and P. Weisbeek. 1995. Multiple outer membrane receptors for uptake of ferric pseudobactins in *Pseudomonas putida* WCS358. *Mol. Genet.* 248: 735-743.
- Kremer, S. M., and P. M. Wood. 1992. Cellobiose oxidase from *Phanerochaete chrysosporium* as a source of Fenton's reagent. *Biochemical Society Transactions*. 20(2): 1105.
- Labarere, J., and M. Bonneau. 1982. Isolation and characterization of plasma membranes from the fungus *Podospira anserina*. *J. Bacteriol.* 151: 648-656.
- Lehner, D., P. Zipper, G. Henriksson, and G. Pettersson. 1996. Small angle X-ray scattering studies on cellobiose dehydrogenase from *Phanerochaete chrysosporium*. *Biochimica et Biophysica Acta*. 1293: 161-169.
- Leong, S. A., and G. Winkelmann. 1998. Molecular biology of iron transport in fungi. *Metal Ions in Biological Systems*. 35:147-186.
- Lesuisse, E., M. Casterassimon, and P. Labbe. 1996. Evidence for the *Saccharomyces cerevisiae* ferrireductase system being a multicomponent electron transport chain. *J. Biol. Chem.* 271: 13578-13583.
- Levier, K., and M. L. Guerinot. 1996. The *Bradyrhizobium japonicum* feqA gene encodes an iron regulated outer membrane protein with similarity to hydroxamate type siderophore receptors. *Journal of Bacteriology*. 178(24): 7265-7275.
- Li, B., S. R. Nagalla, and V. Renganathan. 1996. Cloning of a cDNA encoding cellobiose dehydrogenase, a hemoflavoenzyme from *Phanerochaete chrysosporium*. *Appl. Environ. Microbiol.* 62(4): 1329-1335.
- Li, B., S. R. Nagalla, and V. Renganathan. 1997. Cellobiose dehydrogenase from *Phanerochaete chrysosporium* is encoded by two allelic variants. *Appl. Environ. Microbiol.* 63(2): 796-799.
- Li, R., M. A. Bianchet, P. Talalay, and L. M. Amzel. 1995. The three-dimensional structure of NAD(P)H:quinone reductase, a flavoprotein involved in cancer chemoprotection and chemotherapy: mechanism of the two-electron reduction. *Proceedings of the National Academy of Sciences of the United States of America*. 92: 8846-8850.

- Lind, C., P. Hochstein, and L. Ernster. 1982. DT-diaphorase as a quinone reductase: a cellular control device against semiquinone and superoxide radical formation. *Arch. Biochem. Biophys.* 216: 178-185.
- Lowry, O. H., N. J. Rosebrough, A. L. Farr, and R. J. Randall. 1951. Protein measurement with the Folin phenol reagent. *J. Biol. Chem.* 193: 265-275.
- Lu, J., B. Goodell, J. Liu, A. Enoki, J. Jellison, and F. Fekete. 1994. The role of oxygen and oxygen radicals in one-electron oxidation reactions mediated by low molecular weight compounds isolated from *Gloeophyllum trabeum*. The International Research Group on Wood Preservation. Document IRG/WP94-1457. IRG Secretariat, Box 5607 S-114 86.
- Lundegardh, H. 1945. Absorption, transport and extrudation of inorganic ions by roots. *Arkiv. Bot.* 32(11): 1.
- Majcherczyk, A., and C. Johannes. 2000. Radical mediated indirect oxidation of a PEG-coupled polycyclic aromatic hydrocarbon (PAH) model compound by fungal laccase. *Biochemica et Biophysica Acta.* 1474: 157-162.
- Mansfield, S. D., J. N. Saddler, and G. M. Guebitz. 1998. Characterization of endoglucanases from the brown rot fungi *Gloeophyllum sepiarium* and *Gloeophyllum trabeum*. *Enzyme & Microbial Technology.* 23(1-2): 133-140.
- Martens, R., H. Wetzstein, F. Zadrazil, M. Capelari, P. Hoffmann, and N. Schmeer. 1996. Degradation of the fluoroquinone enrofloxacin by white rot fungi. *Appl. Environ. Microbiol.* 62(11): 4206-4209.
- Medina, M. A., A. D. Castillo-Olivares, and I. N. D. Castro. 1997. Multifunctional plasma membrane redox systems. *BioEssays.* 19(11): 977-984.
- Merk, H. F., and F. K. Jugert. 1991. Cutaneous NAD(P)H:quinone reductase: a xenobiotica-metabolizing enzyme with potential cancer and oxidation stress-protecting properties. *Skin Pharmacology.* 4 (suppl 1): 95-100.
- Micales, J. A. 1995. The role of oxalate decarboxylase in pH regulation by brown rot fungi. *Phytopathology.* 85(10): 1197.
- Milstein, O., R. Gersonde, A. Huttermann, M. Chen, and J. J. Meister. 1992. Fungal biodegradation of lignopolystyrene craft copolymers. *Appl. Environ. Microbiol.* 58(10): 3225-3232.
- Moukha, S. M., T. J. Dumonceaux, E. Record, and F. S. Archibald. 1999. Cloning and analysis of *Pycnoporus cinnabarinus* cellobiose dehydrogenase. *Gene.* 234: 23-33.

- Murphy, T. H., M. J. De Long, and J. T. Coyle. 1991. Enhanced NAD(P)H: quinone reductase activity prevents glutamate toxicity produced by oxidative stress. *J. Neurochem.* 56: 990-995.
- Parra, C., J. Rodriguez, J. Baeza, J. Freer, and N. Duran. 1998. Iron-binding catechols oxidating lignin and chlorolignin. *Biochemical & Biophysical Research Communications.* 251(2): 399-402.
- Paszczynski, A., R. Crawford, D. Funk, and B. Goodell. 1999. De Novo synthesis of 4,5-dimethoxycatechol and 2,5-dimethoxyhydroquinone by the brown rot fungus *Gloeophyllum trabeum*. *App. Environ. Microbiol.* 65(2): 674-679.
- Pracht, J., J. Boenigk, M. Isenbeck-Schroter, F. Keppler, and H. F. Scholer. 2001. Abiotic Fe(III) induced mineralization of phenolic substances. *Chemosphere.* in press.
- Prester, T., H. J. Prochaska, and P. Talalay. 1992. Inhibition of NAD(P)H (quinone acceptor) oxidoreductase by cibacron blue and related anthraquinone dyes: a structure-activity study. *Biochemistry.* 31: 824-833.
- Prochaska, H. J., and P. Talalay. 1986. Purification and characterization of two isofunctional forms of NAD(P)H:quinone reductase from mouse liver. *J. Bio. Chem.* 261:1372-1378.
- Prochaska, H. J., P. Talalay, and H. Sies. 1987. Direct protective effect of NAD(P)H : quinone reductase against menadione-induced chemiluminescence of postmitochondrial fractions of mouse liver. *J. Bio. Chem.* 262: 1931-1934.
- Qi, W., and J. Jellison. 2000. Chelator production and cellobiose dehydrogenase activity of wood-inhabiting fungi. IRG/WP 00-10363. 31st International Research Group on Wood Preservation annual meeting. Kona, Hawaii.
- Qian, Y., and B. Goodell. 1999. The effect of low molecular weight chelators on iron chelation and free radical generation as studied by ESR measurement. IRG 31st International Research Group on Wood Preservation annual meeting. Kona, Hawaii.
- Rabsch, W., W. Voigt, R. Reissbrodt, R. M. Tsois, and A. J. Baumler. 1999. *Salmonella typhimurium* IronN and FepA proteins mediate uptake of enterobactin but differ in their specificity for other siderophores. *Journal of Bacteriology.* 181(11): 3610-3612.
- Raices, M., E. Paifer, J. Cremata, R. Montesino, J. Stahlberg, C. Divne, I. J. Szabo, G. Henriksson, G. Johansson, and G. Pettersson. 1995. Cloning and characterization of a cDNA encoding a cellobiose dehydrogenase from the white rot fungus *Phanerochaete chrysosporium*. *FEBS Letters.* 369: 233-238.

- Rauth, A. M., Z. Goldberg, and V. Misra. 1997. DT-diaphorase: possible roles in cancer chemotherapy and carcinogenesis. *Oncology Research*. 9(6-7): 339-349.
- Rioux, C., D. C. Jordan, and J. B. M. Rattray. 1983. Colorimetric determination of catechol siderophores in microbial cultures. *Anal. Biochem.* 133: 163-169.
- Ritschkoff, A. 1996. Decay Mechanisms of Brown Rot Fungi. Vtt Publications 268. Technical Research Center of Finland. Vuorimiehentie, Finland.
- Ritschkoff, A., J. Buchert, and L. Viikari. 1994. Purification and characterization of a thermophilic xylanase from the brown rot fungus *Gloeophyllum trabeum*. *Journal of Biotechnology*. 32(1): 67-74.
- Roberts, J. J., T. Marchbank, V. P. Kotsaki-Kovatsi, M. P. Boland, F. Friedlos, and R. J. Knox. 1989. Caffeine, aminoimidazolecarboxamide and dicoumarol, inhibitors of NAD(P)H dehydrogenase (quinone) (DT diaphorase), prevent both the cytotoxicity and DNA interstrand crosslinking produced by 5-(aziridin-1-yl)-2,4-dinitrobenzamide (CB 1954) in Walker cells. *Biochemical Pharmacology*. 38: 4137-4143.
- Ryan, H. 1967. Alcohol dehydrogenase activity and electron transport in living yeast. *Biochemical Journal*. 105: 137-143.
- Samejima, M., and K. L. Eriksson. 1992. A comparison of the catalytic properties of cellobiose:quinone oxidoreductase and cellobiose oxidase from *Phanerochaete chrysosporium*. *Eur. J. Biochem.* 207: 103-107.
- Samuels, G. J. 1996. *Trichoderma*: a review of biology and systematics of the genus. *Mycological Research*. 100(8): 923-935.
- Schafer, F. Q., and G. R. Buettner. 2000. Acidic pH amplifies iron-mediated lipid peroxidation in cells. *Free Radical Biology and Medicine*. 28: 1175-1181.
- Schimidhalter, D. R., and G. Canevascini. 1993 (a). Isolation and characterization of two exocellobiohydrolases from the brown rot fungus *Coniophora puteana* (Schum ex Fr) Karst. *Arch. Biochem. Biophys.* 300(2): 551-558.
- Schimidhalter, D. R., and G. Canevascini. 1993 (b). Isolation and characterization of the cellobiose dehydrogenase from the brown rot fungus *Coniophora puteana* (Schum ex Fr.) Karst. *Arch. Biochem. Biophys.* 300(2): 559-563.
- Schmidt, C. J., B. K. Whitten, and D. D. Nicholas. 1981. A proposed role for oxalic acid in non-enzymatic wood decay by brown rot fungi. *Am. Wood Preserv. Assoc.* 77: 157-164.

- Schlager, J. J., and G. Powis. 1990. Cytosolic NAD(P)H: (quinone acceptor) oxidoreductase in human normal and tumor tissue: effects of cigarette smoking and alcohol. *International Journal of Cancer*. 45: 403-409.
- Schoemaker, H. E., E. M. Meijer, M. S. A. Leisola, S. D. Haemmerli, R. Waldner, D. Sanglard, and H. W. H. Schmidt. 1989. Oxidation and reduction in lignin biodegradation. Pp. 454-471. In N. G. Lewis and M. G. Paice (ed.), Plant Cell Wall Polymers: Biogenesis and Biodegradation. American Chemical Society, Washington, D. C.
- Schou, C., G. Rasmussen, M. B. Kalsoft, B. Henrissat, and M. Schulein. 1993. Stereochemistry, specificity and kinetics of the hydrolysis of reduced cellodextrins by nine cellulases. *European Journal of Biochemistry*. 217(3): 947-953.
- Schou, C., M. H. Christensen, and M. Schulein. 1998. Characterization of a cellobiose dehydrogenase from *Humicola insolens*. *Biochem. J.* 330: 565-571.
- Schwyn, B., and J. B. Neilands. 1987. Universal chemical assay for the detection and determination of siderophores. *Anal. Biochem.* 160: 47-56.
- Shimada, M., Y. Akamitsu, T. Tokimatsu, K. Mii, and T. Hattori. 1997. Possible biochemical role s of oxalic acid as a low molecular weight compound involved in brown rot and white rot wood decays. *J. Biotechnol.* 53: 103-113.
- Sjostrom, E. 1993. Wood Chemistry: Fundamentals and Applications. Academic Press., New York.
- Smith, J. E., and D. R. Berry. 1975. The Filamentous Fungi. John Wiley & Sons., New York.
- Stahl, J. D., and S. D. Aust. 1993. Plasma membrane dependent reduction of 2,4,6-trinitrotoluene by *Phanerochaete chrysosporium*. *Biochemical and Biophysical Research Communications*. 192(2): 471-476.
- Stahl, J. D., and S. D. Aust. 1995. Properties of a transplasma membrane redox system of *Phanerochaete chrysosporium*. *Arch. Biochem. Biophys.* 320: 369-374.
- Stahl, J. D., S. J. Rasmussen, and S. D. Aust. 1995. Reduction of quinones and radicals by a plasma membrane redox system of *Phanerochaete chrysosporium*. *Arch. Biochem. Biophys.* 322: 221-227.
- Stookey, L. L. 1970. Ferrozine - A new spectrophotometric reagent for iron. *Analytical Chemistry*. 42(7): 779-781.

- Subramaniam, S. S., S. R. Nagalla, and V. Renganathan. 1999. Cloning and characterization of a thermostable cellobiose dehydrogenase from *Sporotrichum thermophile*. Arch. Biochem. Biophys. 365: 223-230.
- Sun, I. L., E. E. Sun, F. L. Crane, D. J. Morre, A. Lindgren, and H. Low. 1992. Requirement for coenzyme Q in plasma membrane electron transport. Proceedings of the National Academy of Sciences of the United States of America. 89: 11126-11130.
- Talalay, P. 1989. Mechanisms of induction of enzymes that protect against chemical carcinogenesis. Advances in Enzyme Regulation. 28: 237-250.
- Talalay, P., and A. M. Benson. 1982. Elevation of quinone reductase activity by anticarcinogenic antioxidants. Advances in Enzyme Regulation. 20: 287-300.
- Temp, U., and C. Eggert. 1999. Novel interaction between laccase and cellobiose dehydrogenase during pigment synthesis in the white rot fungus *Pycnoporus cinnabarinus*. Appl. Environ. Microbiol. 65(2): 389-395.
- Tien, M., and T. K. Kirk. 1988. Lignin peroxidase of *Phanerochaete chrysosporium*. Methods in Enzymology. 161: 238-249.
- Tsutsumi, Y., T. Haneda, and T. Nishida. 2001. Removal of estrogenic activities of bisphenol A and nonylphenol by oxidative enzymes from lignin-degrading basidiomycetes. Chemosphere. 42(3): 271-276.
- Unbehaun, H., B. Bittler, G. Kuehne, and A. Wagenfuehr. 2000. Investigation into the biotechnological modification of wood and its application in the wood based material industry. Acta Biotechnologica. 20: 305-312.
- Unemoto, T., and M. Hayashi. 1993. Na(+)-translocating NADH-quinone reductase of marine and halophilic bacteria. Journal of Bioenergetics & Biomembranes. 25(4): 385-391.
- Vallim, M. A., B. J. H. Janse, J. Gaskell, A. A. Pizzirani-Kleiner, and D. Cullen. 1998. *Phanerochaete chrysosporium* cellobiohydrolase and cellobiose dehydrogenase transcripts in wood. Appl. Environ. Microbiol. 64(5): 1924-1928.
- Wefers, H., T. Komai, P. Talalay, and H. Sies. 1984. Protection against reactive oxygen species by NAD(P)H:quinone reductase induced by the dietary antioxidant butylated hydroxyanisole (BHA). Decreased hepatic low-level chemiluminescence during quinone redox cycling. FEBS Letter. 169: 63-66.

- Weger, L. A. D., R. V. Boxtel, B. V. D. Burg, R. A. Gruters, F. P. Geels, B. Schippers, and B. Lugtenberg. 1986. Siderophore and outer membrane proteins of antagonistic, plant growth stimulating, root colonizing *Pseudomonas spp.* *Journal of Bacteriology*. 165(2): 585-594.
- Westermarck, U., and K. E. Eriksson. 1975. Purification and properties of cellobiose: quinone oxidoreductase from *Sporotrichum pulverulentum*. *Acta Chem. Scand. B29*: 419-424.
- Wetzstein, H., M. Stadler, H. Tichy, A. Dalhoff, and W. Karl. 1999. Degradation of ciprofloxacin by basidiomycetes and identification of metabolites generated by the brown rot fungus *Gloeophyllum striatum*. *App. Environ. Microbiol.* 65(4): 1556-1563.
- Wiley, W. R. 1974. Isolation of spheroplast and membrane vesicles from yeast and filamentous fungi. *Methods in Enzymology*. 31: 609-627.
- Wood, P. M. 1993. Pathways for production of Fenton's reagent by wood-rotting fungi. *FEMS Microbiol. Rev.* 13: 313-320.
- Worrall, J. J., S. E. Anagnost, and R. A. Zabel. 1997. Comparison of wood decay among diverse lignicolous fungi. *Mycologia*. 89(2): 199-219.
- Yajima, Y. A., M. B. Enoki, M. Mayfield, and M. H. Gold. 1979. Vanillate hydroxylase from the white rot basidiomycete *Phanerochaete chrysosporium*. *Arch. Microbiol.* 123: 319-321.
- Zabel, R. A., and J. J. Morrell. 1992. Wood Microbiology: Decay and Its Prevention. Academic Press, Inc., San Diego, California.
- Zuo, Y., and J. Hoigne, 1994. Photochemical decomposition of oxalic, glyoxalic, and pyruvic acids catalyzed by iron in atmospheric waters. *Atmos. Environ.* 28: 1231-1239.

Appendix A

HIGHLEY'S LIQUID MEDIA

Ingradients

NH ₄ NO ₃	2.0 g/l	H ₃ BO ₄ *	0.57 mg/l
KH ₂ PO ₄	2.0 g/l	MnCl ₂ .4H ₂ O *	0.036 mg/l
MgSO ₄ .7H ₂ O	0.5 g/l	ZnSO ₄ .7H ₂ O *	0.31 mg/l
CaCl ₂ .2H ₂ O	0.1 g/l	CuSO ₄ .5H ₂ O *	0.039 mg/l
Cellulose	10 g/l	(NH ₄) ₆ Mo ₇ O ₂₄ .4H ₂ O *	0.018 mg/l
Glucose	2 g/l	FeSO ₄ .7H ₂ O **	5.56 mg/l

* Stock solutions:

H₃BO₄: 0.57 mg/mL, use 1 mL per liter media.

MnCl₂.4H₂O: 0.36 mg/mL, use 100 ul per liter media.

ZnSO₄.7H₂O: 0.31 mg/mL, use 1 mL per liter media.

CuSO₄.5H₂O: 0.39 mg/mL, use 100 ul per liter media.

(NH₄)₆Mo₇O₂₄.4H₂O: 0.18 mg/mL, use 100 ul per liter media.

** Prepare fresh solution (55.6 mg/mL) each time before use. Use 100 ul per liter media.

Preparation

Add 2 g of cellulose powder into one 500 mL flask. Then add 200 mL of liquid media into the flask. Autoclave for 20 minutes at 15 PSI. If only glucose is used as the carbon source, 10 gram of glucose is used for 1 liter of media.

Appendix B
BASAL MEDIA

Media Composition

Basal III solution, 100 mL
Trace elements solution, 60 mL
10% glucose, 100 mL
0.1 M 2,2-dimethylsuccinate, pH 4.2, 100 mL
100 mg/l Thiamin, 10 mL
8 g/l ammonium tartrate, 25 mL
0.4 M Veratryl alcohol, 100 mL
deionized distilled water, 405 mL

Stock Solutions

Trace elements solution (per liter)

MgSO₄: 3 g

MnSO₄: 0.5 g

NaCl: 1.0 g

FeSO₄·7H₂O: 0.1 g

CoCl₂: 0.1 g

ZnSO₄·7H₂O: 0.1 g

CuSO₄: 0.1 g

AlK(SO₄)₂·12H₂O: 10 mg

H₃BO₃: 10 mg

$\text{Na}_2\text{MoO}_4 \cdot 2\text{H}_2\text{O}$: 10 mg

Nitrilotriacetate: 1.5 g

Filter sterilized.

Basal III solution (per liter)

KH_2PO_4 : 20 g

MgSO_4 : 5 g

CaCl_2 : 1 g

Trace elements solution: 100 mL

Filter sterilized.

10% glucose, autoclave for 20 minutes at 121 °C

0.1 M 2,2-dimethylsuccinate, pH 4.2, autoclave for 20 minutes at 121 °C

100 mg/l Thiamin, autoclave for 20 minutes at 121 °C

8 g/l ammonium tartrate, autoclave for 20 minutes at 121 °C

0.4 M Veratryl alcohol, filter sterilized.

Appendix C

LINEWEAVER-BURK PLOTS DETERMINING KINETIC CONSTANTS

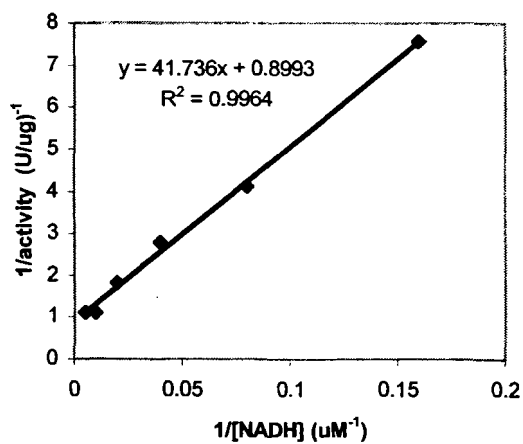


Figure C.1. Lineweaver-Burk plot of NADH oxidization by the *G. trabeum* quinone reductase.

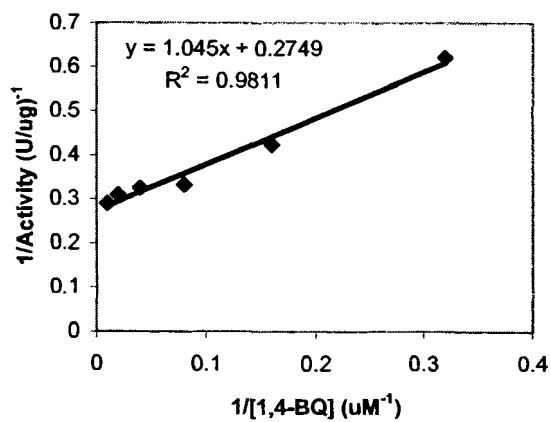


Figure C.2. Lineweaver-Burk plot of 1,4-benzoquinone reduction by the *G. trabeum* quinone reductase.

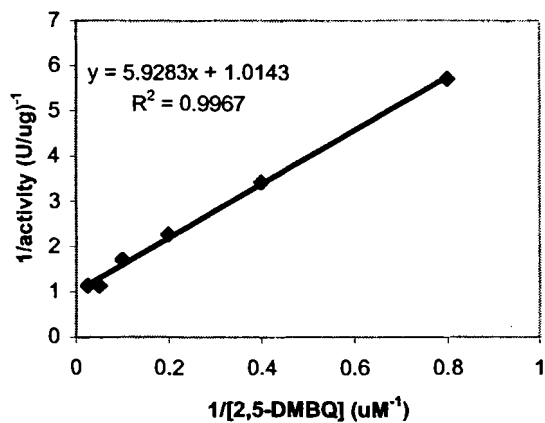


Figure C.3. Lineweaver-Burk plot of 2,5-dimethoxy-1,4-benzoquinone reduction by the *G. trabeum* quinone reductase.

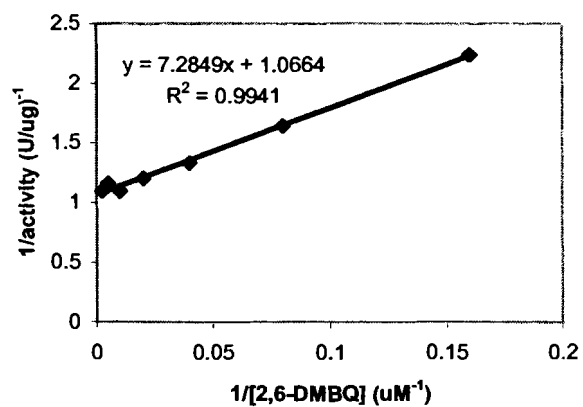


Figure C.4. Lineweaver-Burk plot of 2,6-dimethoxy-1,4-benzoquinone reduction by the *G. trabeum* quinone reductase.

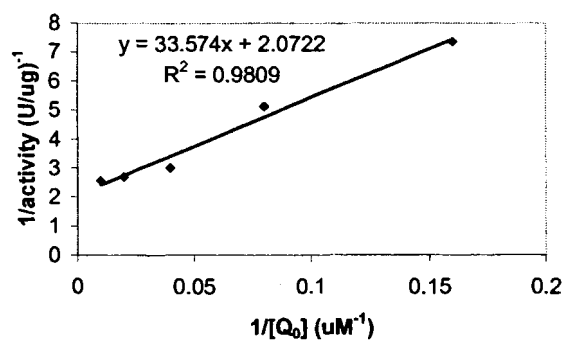


Figure C.5. Lineweaver-Burk plot of 2,3-dimethoxy-5-methyl-1,4-benzoquinone reduction by the *G. trabeum* quinone reductase.

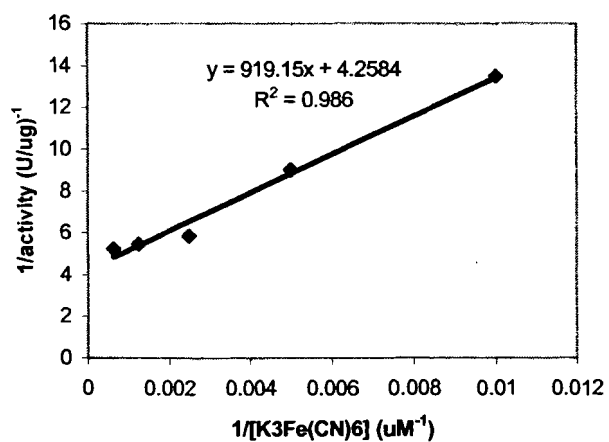


Figure C.6. Lineweaver-Burk plot of potassium ferricyanide reduction by the *G. trabeum* quinone reductase.

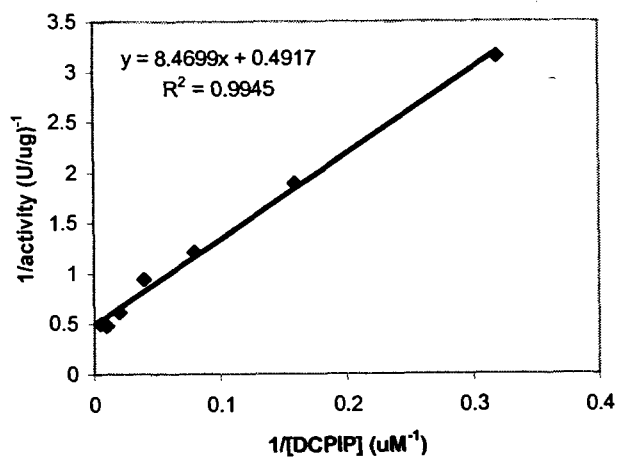


Figure C.7. Lineweaver-Burk plot of 2,6-dichloro-indophenol reduction by the *G. trabeum* quinone reductase.

Appendix D

HPLC ANALYSIS OF BIOCHELATOR FRACTIONS

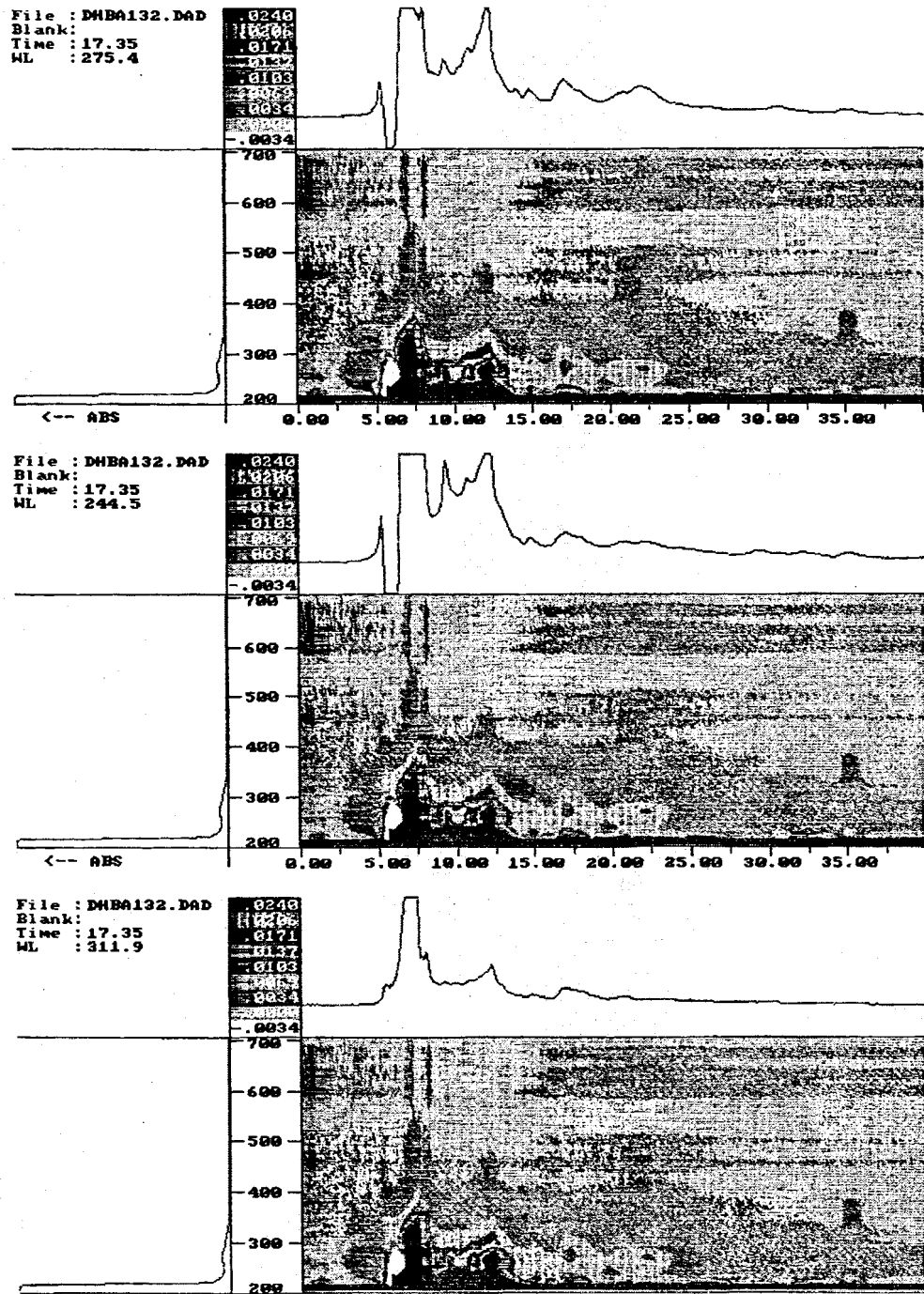


Figure D.1. HPLC analysis of the culture filtrate from *G. trabeum* at 275.4, 244.5 and 311.9 nm, where the characteristic absorbance peaks of DHBA are expected.

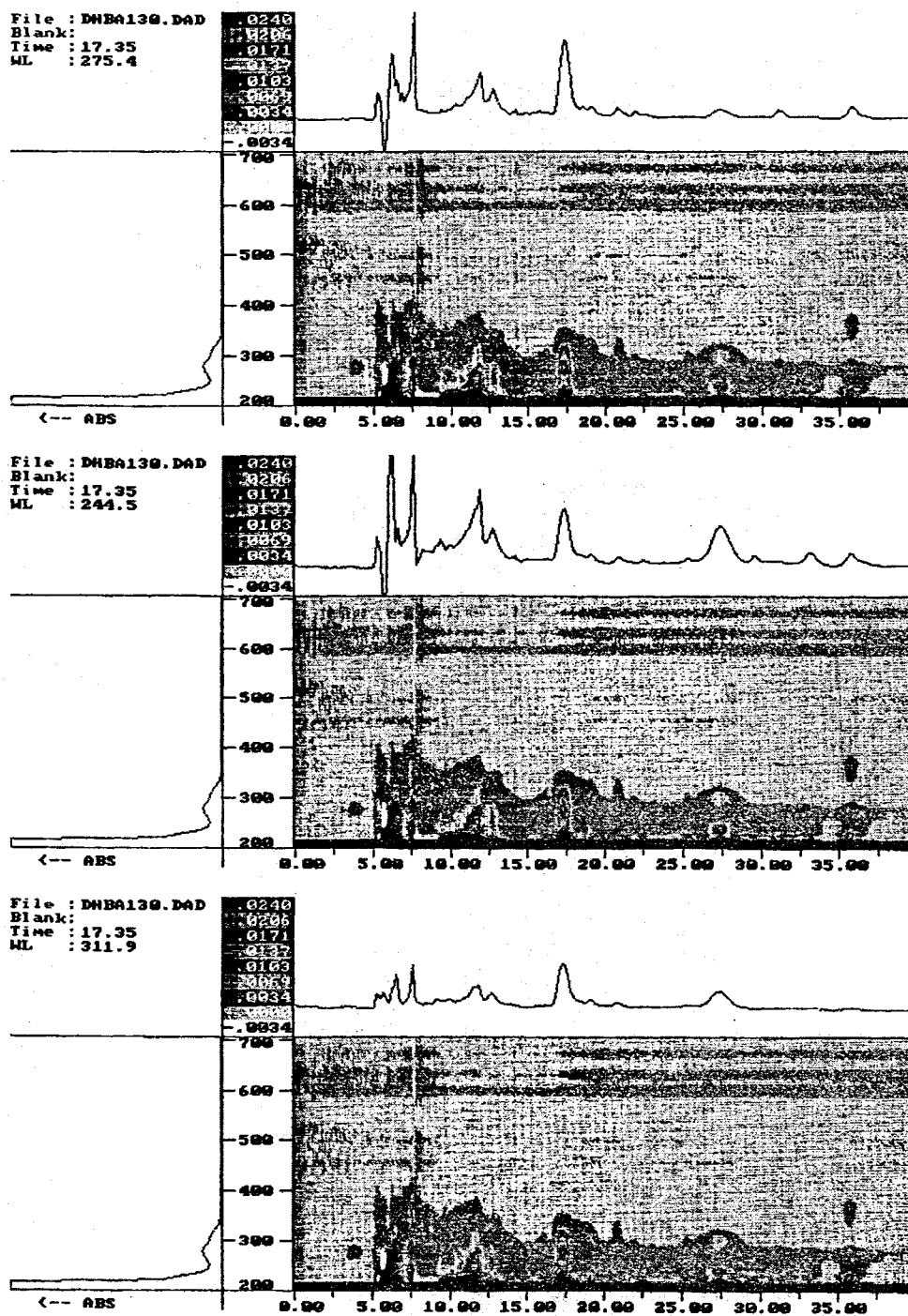


Figure D.2. HPLC analysis of the ethyl acetate extract from the *G. trabeum* culture filtrate at 275.4, 244.5 and 311.9 nm, where the characteristic absorbance peaks of DHBA are expected.

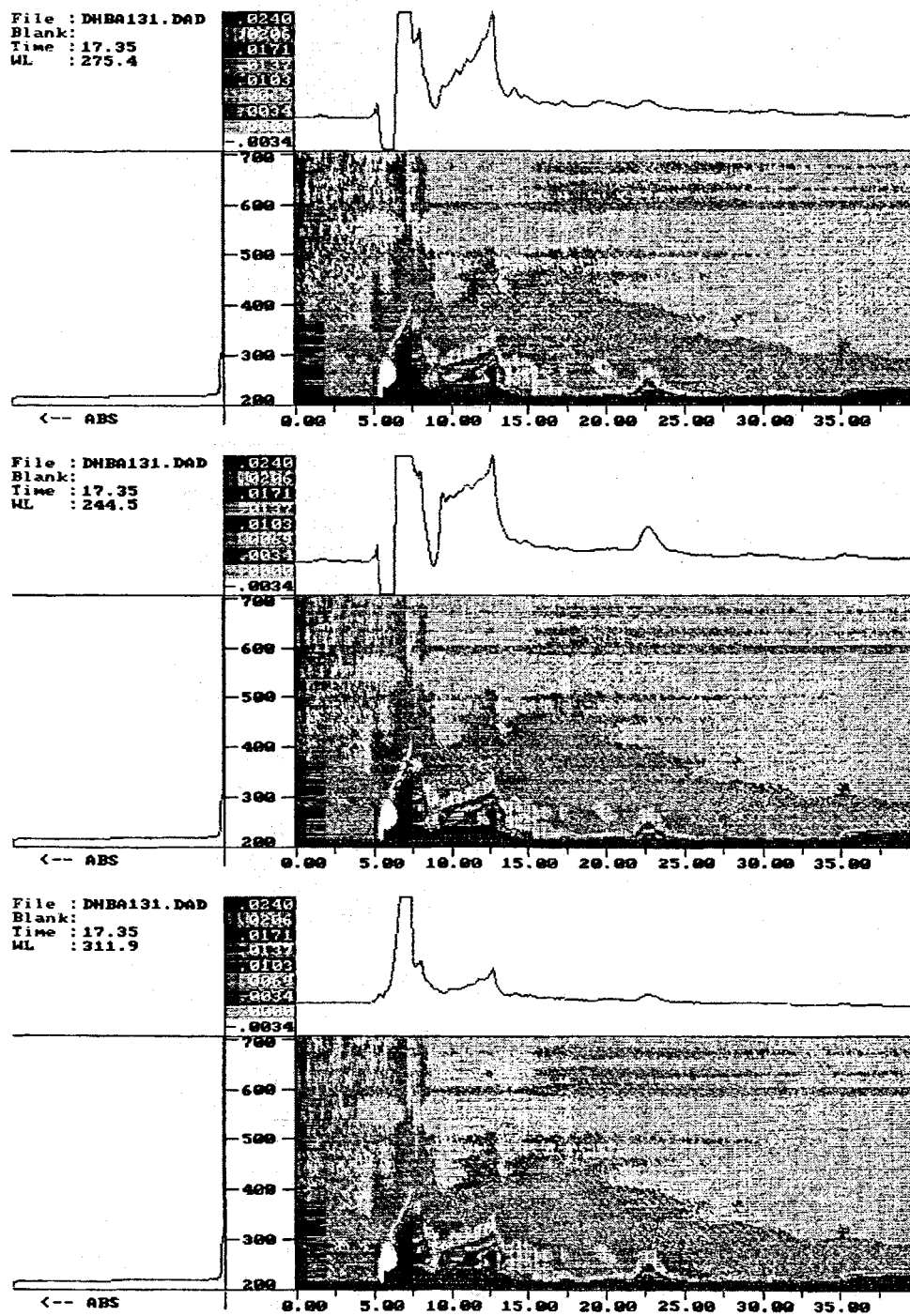


Figure D.3. HPLC analysis of the aqueous residual from the *G. trabeum* culture filtrate at 275.4, 244.5 and 311.9 nm, where the characteristic absorbance peaks of DHBA are expected.

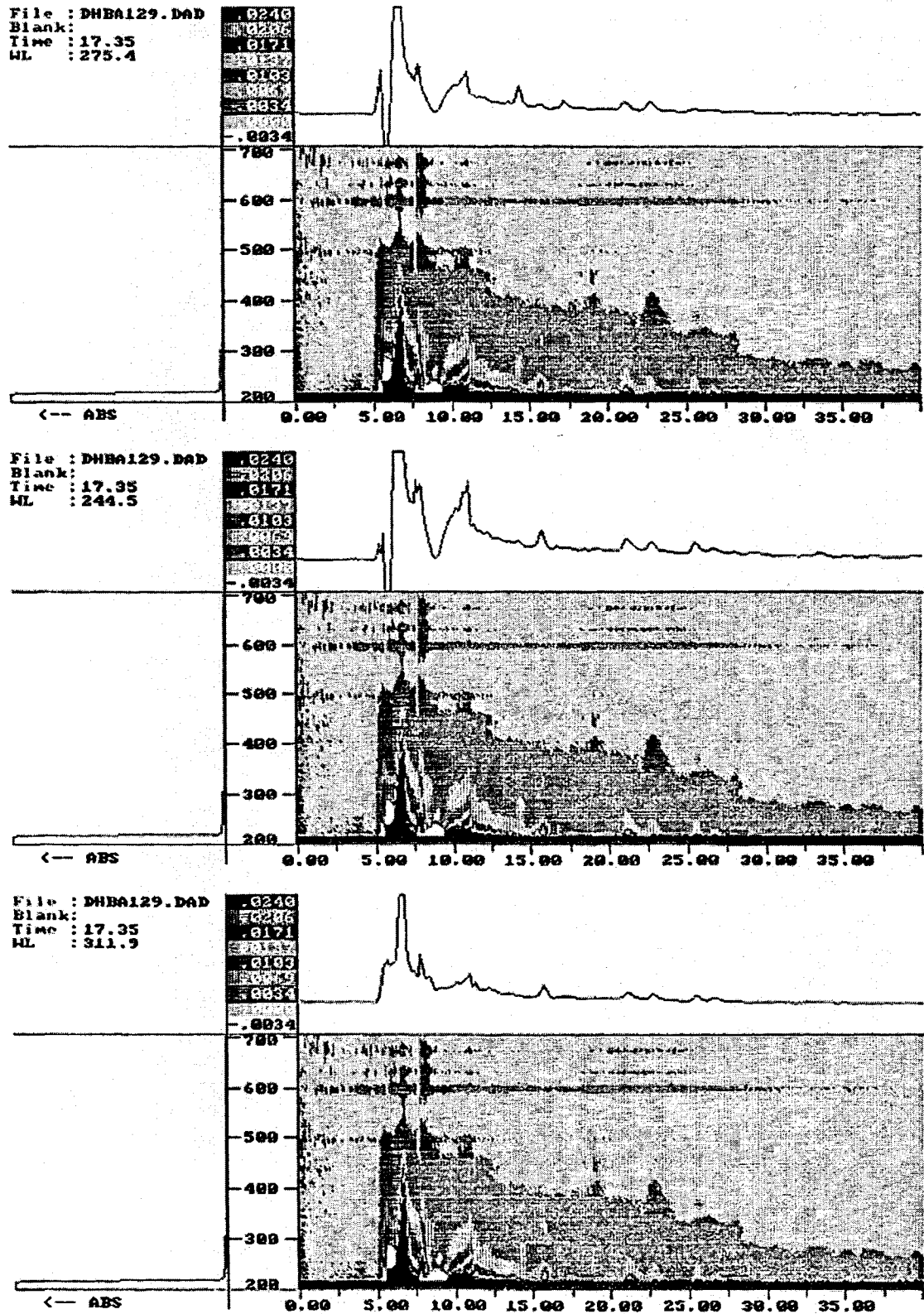


Figure D.4. HPLC analysis of the ethyl acetate extraction from the *P. chrysosporium* culture filtrate at 275.4, 244.5 and 311.9 nm, where the characteristic absorbance peaks of DHBA are expected.

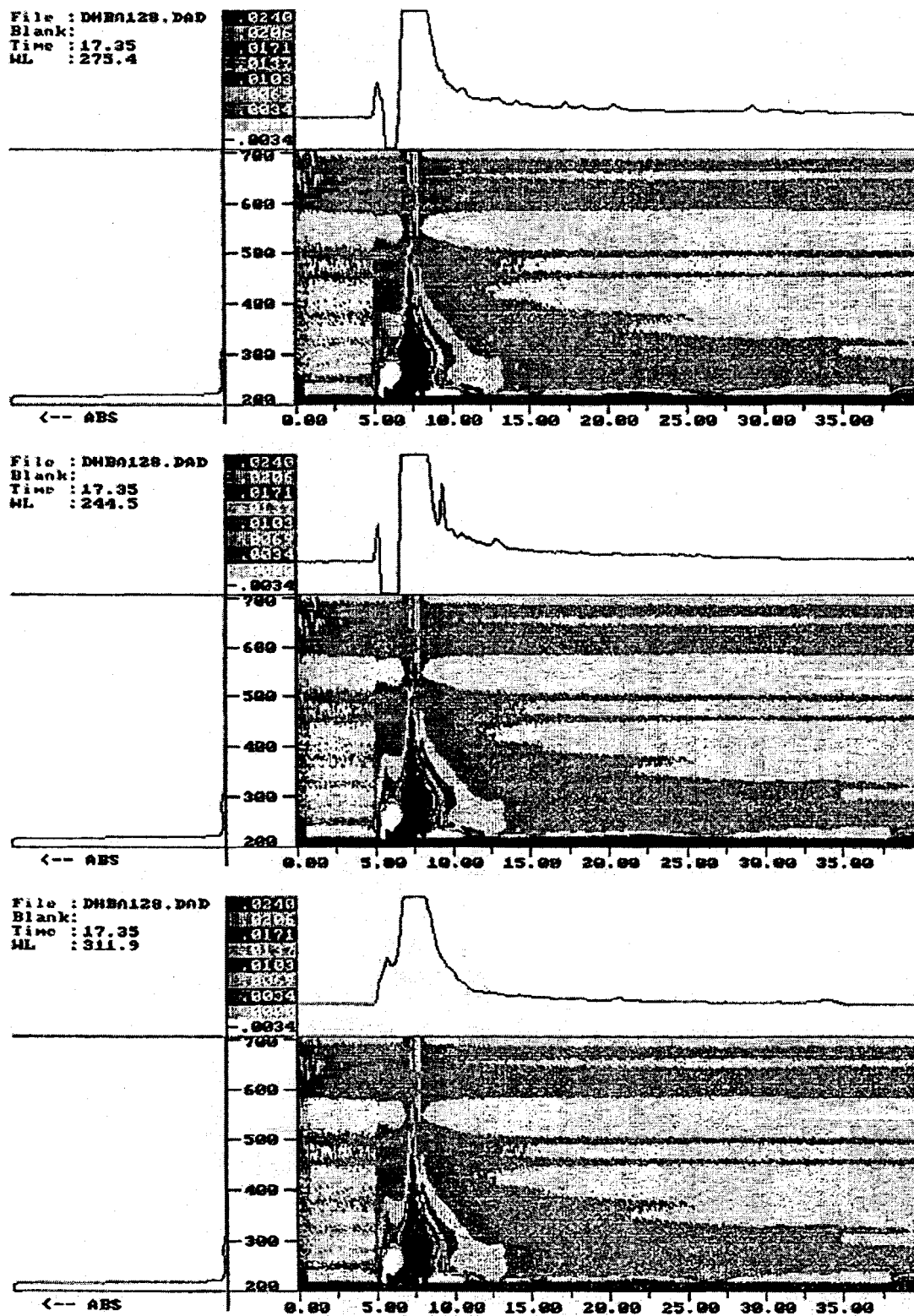


Figure D.5. HPLC analysis of the aqueous residual from the *P. chrysosporium* culture filtrate at 275.4, 244.5 and 311.9 nm, where the characteristic absorbance peaks of DHBA are expected.

BIOGRAPHY OF THE AUTHOR

Weihong Qi was born in Harbin, China on July 6, 1972. She was raised in Guilin, Guangxi and graduated from Guilin High School in 1990. She attended Wuhan University and graduated in 1994 with a Bachelor degree in Ecology. She was admitted into the graduate school of the Chinese Academy of Science and graduated in 1997 with a Master degree in Microbiology. She entered the Biological Science graduate program at the University of Maine in the summer of 1997. Weihong is a candidate for the Doctor of Philosophy degree in Biological Sciences from The University of Maine in December, 2001.